

FOR REFERENCE ONLY

41 0566368 5



ProQuest Number: 10182990

All rights reserved

INFORMATION TO ALL USERS

The quality of this reproduction is dependent upon the quality of the copy submitted.

In the unlikely event that the author did not send a complete manuscript and there are missing pages, these will be noted. Also, if material had to be removed, a note will indicate the deletion.



ProQuest 10182990

Published by ProQuest LLC (2017). Copyright of the Dissertation is held by the Author.

All rights reserved.

This work is protected against unauthorized copying under Title 17, United States Code  
Microform Edition © ProQuest LLC.

ProQuest LLC.  
789 East Eisenhower Parkway  
P.O. Box 1346  
Ann Arbor, MI 48106 – 1346

THE SYNTHESIS AND SCREENING OF SUBSTITUTED SULPHUR HETEROCYCLES  
FOR LANGMUIR-BLODGETT FILMS AND NON-LINEAR OPTICS.

By

P. Routledge, B.Sc.

A Thesis submitted for the degree of

Doctor of Philosophy in

**THE NOTTINGHAM TRENT UNIVERSITY**

OCTOBER 1995.

REF.

PH-D|CP|95

ROU

## **ACKNOWLEDGEMENTS**

During the passage of time while researching at The Nottingham Trent University, I have become indebted to many people who I would now like to acknowledge with the following expression of my gratitude.

I would especially like to thank my supervisors' Dr DB Neal and Dr JM Barker for their invaluable advice, effort and encouragement towards me during this project. I would also like to thank Dr M Newton for proof reading this thesis. I would like to thank the technical staff for their assistance especially Mr ML Wood for the  $^1\text{H}$  and  $^{13}\text{C}$  NMR spectra he produced for me. I would also like to thank Dr GH Cross and his colleagues at Durham University for their collaboration in doing the SHG measurements on the Langmuir-Blodgett films.

I would also like to thank Dr F Grunfeld of Nima Technology for his advice and technical assistance throughout, and sponsorship in the latter part of this project.

A special thanks to my family for their unconditional love and unwavering conviction in my ability. Finally thank you to all my the friends and colleagues that kept me sane throughout the whole duration of this project, by taking me down the pub and helping me put everything back into perspective.

## ABSTRACT

Over recent years there has been a great increase in research into Langmuir-Blodgett (LB) thin films, as the LB method is an organic fabrication technique appropriate for the formation of monolayer and multilayer structures that have a high degree of anisotropy and structural order as well as a precise and uniform thickness. In particular, considerable interest in the second-order non-linear optical properties of molecules that can be deposited as LB films has arisen, since the technique enables them to be readily assembled into non-centrosymmetric structures that ensures that the individual second-order hyperpolarisabilities do not cancel one another.

One group of materials that have been investigated extensively, and which have produced exciting results are hemicyanine dyes, which have a D- $\pi$ -A system (donor and acceptor groups linked by a conjugated  $\pi$  system) containing a stilbene unit bonded to a heterocyclic group containing nitrogen. In this study a thiophene moiety was incorporated into the molecule instead of the nitrogen heterocycle. The inclusion of a  $\pi$ -excessive centre into a stilbene type molecule of this type may enhance the second-order non-linear optical properties of the material. Background experiments have been performed in which the thiophene units were incorporated into various simple long chain molecules, in order to establish how this moiety was likely to effect the film forming capabilities, film stability at the air/subphase interface and the transfer ratio and mode of transfer onto the solid substrate.

The design, synthesis and subsequent systematic characterisation of several members of three homologous series of novel thiophene based compounds, which are amphiphilic in nature, is described. The characterisation of these films involved the production of isotherms under subphase conditions that were varied systematically; subsequently the area per molecule, decay rate of the film on the subphase, transfer ratio of the film to a substrate and the mode of transfer of the films have been determined. A systematic investigation into the effects on monolayer stability and transferability of introducing a thiophene moiety at various positions in the alkyl chain of stearic acid is also reported.

Subsequent work focused on the design, synthesis and characterisation of a few members of another homologous series of thiophene based amphiphilic compounds. The members of this series were somewhat more complicated in structure as compared to the first few series. These molecules incorporated an extended region of  $\pi$ -conjugated bonds, which was bounded at one end by an electron donating group and at the other end by an electron accepting group. This gives a Donor- $\pi$ -Acceptor (D- $\pi$ -A) system. There was also a long alkyl chain to confer the required water insolubility to the system.

Once again these molecules have been subjected to a systematic investigation of LB characteristics; this screening was extended to include a study of the characteristics of heterogeneous films incorporating various percentages of arachidic acid. Since these films adopted the centrosymmetric Y-type mode of deposition onto a solid substrate, alternate layer structures would be required if any second-order non-linear properties of the molecules are to be exploited. Preliminary second harmonic generation experiments on a series of such structures, performed in collaboration with a group at Durham University, indicate that the material is not significantly more active than other materials reported in the literature.

## CONTENTS

|  |     |
|--|-----|
| ABSTRACT . . . . .   | i   |
| CONTENTS . . . . .   | iii |
| 1.0 INTRODUCTION . . . . .   | 1   |
| 2.0 NON-LINEAR OPTICAL EFFECTS. . . . .  | 6   |
| 2.1 Introduction . . . . .   | 6   |
| 2.2 Origin and Classification of Non-Linear Optical Effects. . . . .           | 6   |
| 2.2.1 Physical Origins. . . . .  | 9   |
| 2.2.2 Linear Polarisation . . . . .  | 12  |
| 2.2.3 Quadratic Polarisation . . . . .   | 12  |
| 2.2.4 Cubic Polarisation . . . . .   | 14  |
| 2.3 Optimization of Molecular Structure . . . . .                              | 15  |
| 2.4 Crystal Structure Considerations . . . . .                                 | 21  |
| 2.5 Use of the Principles for the Optimization of Non-Linear Response. . . . . | 23  |
| 2.6 Applications of Non-Linear Optical Phenomena. . . . .                      | 36  |
| 3.0 LANGMUIR-BLODGETT FILM TECHNOLOGY. . . . .                                 | 41  |
| 3.1 Basic Concepts. . . . .  | 41  |
| 3.1.1 Historical introduction . . . . .  | 41  |
| 3.1.2 Langmuir-Blodgett films . . . . .  | 42  |
| 3.1.3 Deposition principles . . . . .  | 43  |
| 3.2 Materials . . . . .  | 46  |
| 3.2.1 Introduction . . . . .   | 46  |
| 3.2.2 Classical materials . . . . .  | 46  |
| 3.2.3 Novel materials from the literature . . . . .                            | 49  |
| 3.2.4 Novel materials used in this project. . . . .                            | 52  |
| 3.3 Hardware . . . . .   | 52  |
| 3.3.1 Mechanical Construction of the Langmuir Trough . . . . .                 | 52  |
| 3.3.2 Pressure sensors. . . . .  | 56  |
| 3.3.3 Barriers . . . . .   | 56  |
| 3.3.4 Dipper Mechanisms . . . . .  | 58  |
| 3.3.5 Trough control . . . . .   | 60  |
| 3.3.6 Reduction of contamination . . . . .                                     | 60  |
| 3.4 Quality Assessment . . . . .   | 61  |

|         |  |     |
|---------|--|-----|
| 3.5     | Possible applications for Langmuir-Blodgett films. . . . .                             | 65  |
| 3.5.1   | Devices that have been demonstrated. . . . .   | 67  |
| 4.0     | DISCUSSION OF THE CHEMISTRY. . . . .   | 70  |
| 4.1     | Introduction. . . . .  | 70  |
| 4.2     | Structure of Thiophene. . . . .  | 71  |
| 4.3     | Reactions. . . . .   | 74  |
| 4.3.1   | Friedel-Crafts Acylation. . . . .  | 74  |
| 4.3.1.1 | Catalysts. . . . .   | 74  |
| 4.3.1.2 | Choice of Solvent. . . . .   | 76  |
| 4.3.1.3 | The Friedel-Crafts Acylation of Thiophene. . . . .                                     | 77  |
| 4.3.2   | Reduction of the carbonyl function to methylene (CH <sub>2</sub> ) in ketones. . . . . | 78  |
| 4.3.3   | The Wittig Reaction . . . . .  | 81  |
| 4.3.4   | Reduction of nitro groups. . . . .   | 82  |
| 4.4     | Synthesis of Thiophenes for Study. . . . .   | 82  |
| 4.4.1   | Retrosynthetic analysis of compounds 1. and 2. . . . .                                 | 84  |
| 4.4.2   | Synthesis of compounds 1 and 2. . . . .  | 85  |
| 4.4.3   | Retrosynthetic analysis of compound 3. . . . .   | 87  |
| 4.4.4   | Synthesis of compound 3. . . . .   | 88  |
| 4.5     | Synthesis of Materials for Non-linear Optics. . . . .                                  | 90  |
| 4.5.1   | Retrosynthetic analysis of compounds 19. . . . .                                       | 90  |
| 4.5.2   | Retrosynthetic analysis of compounds 20. . . . .                                       | 91  |
| 4.5.3   | Synthesis of compounds 20. . . . .   | 92  |
| 4.5.4   | Retrosynthetic analysis of compound 21. . . . .  | 97  |
| 4.5.5   | Synthesis of compound 21. . . . .  | 98  |
| 4.5.6   | Retrosynthetic analysis of compounds 22. . . . .                                       | 99  |
| 4.5.7   | Synthesis of compounds 22. . . . .   | 100 |
| 4.5.8   | Retrosynthetic analysis of compound 24. . . . .  | 101 |
| 4.5.9   | Synthesis of compound 24. . . . .  | 102 |
| 4.5.10  | Retrosynthetic analysis of compound 25. . . . .  | 103 |
| 4.5.11  | Synthesis of compound 25. . . . .  | 104 |
| 4.5.12  | Synthesis of compound 54. . . . .  | 104 |
| 4.6     | Langmuir-Blodgett discussion. . . . .  | 107 |
| 5.0     | LANGMUIR-BLODGETT MATERIAL SYNTHESIS<br>EXPERIMENTAL . . . . .                         | 135 |
| 5.1     | Preparation of mono methyl succinate. . . . .  | 135 |
| 5.2     | Preparation of methyl half ester succinyl chloride. . . . .                            | 135 |



|         |   |     |
|---------|---|-----|
| 5.3     | Preparation of compounds 1 and 2. (via compounds 3-6) . . . . .                             | 136 |
| 5.3.1   | Step 1: Friedel-Crafts acylation. . . . .   | 136 |
| 5.3.2   | Step 2: Huang-Minlon modification to the Wolff-Kishner<br>reduction. . . . .                | 139 |
| 5.3.3   | Step 3: Friedel-Crafts acylation. . . . .   | 140 |
| 5.3.4   | Step 4: Huang-Minlon reduction of 2-(3'-<br>carbmethoxypropanoyl)-5-alkylthiophene. . . . . | 143 |
| 5.4     | Preparation of compounds 3 . . . . .  | 147 |
| 5.4.1   | Step 1: esterification of thiophene-2-ethanoic acid. . . . .                                | 147 |
| 5.4.2   | Step 2: Friedel-Crafts acylation. . . . .   | 147 |
| 5.4.3   | Step 3: Huang-Minlon reduction of 2-(2'-carbmethoxyethyl)-5-<br>alkanoyl-thiophene. . . . . | 148 |
| 5.5     | Synthesis of 2-nitrothiophene-5-ethanoic acid . . . . .                                     | 149 |
| 5.5.1   | Nitration of thiophene-2-ethanoic acid . . . . .  | 150 |
| 5.5.2   | Nitration of 2'-(2-carbmethoxyethyl)-thiophene. . . . .                                     | 150 |
| 5.5.2.1 | Saponification of 2'-(2-carbmethoxyethyl)-5-<br>nitrothiophene. . . . .                     | 150 |
| 5.6     | Chloromethylation of nitrothiophene . . . . .   | 151 |
| 5.7     | Preparation of 2-acetylamidothiophene . . . . .   | 151 |
| 5.7.1   | Method 1 . . . . .  | 151 |
| 5.7.1.1 | Preparation of methyl 2-aminothiophene-3-<br>carboxylate. . . . .                           | 151 |
| 5.7.1.2 | Preparation of methyl 2-acetylamidothiophene-3-<br>carboxylate. . . . .                     | 152 |
| 5.7.1.3 | Preparation of 2-acetylamidothiophene-3-<br>carboxylic acid. . . . .                        | 152 |
| 5.7.1.4 | Decarboxylation of 2-acetylamidothiophene-3-<br>carboxylic acid. . . . .                    | 153 |
| 5.7.2   | Method 2: The Beckmann rearrangement. . . . .   | 153 |
| 5.7.2.1 | Preparation of 2-acetylthiophene oxime. . . . .   | 153 |
| 5.7.2.2 | Beckmann rearrangement. . . . .   | 154 |
| 5.7.3   | Method 3: The reductive acetylation of 2-nitrothiophene. . . . .                            | 154 |
| 5.7.3.1 | Nitration of thiophene. . . . .   | 154 |
| 5.7.3.2 | Reductive acetylation of 2-nitrothiophene. . . . .  | 158 |
| 5.8     | Preparation of N-alkylated 2-acetamidothiophene. . . . .                                    | 158 |
| 5.9     | Formylation of N-alkyl-2-acetamidothiophene. . . . .  | 161 |
| 5.10    | Synthesis of the triphenylphosphine salt of 4-nitrobenzylbromide . . . . .                  | 163 |
| 5.11    | Wittig Reaction . . . . .   | 163 |
| 5.12    | LANGMUIR-BLODGETT FILM EXPERIMENTAL . . . . .   | 166 |

|   |     |
|---|-----|
| 5.12.1 Monolayer spreading. . . . .               | 166 |
| 5.12.2 Pressure-area isotherms. . . . .           | 167 |
| 5.12.3 Monolayer Stability Studies. . . . .       | 172 |
| 5.12.4 Monolayer mobility. . . . .                | 173 |
| 5.12.5 Langmuir-Blodgett Film Deposition. . . . . | 174 |
| 5.12.6 Second Harmonic Generation. . . . .        | 175 |
| CONCLUSIONS . . . . .                             | 176 |
| REFERENCES . . . . .                              | 180 |

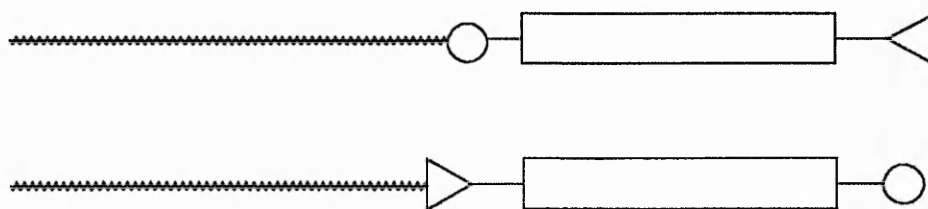
## ABBREVIATIONS

|     |                   |   |                                 |
|-----|-------------------|---|---------------------------------|
| R:- | (a)               | = | i-C <sub>3</sub> H <sub>7</sub> |
|     | (b)               | = | n-C <sub>3</sub> H <sub>7</sub> |
|     | (c)               | = | C <sub>5</sub> H <sub>11</sub>  |
|     | (d)               | = | C <sub>6</sub> H <sub>13</sub>  |
|     | (e)               | = | C <sub>7</sub> H <sub>15</sub>  |
|     | (f)               | = | C <sub>9</sub> H <sub>19</sub>  |
|     | (g)               | = | C <sub>13</sub> H <sub>27</sub> |
|     | (h)               | = | C <sub>15</sub> H <sub>31</sub> |
|     | (i)               | = | C <sub>16</sub> H <sub>33</sub> |
|     | (j)               | = | C <sub>17</sub> H <sub>35</sub> |
|     | (k)               | = | C <sub>21</sub> H <sub>43</sub> |
|     | g                 | = | grammes                         |
|     | ml                | = | millilitres                     |
|     | mm                | = | millimetres                     |
|     | ppm               | = | parts per million               |
|     | NMR               | = | nuclear magnetic resonance      |
|     | DMSO              | = | deuterated dimethylsulphoxide   |
|     | CDCl <sub>3</sub> | = | deuterated chloroform           |
|     | def               | = | deformation                     |
|     | str               | = | stretch                         |
|     | w                 | = | weak                            |
|     | m                 | = | medium                          |
|     | st                | = | strong                          |
|     | b                 | = | broad                           |
|     | s                 | = | singlet                         |
|     | d                 | = | doublet                         |
|     | t                 | = | triplet                         |
|     | q                 | = | quartet                         |
|     | mult              | = | multiplet                       |

# Introduction

## 1.0 INTRODUCTION.

In recent years there has been great interest in organic materials that exhibit large non-linear optical coefficients, often considerably greater than those displayed by 'conventional' inorganic dielectrics such as lithium niobate or potassium dihydrogen phosphate<sup>(1)</sup>. The tendency of organic molecules to crystallize centrosymmetrically means that any inherent second-order molecular non-linearity rarely manifests itself at the macroscopic level because of the cancelling of the contributions made by each individual molecule. The Langmuir-Blodgett technique is an elegant method of assembling amphiphilic organic molecules into layers of a well-defined thickness and alignment<sup>(2)</sup>; furthermore, non-centrosymmetric structures can be generated, providing a means to exploit the non-linear optical properties of the individual molecules. This may be achieved in several ways: first, and probably the least satisfactory, is deposition by the X or Z modes (see chapter 3). This is the easiest method to use if a compound and conditions can be found such that deposition does occur in one of these modes; however, whether or not these deposition modes are possible cannot be predicted from the structure of the molecules alone. The second method is to employ an alternate layer structure in which the active molecule layer is spaced by an inert layer of fatty acid<sup>(3-4)</sup>. One major drawback is that the non-linear optical response is likely to be diluted. The final method is to use two different types of active molecules in which the donor and acceptor groups have been transposed (see Fig. 1.1). In this system the non-linear effects should at least be additive; however, in certain cases these have shown a greater than expected result<sup>(5)</sup>.



~~~~~ long alkyl chain.

□ extended region of conjugation.

△ acceptor group.

○ donor group.

**Figure 1.1** Schematic diagram of the two types of active molecules which are amphiphilic in nature.

Criteria for materials to be used to fabricate Langmuir-Blodgett films are:

1. They must be amphiphilic in nature (ie contain both a hydrophilic 'head' group and a hydrophobic 'tail' group).
2. This 'tail' must be of sufficient length to increase the hydrophobic nature of the molecule to make it insoluble in the subphase.

The additional features that have to be included to produce second-order non-linear optical effects are:

3. An extended region of conjugation (this region of conjugation can be any system of alternating multiple and single bonds).
4. Donor and acceptor groups positioned at either end of the region of  $\pi$ -conjugation (the selection criteria for the donor and acceptor groups are given later, in chapter 2).

The aims of this project were to design, synthesise and subsequently systematically characterise several members of three homologous series of novel thiophene based compounds which were amphiphilic in nature (criteria 1 and 2 above). The characterisation of the films involved the production of isotherms that were produced under subphase conditions that were varied systematically; subsequently the area per molecule, decay rate of the film on the subphase surface, transfer ratio of the film to a substrate and the mode of transfer were determined. This was extended to systematically investigate the effect on monolayer stability and transferability of introducing a thiophene moiety at various positions in the alkyl side chain of carboxylic acids such as stearic acid.

The project then progressed to the design of novel thiophene based molecules that would exhibit second harmonic generation using all the criteria outlined above.

These were synthesised and then subjected to the same systematic investigation of their LB characteristics as in the earlier series. This screening was extended to include an investigation of the characteristics of heterogeneous films incorporating various percentages of arachidic acid. The monolayer formation on the subphase and subsequent transfer to a substrate has been found to be not very good for some of these materials. Mixed monolayers of the active molecule and an inert fatty acid were employed in order to remedy this. This might be expected to dilute the non-linear optical response; however, it has been noted that in certain mixture ratios the non-linear response has been enhanced and been found to be greater than that of the pure monolayer<sup>(6)</sup>. These films when transferred to a substrate adopt a Y-type mode of deposition, so in order to exploit any second-order non-linear properties alternate layer structures were manufactured. Preliminary second harmonic generation experiments were then performed in collaboration with a group at Durham University.

Thiophene was chosen to be the basic central aromatic moiety in the synthesis of the novel amphiphilic compounds because it is very similar in reactions and structure to benzene and should behave similarly to benzene. There have been many Langmuir-Blodgett non-linear optical materials containing benzene. Thiophene, however, is not a totally symmetrical molecule, and therefore possesses a dipole moment. Thiophene is also a  $\pi$ -excessive aromatic compound (ie it has a greater electron density per carbon atom in the ring than benzene). The delocalisation energy of thiophene is lower than that of benzene and therefore its substitution in donor-acceptor compounds should be expected to result in enhanced charge transfer properties and nonlinear responses over benzenoid ring systems.

A general introduction to non-linear effects, their origins, classification, and



applications is given in chapter 2. Furthermore, a comparison of materials that exhibit significant second-order non-linearities is presented, with some guidelines for the synthesis of highly efficient materials. Langmuir-Blodgett film technology is reviewed in chapter 3. A brief account of the structure and relevant chemistry of thiophene is given in chapter 4, followed by an in depth discussion of the experimental results. Chapter 5 details the experimental chemistry employed in this research. Chapter 6 gives an account of Langmuir-Blodgett experimental work followed by a discussion of the findings; it also contains a discussion of some preliminary non-linear second-harmonic generation experiments. There are also two energy minimised structure diagrams of compound 54k produced using the computer molecular modelling package Chem-X and some Atomic Force Microscope images of a monolayer of compound 54k on silicon. The final chapter is a summary of the conclusions drawn in this thesis and some suggestions for possible further work.

Non-Linear

Optical Effects

## 2.0 NON-LINEAR OPTICAL EFFECTS.

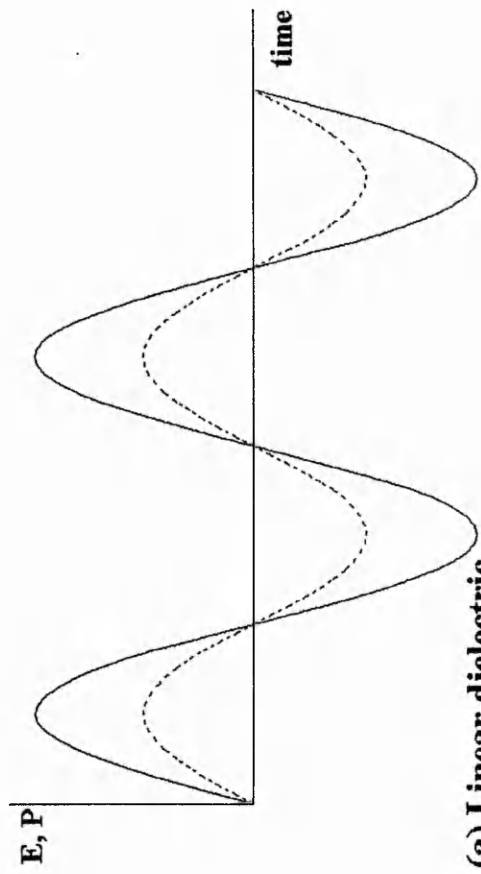
### 2.1 Introduction

This chapter is concerned with a general discussion of non-linear optical effects and materials. Following a brief introduction, in which the roots of non-linear behaviour in electromagnetic theory are examined, together with the technological progress that has made such effects significant, the physical origins of non-linearity are discussed. The various non-linear optical phenomena are then classified according to the order of polarization field associated with them. Sections 2.3 and 2.4 detail the molecular and structural features required for an organic material to display highly non-linear behaviour and explains how they can be obtained in practice. Section 2.5 gives a comparison of the organic and inorganic materials in current use. Finally, section 2.6 deals with the applications of non-linear optical phenomena.

### 2.2 Origin and Classification of Non-Linear Optical Effects.

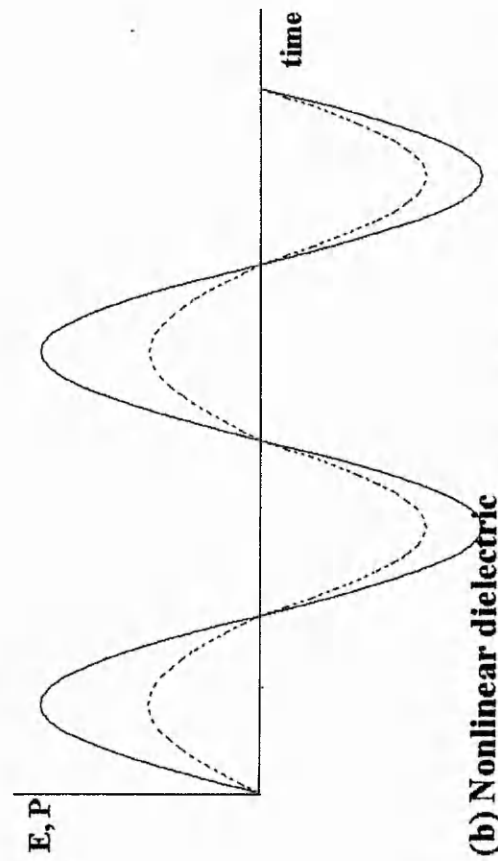
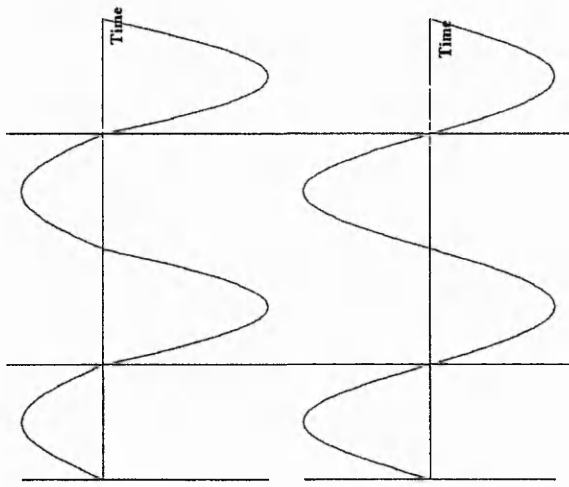
Advances in non-linear optics have relied heavily on the development of Q-spoiled lasers<sup>(7)</sup>. Such lasers have outputs consisting of a series of intense coherent pulses. These are typically 30-100 ns long, and the power density is about a few MW cm<sup>-2</sup>. For a power density of 1 MW cm<sup>-2</sup>, the peak electric field strength in a pulse is  $E_1 \sim 30 \text{ kV cm}^{-1}$ , a figure that is still very small when compared to typical atomic field strengths:  $E_a \sim 3 \times 10^5 \text{ kV cm}^{-1}$ . However, under ideal conditions the characteristic length for significant second harmonic generation (SHG) or parametric amplification is<sup>(7)</sup>  $L \sim \lambda E_a/E_1$ : where  $\lambda \sim 10^{-4} \text{ cm}$  is the wavelength of the light. Thus  $L \sim 1 \text{ cm}$  for a power density of 1 MW cm<sup>-2</sup>, and since much higher power densities than this can be achieved either by focusing the pulse with a lens system or by amplifying it with a

laser amplifier it is now possible to achieve significant non-linear optical effects in samples of suitable materials with dimensions significantly smaller than a centimetre.



Optical  
Polarisation

Fundamental  
Polarisation



Second-  
Harmonic  
Polarisation

Steady d. c.  
Polarisation

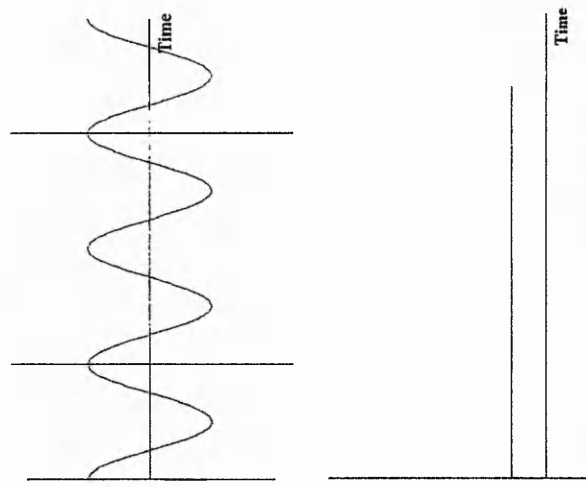


**Figure 2.2** Polarisation resulting from an applied sinusoidal electric

field. \_\_\_\_\_ Optical Field (E), - - - - - Polarisation (P).

**Figure 2.3** Components of the non-

linear polarisation wave of Fig 2.2(b).

### 2.2.2 Linear Polarisation: $P^{(1)} = \epsilon_0 \chi^{(1)} E$

The linear polarisation is responsible for refraction and attenuation. When the applied optical field is a wave with frequency  $\omega$ , the linear polarisation also has frequency  $\omega$ , radiating into the medium and modifying the way in which the wave propagates.

The electric flux density,  $D$  is given by

$$D = \epsilon_0 E + P^{(1)} = \epsilon_0 \epsilon_r E \quad (2.2)$$

where  $\epsilon_r$  is the dielectric constant. It therefore follows that  $\epsilon_r = 1 + \chi^{(1)}$ . Now, the refractive index,  $n$ , is given by:

$$n = \frac{c}{v} = \left( \frac{\epsilon \mu}{\epsilon_0 \mu_0} \right)^{\frac{1}{2}} = (\epsilon_r \mu_r)^{\frac{1}{2}} \quad (2.3)$$

where  $v$  and  $c$  are the velocities of light in the medium and in a vacuum, respectively.

If a relative permeability ( $\mu_r$ ) of unity is assumed then the refractive index will be  $(1 + \chi^{(1)})^{\frac{1}{2}}$  and the propagation constant,  $k$ , is  $(1 + \chi^{(1)})^{\frac{1}{2}} \omega/c$ . In practice  $\chi^{(1)}$  is a complex quantity and the components of  $P^{(1)}$  in quadrature with the field results in losses and therefore attenuation.

When the optical field contains several waves at different frequencies, they propagate independently of one another in the linear regime.

### 2.2.3 Quadratic Polarisation: $P^{(2)} = \epsilon_0 \chi^{(2)} E E$

The effects arising from the quadratic polarisation are all mixing phenomena, involving the generation of sum and difference frequencies, but they take a variety of forms.

- (i) When the applied optical field contains one frequency, a Fourier analysis of the non-linear polarization wave shows that it contains an

average (dc) term and a term oscillating at twice the applied frequency. This can readily be seen for a light wave of the form  $E = E_0 \sin \omega t$ , giving a quadratic polarization of the form:

$$P^{(2)} = \epsilon_0 \chi^{(2)} E_0^2 \sin^2 \omega t \quad (2.4)$$

This can be rewritten as

$$P^{(2)} = \frac{\epsilon_0 \chi^{(2)}}{2} E_0^2 (1 - \cos 2\omega t) \quad (2.5)$$

The dc polarization produces a dc electric field in the medium (optical rectification), and the polarization at twice the applied frequency radiates into the medium (second harmonic generation).

- (ii) When the optical field contains two frequencies, a new range of effects occurs.
  - (a) The simplest case is where one frequency is zero (a monochromatic wave propagated through the medium in the presence of a dc electric field).  $P^{(2)}$  then contains a term that is proportional to the product of the dc and optical fields. This leads to an extra term in the total polarization that is linear in the optical field whose size is proportional to the dc field. The effect of this extra term on the optical wave is equivalent to changing  $\chi^{(1)}$  by a shunt proportional to the dc field; this is the linear electro-optic or Pockels effect.
  - (b) If a small optical signal (frequency  $\omega_s$ ) is propagated through the medium in the presence of a powerful 'pump' optical field (at a higher frequency  $\omega_p$ ) an extra term in the total polarisation which is linear in the signal field and whose effect on the latter is equivalent to changing

$\chi^{(1)}$  by an amount proportional to the pump intensity. Therefore, the propagation constant at the signal frequency depends on the pump intensity. This effect is called parametric interaction because the pump field may be regarded as modulating the parameter  $\chi^{(1)}$  at the pump frequency.

#### 2.2.4 Cubic Polarisation: $P^{(3)} = \epsilon_0 \chi^{(3)} E E E$

For a monochromatic wave of the form  $E = E_0 \sin \omega t$  we have

$$P^{(3)} = \epsilon_0 \chi^{(3)} E_0^3 \sin^3 \omega t \quad (2.6)$$

$$P^{(3)} = \frac{\epsilon_0 \chi^{(3)}}{4} E_0^3 (3 \sin \omega t - \sin 3\omega t) \quad (2.7)$$

Thus, the cubic polarization produces third harmonic generation and related mixing phenomena. An example of such a phenomenon is the change in refractive index that occurs when a monochromatic wave propagates through the medium in the presence of a dc field. This change is proportional to the square of the dc field and is the quadratic electro-optic or Kerr effect frequently used in the electronic shutter in Q-spoiled lasers.

Also the low frequency, essentially classical, mixing phenomena,  $P^{(3)}$  also produces some quantal effects that arise for certain frequency combinations when a small signal wave of frequency  $\omega_s$  propagates through the medium in the presence of a strong pump wave at frequency  $\omega_p$ . If  $\omega_s$  and  $\omega_p$  are selected such that  $\omega_p + \omega_s = \omega_i$ , where  $\omega_i$  is some transition frequency of the medium, then the transition can take place through the simultaneous absorption of a pump and a signal photon. This process



of two-photon absorption produces signal attenuation although the signal frequency itself is not equal to a transition frequency of the medium, unlike one-photon absorption processes that arise from  $\chi^{(1)}$  and disappear when  $\omega_s \neq \omega_i$ . Conversely, if  $\omega_s$  and  $\omega_p$  are chosen such that  $\omega_p - \omega_s = \omega_i$ , then the transition can take place by the simultaneous absorption of a pump photon and emission of a signal photon, resulting in signal amplification. In this stimulated Raman effect the signal field stimulates the emission of signal photons, unlike the incoherent Raman effect where the transitions are spontaneous. The two-photon effects both arise from the term in  $P^{(3)}$  that is proportional to the product of the signal field and pump intensity. The effect of this term on the signal wave is equivalent to changing  $\chi^{(1)}$  by an amount proportional to the pump intensity, the propagation constant at the signal frequency being similarly modified.

### 2.3 Optimization of Molecular Structure

This section is devoted to the molecular engineering required to optimize  $\beta$  for a molecule and neglects any additional constraints arising from crystal structure considerations.

The dipole moment of a molecule is defined by Eqn 2.8:

$$\underline{\mu} = e \underline{l} \quad (2.8)$$

where  $e$  is the magnitude of the charge separated by the vectorial distance  $\underline{l}$ . A large value of  $\Delta\mu$  is desirable for non-linear effects, and since molecules with large ground state dipole moments tend to have correspondingly large excited state dipole moments, the treatment of ground state dipoles is usually sufficient. In aliphatic systems the dipole moments are usually small and the  $\beta$  values correspondingly low. However, large dipole moments can result from partial charge transfer between donor and

acceptor groups terminating a conjugated chain, and molecules possessing these features exhibit very large optical non-linearities. The major polarisable medium in these materials is the  $\pi$ -electron system, and the origin of the non-linear behaviour lies in the excited  $\pi$ -electron states, particularly those possessing large charge correlations<sup>(11)</sup>.

It is often convenient to split the contributions to the molecular (hyper)polarizabilities into those made by the length,  $L$ , of the conjugated system, and those arising from the substituent perturbations on it. It is well known that  $\alpha \propto L^3$ , and theory predicts<sup>(12)</sup> that  $\beta \propto L^3$  and  $\gamma \propto L^5$ . More qualitative relationships between conjugation length and  $\beta$  have been found; for example, the  $\beta$  values for substituted stilbenes are consistently an order of magnitude larger than those for comparably substituted benzene analogues. It is interesting to note that conjugated systems can be either one dimensional (as in the case of polyenes) or two dimensional (as formed by benzene-type hexagonal rings) but not three dimensional, since the conjugation arises from the electrons in the p-orbitals which are not participating in sp hybridization to form the skeleton of the saturated bonds and so cannot be present if all four electrons are involved in four different bonding directions. The optical properties of two dimensional conjugated systems will be very different across the plane compared to parallel to it.

There have been several models proposed to explain the enhanced optical non-linearities of polarized conjugated molecules; in one such model Oudar and Chemla relate the  $\beta$  of a molecule to an equivalent electric field due to the substituents which biases the hyperpolarizabilities<sup>(13)</sup>. The  $\pi$ -electron contribution to  $\beta$  is the dominant effect in a series of monosubstituted aromatic molecules. When both donor and

acceptor groups are present simultaneously and are spaced by a conjugated system, their effects are superadditive due to the phenomenon of charge transfer which involves the entire disubstituted molecule; the contribution of this effect to the optical non-linearity can be quantified<sup>(14)</sup>. Quantum mechanical models for  $\beta$  have been described by various authors<sup>(15)</sup>.

In order for a material to be of practical use for second harmonic generation it must be closely matched to the laser it is to double; the absorption edge should be near the wavelength of the second harmonic but must not include it<sup>(12)</sup>. Now, as the length of conjugation is increased there is a gradual bathochromic shift in the absorption edge (from 200nm in ethylene to a maximum in the range of 600-700nm for an infinite series of double bonds), and the addition of donor and acceptor substituents produces a further dramatic bathochromic shift as a result of stabilization due to the mixing of nonbonded and charge transfer states<sup>(16)</sup>. Thus there has to be a trade off between transparency and efficiency when selecting the appropriate donor and acceptor groups and conjugated systems for a material destined to be used as a frequency doubler.

In order to select the best combinations of donors and acceptors one must consider the relative strengths of the range of available groups. An approximate measure of donor strength is given by the first ionization potential of a simple, nonconjugated molecule containing the relevant group, since this represents the ease with which it releases electrons. Any atom possessing lone pair electrons in a high energy orbital, such as oxygen, nitrogen and sulphur, can act as an electron donor, provided that this lone pair is available for efficient overlap with the  $\pi$ -electron system of the chromophore. Table 2.1 gives the ionization potentials of the most frequently

encountered neutral groupings containing these atoms<sup>(17)</sup>. From this table it can be seen that electron donating ability depends not only on the heteroatom concerned, but also on the nature of the substituents attached to it (for example, electron withdrawing groups will decrease the overall strength of the donor). Imparting a negative charge to the atom, as in  $-O^-$ ,  $-S^-$ , and  $-NR^-$ , for example by deprotonation, can greatly enhance the donor strength of a particular group.

The effectiveness of acceptor groups tends to be more variable than is the case with donor groups, and the nature of the rest of the chromophore can have an important influence. Simple acceptor groups contain at least two multiple bonded atoms, and the terminal atoms of such groupings are always more electronegative than carbon. The Hammett para  $\sigma^-$  constant for a group gives an indication of acceptor strength, and values of this quantity for some typical acceptors are given in table 2.2<sup>(17)</sup>.

**Table 2.1**

Relative effectiveness and ionization potentials for some typical electron donor groups<sup>(17)</sup>.

| <b>Donor Group, X</b> | <b>Ionization Potential of CH<sub>3</sub>X (eV)</b> | <b>Relative Effectiveness</b>                                     |
|-----------------------|-----------------------------------------------------|-------------------------------------------------------------------|
| -OAc                  | 11.0                                                | Least effective<br><br><br><br><br><br><br><br><br>Most effective |
| -OH                   | 10.8                                                |                                                                   |
| -NHAc                 | 10.2                                                |                                                                   |
| -OMe                  | 10.0                                                |                                                                   |
| -SH                   | 9.4                                                 |                                                                   |
| -NH <sub>2</sub>      | 9.0                                                 |                                                                   |
| -SMe                  | 8.7                                                 |                                                                   |
| -NHMe                 | 8.2                                                 |                                                                   |
| -NMe <sub>2</sub>     | 7.9                                                 |                                                                   |

**Table 2.2**

Relative effectiveness and Hammett para  $\sigma$ -constants for some typical electron acceptor groups<sup>(17)</sup>.

| Acceptor Group                   | $\sigma$ -para | Relative Effectiveness                                                            |
|----------------------------------|----------------|-----------------------------------------------------------------------------------|
| -CO <sub>2</sub>                 | 0.0            | Least effective<br><br><br><br><br><br><br><br><br><br><br><br><br>Most effective |
| -NO                              | 0.12           |                                                                                   |
| -CHO                             | 0.36           |                                                                                   |
| -CONH <sub>2</sub>               | 0.36           |                                                                                   |
| -CO <sub>2</sub> Me              | 0.39           |                                                                                   |
| -CO <sub>2</sub> H               | 0.41           |                                                                                   |
| -SOMe                            | 0.49           |                                                                                   |
| -COMe                            | 0.50           |                                                                                   |
| -CN                              | 0.66           |                                                                                   |
| -SOCF <sub>3</sub>               | 0.69           |                                                                                   |
| -SO <sub>2</sub> Me              | 0.72           |                                                                                   |
| -NO <sub>2</sub>                 | 0.78           |                                                                                   |
| -SO <sub>2</sub> CF <sub>3</sub> | 0.93           |                                                                                   |

## 2.4 Crystal Structure Considerations

In section 2.2.1 it was pointed out that only noncentrosymmetric crystals have finite second-order susceptibilities; this is because the  $\beta$ -tensors of the constituent molecules are orientationally averaged to zero in random media or centrosymmetric crystals. Even noncentrosymmetric crystals usually do not take full advantage of the intrinsic non-linearities of their constituent molecules, due to non ideal packing arrangements. The molecular parameters that decide crystal structure are very subtle and mutually interactive, which makes them extremely difficult to separate. Thus, it is very difficult to predict the crystal structure solely from the molecular structure. Apparently very slight changes to a molecule can result in drastic changes in the bulk packing and consequently in huge differences in non-linear efficiencies.

The crystal structure of organic materials is influenced by a variety of factors, such as molecular shape (close-packing principle), van der Waal's forces, hydrogen bonding (if present) and multipolar interactions. These forces are all associated with much smaller energies than those involved with intramolecular bonding. Dipolar interaction energies are proportional to the square of the ground state dipole moment and are dependent on the crystal space group. The dipole energy contribution to the total intramolecular binding energy in a crystal varies slowly with structural parameters, and will not bring structures out of a position of minimum energy resulting from van der Waal's interaction in a close-packed situation<sup>(18)</sup>. However, molecules designed to have large  $\beta$  tensors are atypical in that they often have very large ground state dipole moments, so that dipolar interactions tend to favour centrosymmetric crystal structures in which the dipoles are opposed or at least brought out of net alignment. One possible way of overcoming this undesirable influence is

by the incorporation of hydrogen bonding groups into the molecules. The energies associated with hydrogen bonding are comparable with those of the dipolar forces, so that the presence of such bonding could help to cause a favourable molecular orientation.

One way of guaranteeing a finite  $\chi^{(2)}$  is to use pure enantiomers, which must crystallize non-centrosymmetrically. However, in practice great differences in efficiency are found between related optically active compounds, and such complications as racemization, optical purity and resolution, which occur in the synthesis of such materials, must be dealt with.

Apart from the enantiomeric ones, only 10 of the 32 classes of crystallographic point groups that organic materials can adopt are suitable for such phenomena as second harmonic generation, and most compounds adopt centrosymmetric point groups<sup>(12)</sup>. In addition, the choice of molecular orientations is further limited by the fact that most materials that do adopt useful crystal point groups belong to either of only two space groups. This produces a severe statistical constraint on the number of single crystal organic materials likely to have a useful  $\chi^{(2)}$ . Another fact to consider is that for a crystal to be of use in non-linear optics it must be capable of being grown to a high degree of perfection.

Further complications arise when single crystals are used for optical mixing, since it is necessary for the interacting waves to have their phases matched. For example, a prerequisite for efficient second harmonic generation is that  $k^{(2\omega)}=2k^{(\omega)}$ , or equivalently  $n^{(2\omega)}=n^{(\omega)}$ . If this condition is not met, then the second-harmonic power generated at some plane, say  $Z_1$ , having propagated to another plane ( $Z_2$ ), is not in phase with the second-harmonic wave generated at  $Z_2$ , and interference will result. For



normally dispersive materials  $n$  increases with  $\omega$  and so  $n^{(2\omega)} \neq n^{(\omega)}$ . However, in crystals that are naturally birefringent the refractive indices in the ordinary and extraordinary directions are not equal at a given  $\omega$ , so that by a technique known as 'angle phase matching' the fundamental and second harmonic can be propagated in such directions that now  $n^{(2\omega)} = n^{(\omega)}$ . Quasi-phase-matching techniques can be used with materials that are isotropic or are inadequately birefringent; however, in practice these tend to be difficult to carry out and offer only low conversion efficiencies<sup>(19)</sup>.

### **2.5 Use of the Principles for the Optimization of Non-Linear Response.**

A few examples of organic non-linear optical materials that have been produced following the consideration of the criteria detailed in the previous two sections will now be described. Many of these principles can be extended to thin films of organic materials, and their fabrication into wave-guiding structures can help to overcome such problems as phase matching.

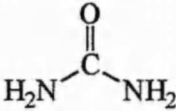
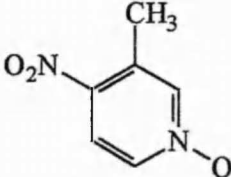

Table 2.3 summarizes most of the single crystal organic non-linear materials that have appeared in the literature<sup>(12,20,21)</sup>. The relative efficiencies refer to second harmonic generation (SHG) experiments performed on powdered samples using the Kurtz technique; the values are only semi-quantitative because powder efficiency depends on particle size distribution, among other factors. Where  $\beta$  values are available, they are also given in the table. Urea has been chosen as a reference because it has non-linear properties that are comparable to the best inorganic materials<sup>(22)</sup>; the difficulty in growing large high quality crystals is its only drawback.

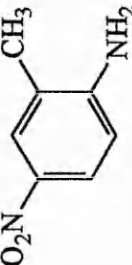
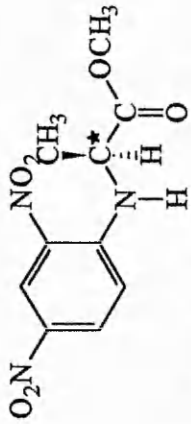
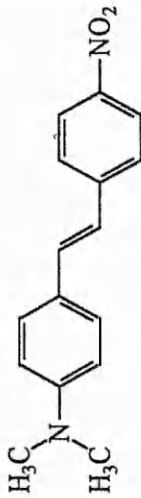
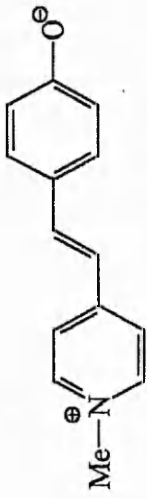
Compounds (B-F) have received extensive treatment in the past. They all possess donor and acceptor groups linked by a conjugated system, and consequently have quite large values of  $\beta$ ; this is particularly noticeable in (F), in which the

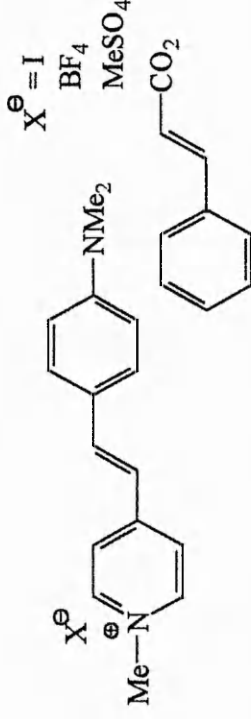
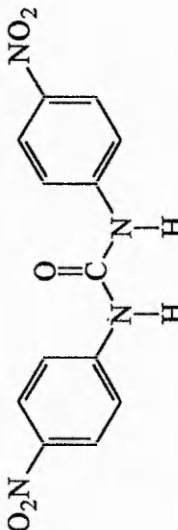
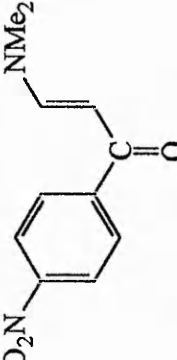
conjugation length is greatest. However, (F), like *para*-nitroaniline (C), crystallizes with a centrosymmetric structure and thus does not display SHG. Addition of a methyl group to *para*-nitroaniline to form MNA<sup>(22)</sup> (D), which has a significant powder efficiency, is an example of how the introduction of an extra substituent can alter the crystal structure.

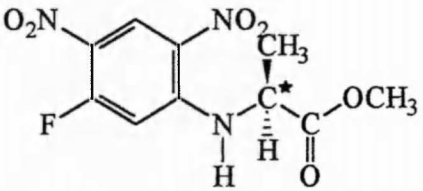
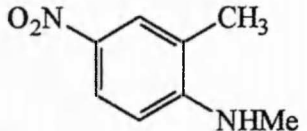
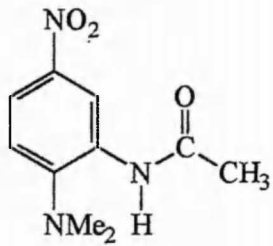
**Table 2.3**

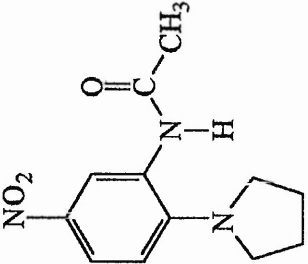
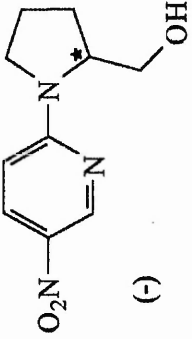
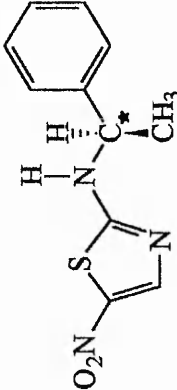
Organic non-linear materials in the literature. Bracketed efficiency factors apply to crystallographically optimal materials<sup>(12,20,22)</sup>.

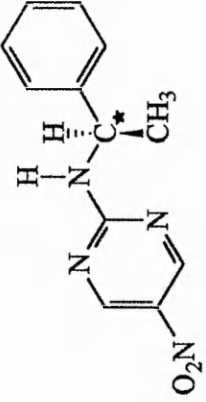
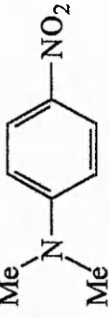
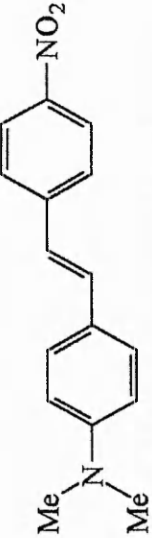
| Ref. No. | Structure.                                                                                                                  | $\beta(10^{-50}\text{C}^3\text{m}^3\text{J}^2)$ | Eff<br>(x urea) |
|----------|-----------------------------------------------------------------------------------------------------------------------------|-------------------------------------------------|-----------------|
| A        | <br>Urea                                   | 0.17                                            | 1.0 [x2.5]      |
| B        | <br>3-methyl-4-nitropyridine-N-oxide (POM) | 2                                               | 13 [x4]         |
| C        | <br>4-nitroaniline (p-NA)                | 13                                              | 0.0             |

|   |                                                                                                                                                            |     |           |
|---|------------------------------------------------------------------------------------------------------------------------------------------------------------|-----|-----------|
| D |  <p>2-methyl-4-nitroaniline (MNA)</p>                                   | 16  | 22 [x3.5] |
| E |  <p>methyl-2-(2',4'-dinitrophenyl)-aminopropanoate (MAP)</p>            | 82  | 10 [x6.7] |
| F |  <p>N,N-dimethylamino-4'-nitrostilbene</p>                               | 170 | 0.0       |
| G |  <p>E-1-(4'-phenoxy)-2-(4'-N-methylpyridinium) ethene (merocyanine)</p> | 370 | 0.0       |

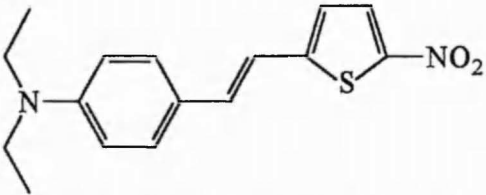
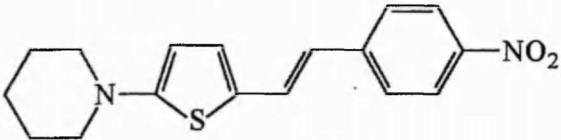
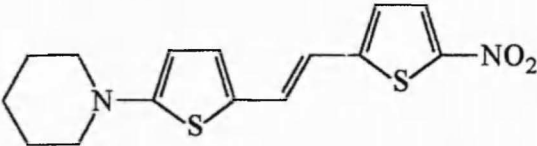
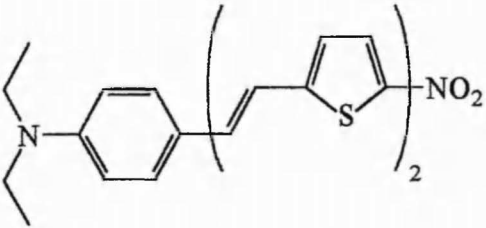
| Ref No. | Structure                                                                                                                                                                                                     | Eff<br>(x Urea)         |
|---------|---------------------------------------------------------------------------------------------------------------------------------------------------------------------------------------------------------------|-------------------------|
| H       |  <p data-bbox="589 493 626 1627">E-1-(4'-dimethylaminophenyl)-2-(4'-N-methylpyridium) ethene (styrylpyridinium cyanine)</p> | 0<br>~83<br>~250<br>~13 |
| I       |  <p data-bbox="866 829 902 1291">N,N'-bis(4'-nitrophenyl)urea (DNPU)</p>                                                    | 8.8                     |
| J       |  <p data-bbox="1142 703 1179 1417">2-dimethylaminovinyl-4-nitrophenyl ketone (DMA-NAP)</p>                                 | 7.5                     |

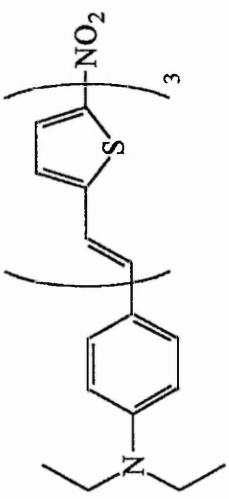
|   |                                                                                                                                                                                     |     |
|---|-------------------------------------------------------------------------------------------------------------------------------------------------------------------------------------|-----|
| K |  <p style="text-align: center;"><b>methyl 2-(2,4'-dinitro-5'-fluorophenyl)aminopropanoate</b></p> | 21  |
| L |  <p style="text-align: center;"><b>2-methyl-4-nitro-methylaniline (MNMA)</b></p>                  | 80  |
| M |  <p style="text-align: center;"><b>2-N,N-dimethylamino-5-nitroacetanilide (DAN)</b></p>           | 115 |

|   |                                                                                                                                                                                                               |     |
|---|---------------------------------------------------------------------------------------------------------------------------------------------------------------------------------------------------------------|-----|
| N |  <p style="text-align: center;"><b>2-N-pyrrolidino-5-nitroacetamide (PAN)</b></p>                                           | 80  |
| O |  <p style="text-align: center;"><b>(-)</b></p> <p style="text-align: center;"><b>2-N-prolinol-5-nitropyridine (PNP)</b></p> | 160 |
| P |                                                                                                                            | 8   |

|         |                                                                                                                             |                                                                  |
|---------|-----------------------------------------------------------------------------------------------------------------------------|------------------------------------------------------------------|
| Q       |                                           | 4                                                                |
| Ref No. | Structure                                                                                                                   | $\beta\mu$<br>( $10^{-6}$ esu) at<br>$\lambda=1.907 \mu\text{m}$ |
| R       |  <p>N,N-dimethyl-4-nitroaniline</p>       | 110 <sup>(21)</sup>                                              |
| F       |  <p>N,N-dimethylamino-4-nitrostilbene</p> | 580 <sup>(21)</sup>                                              |



|   |                                                                                                                                                       |                      |
|---|-------------------------------------------------------------------------------------------------------------------------------------------------------|----------------------|
| S |  <p>1-(N,N-diethylamino-4'-phenyl)-2-(5''-nitrothienyl) ethene</p>  | 600 <sup>(21)</sup>  |
| T |  <p>1-(5'-cyclohexylaminothienyl)-2-(4''nitrophenyl) ethene</p>     | 660 <sup>(21)</sup>  |
| U |  <p>1-(5'-cyclohexylaminothienyl)-2-(5''-nitrothienyl) ethene</p>   | 1040 <sup>(21)</sup> |
| V |  <p>1-(N,N-diethylamino-4'-phenyl)-2-(5''-nitrothienyl) ethene</p> | 1400 <sup>(21)</sup> |

|   |                                                                                                                                                                                                                                                                                                                                                                                                                                                                                                                                                                                                                                                                                                                                                         |                      |
|---|---------------------------------------------------------------------------------------------------------------------------------------------------------------------------------------------------------------------------------------------------------------------------------------------------------------------------------------------------------------------------------------------------------------------------------------------------------------------------------------------------------------------------------------------------------------------------------------------------------------------------------------------------------------------------------------------------------------------------------------------------------|----------------------|
| W |  <p>The chemical structure shows a copolymer chain with two repeating units. The first unit is a diethylamino styrene unit, represented as a benzene ring with a para-substituted diethylamino group (-N(CH<sub>2</sub>CH<sub>3</sub>)<sub>2</sub>) and a vinyl group (-CH=CH<sub>2</sub>) attached to the same carbon. The second unit is a 2-nitrothiophene unit, represented as a thiophene ring with a nitro group (-NO<sub>2</sub>) at the 2-position and a vinyl group (-CH=CH<sub>2</sub>) at the 5-position. The units are connected by a backbone of alternating single and double bonds, with a subscript '3' indicating the number of repeating units.</p> | 2100 <sup>(21)</sup> |
|---|---------------------------------------------------------------------------------------------------------------------------------------------------------------------------------------------------------------------------------------------------------------------------------------------------------------------------------------------------------------------------------------------------------------------------------------------------------------------------------------------------------------------------------------------------------------------------------------------------------------------------------------------------------------------------------------------------------------------------------------------------------|----------------------|

The asymmetrical addition of bulky substituents results in molecules that are less geometrically simple, and such changes can mean that the dipolar forces that favour antiparallel alignment are overcome to satisfy the general requirement for dense molecular packing. MAP (E) presents a further example of this principle<sup>(22,23)</sup>, with the influence of chirality also playing a part in the production of a non-centrosymmetric crystal structure.

The large  $\beta$  value of the merocyanine (G) shows how the presence of a charge can enhance the strengths of donors and acceptors, but unfortunately it crystallizes centrosymmetrically. In the series of cationic dyes (H), the importance of the counter ion is shown. For such materials, monopolar interactions should be dominant over the deleterious dipolar effects in deciding the alignment of the  $\beta$ -enhanced cations. With this cation, medium-small, largely pseudo tetrahedral anions were found to favour the production of an acentric crystal structure<sup>(20)</sup>.

If a molecule could be produced in which dipolar interactions are eliminated, a non-centrosymmetric crystal structure is not guaranteed but at least the structure should be more sensitive to other influences, such as minor molecular substitutions, which are potentially able to prevent centrosymmetry but which are normally overshadowed by stronger electrostatic forces. This idea has been successfully employed in 3-methyl-4-nitropyridine-1-oxide (POM) (B), which has a vanishing ground state dipole moment and crystallizes non-centrosymmetrically<sup>(22,24,25)</sup>. There is an apparent contradiction in the desire for zero dipole moment and conjugated charge transfer, which normally leads to a highly polar structure making significant resonant contributions to the ground state of the molecule. However, in POM this is not a problem because the localized dipole moment of the N-oxide semi-polar bond opposes

and cancels that of nitrobenzene, giving a negligible total dipole moment. In a heterocyclic molecule such as this, the N-oxide group may act as a donor or an acceptor depending on the electronic nature of the substituent para to it; in POM, the nitro group is an acceptor and so promotes the donor nature of the N-oxide. The methyl group does not interfere with the basic charge transfer process but does help to dictate the crystal structure. The reduction of the ground state dipole moment is also favourable for the growth of large, high quality crystals from solution, since disruptive molecular associations should be reduced.

Twieg and Jain<sup>(12)</sup> have described the assessment of several different groups of materials using the powder technique, and compounds (I-R) represents the best from each class.

- (i) Urea derivatives (eg I). This was an attempt to combine the large non-linearity of nitroaniline molecules with the non-centrosymmetric crystal structure of urea.
- (ii) Polarized enones (eg J). These were related to diethylaminomethylcoumarin, a material studied by other workers<sup>(26)</sup>. Compounds that were identical except that a nitrile group replaced the nitro group all showed zero activity.
- (iii) Analogues of MAP (eg K). Both the amine donor and the substituents on the aromatic ring were changed. A wide range of activity was observed in the series, illustrating the important effects that slight changes in molecular structure can have on crystal structure.
- (iv) Analogues of MNA. Compound (L) was the only achiral derivative studied that showed any activity, and its efficiency was approximately four times

that of MNA itself. The origins of this improvement could lie in its stronger donor or in its different crystal space group. Hydrogen bonding between the amide hydrogen and the nitro group of an adjacent molecule is important in deciding this crystal structure.

- (v) Bifunctional nitrobenzenes (eg M, N). The efficiency DNPU (I) is limited by the fact that the urea group, required to promote acentric crystallization via hydrogen bonding, is a poor donor. Therefore in this series other nitroaniline derivatives were studied in which a variety of hydrogen bonding groups were placed at alternative locations in the molecule, and a wide range of efficiencies were observed.
- (vi) Nitropyridines. Donor-acceptor substituted benzene derivatives are only a small class in a whole range of non-linear materials. This section introduces the basis for a new class of compounds that have several advantages over the benzene derivatives, including cutoffs at shorter wavelengths and easier synthesis. PNP (O) contains a very strong donor and was found to be very active, with hydrogen bonding contributing to the production of a favourable molecular alignment in the crystal. NPP, which is the benzene analogue of PNP, is even more active, a property that has been attributed to a structure that is optimal from the stand point of phase-matching requirements<sup>(15)</sup>.
- (vii) Thiazoles (eg P) and pyrimidines (eg Q). These were selected for their favourable absorption edges and the availability of precursors for synthesis. However, the efficiencies observed so far have been relatively low.

This section has illustrated the great difficulties encountered in obtaining a non-centrosymmetric crystal containing highly non-linear molecules. The subject of this thesis is a novel way of bypassing such problems; the Langmuir-Blodgett (LB) technique can be used to form thin films containing the new non-linear species arranged in a way that guarantees the absence of a centre of symmetry. Such films are ideal for applications in integrated optics where single crystals may be inappropriate.

Electric field induced nonlinear second harmonic generation (EFISH) measurements of compounds (R-W) were taken from reference 21 and the dialkylamino-nitrostilbene molecule is entered twice in order that comparisons between the different compounds measured using differing wavelengths can be achieved. The values given for compounds (R-W) are for  $\beta\mu$  and not just  $\beta$ ; this is because of the differing ways authors present results in the literature. It can be seen that replacing just one of the benzene moieties with a thiophene (eg S and T) has a small enhancing effect on the nonlinearity. Replacing both benzenes (eg U) has a much greater effect, and increasing the overall conjugation length (eg V and W) has a dramatic effect upon the nonlinearity observed. Rao<sup>(27)</sup> *et al* report that a log-log plot reveals a power law dependence of  $\beta\mu$  on the number of conjugated  $\pi$ -electrons. Unlike purely benzene systems<sup>(28)</sup> there was no saturation observed in the thiophene series.

## 2.6 Applications of Non-Linear Optical Phenomena.

The large range of non-linear optical phenomena described earlier produce a wealth of potential applications. Each application can be classified according to the particular process that it exploits, as in the summary provided in table 2.4. There are two general classes of process: passive and active, the former giving rise to most of the practical applications. In passive processes the non-linear material is effectively

acting like a catalyst, and the susceptibilities involved are predominantly real. Imaginary terms in the susceptibilities start to dominate as resonances are approached, causing the active processes such as Raman scattering and two photon absorption<sup>(8)</sup>.

The major interest in non-linear optics stems from the telecommunications industry's need for high-bandwidth optical switching and processing devices to service current information and data transmission needs. In addition, the need for new methods of tailoring individual laser pulses to perform specific functions or to be readily detected in complex experiments has become apparent from the use of a host of sophisticated laser tools.

**TABLE 2.4.**

Passive Non-Linear Optical Phenomena and their uses<sup>(1,8,22)</sup> ( $\omega=0$  refers to a dc electric field).

| Susceptibility | Process                                                                                                                                   | Application                                                                                                                         |
|----------------|-------------------------------------------------------------------------------------------------------------------------------------------|-------------------------------------------------------------------------------------------------------------------------------------|
| $\chi^{(1)}$   | Linear dispersion, refraction                                                                                                             | Optical fibres                                                                                                                      |
| $\chi^{(2)}$   | Optical rectification (inverse electro-optic effect) $\omega_1, -\omega_1 \rightarrow 0$                                                  | Hybrid bistable device                                                                                                              |
| $\chi^{(2)}$   | Electro-optic (Pockels) effect $\omega_1 + 0 \rightarrow \omega_1$                                                                        | Modulators, variable phase retarders                                                                                                |
| $\chi^{(2)}$   | Frequency doubling $\omega_1 + \omega_1 \rightarrow 2\omega_1$                                                                            | Second harmonic generation                                                                                                          |
| $\chi^{(2)}$   | Frequency mixing $\omega_1 \pm \omega_2 \rightarrow \omega_3$                                                                             | Optical mixers                                                                                                                      |
| $\chi^{(2)}$   | Parametric amplification $\omega_3 \rightarrow \omega_1 + \omega_2$                                                                       | Optical parametric oscillators                                                                                                      |
| $\chi^{(3)}$   | Frequency tripling $\omega_1 + \omega_1 + \omega_1 \rightarrow 3\omega_1$                                                                 | Deep U.V. conversion                                                                                                                |
| $\chi^{(3)}$   | Quadratic electro-optic effect $\omega_1 + 0 + 0 \rightarrow \omega_1$                                                                    | Variable phase retardation, liquid-crystal displays                                                                                 |
| $\chi^{(3)}$   | Intensity-dependent refractive index $\omega_1 + \omega_1, -\omega_1 \rightarrow \omega_1$                                                | -                                                                                                                                   |
| $\chi^{(3)}$   | AC electro-optic effect, AC Kerr effect, Brillouin scattering, Raman scattering $\omega_1 + \omega_2, -\omega_2 \rightarrow \omega_3$     | Ultra high speed optical gates                                                                                                      |
| $\chi^{(3)}$   | AC electro-optic effect, AC Kerr effect, self focusing, degenerate four-wave mixing $\omega_1 + \omega_1, -\omega_1 \rightarrow \omega_1$ | Optical bistability phase conjugation (image processing), real-time holography, optical transistors, amplifiers, amplitude choppers |



Second harmonic generation already finds extensive use for doubling the frequency of radiation to take it from the infrared to the ultraviolet, as well as for producing radiation of a suitable wavelength for pumping dyes and for the analysis of short pulses. For example, there should be a variety of applications in such fields as electrophotography, scanning, and optical storage for a device based on a frequency doubled GaAs laser<sup>(12)</sup>. The frequency modulation of a laser carrier beam, optical parametric oscillation and amplification for solid state infrared tunable coherent devices<sup>(15)</sup> represent some further applications in the field of integrated optics. Highly efficient non-linear materials can provide such functions on a reduced scale and without a delaying electron-photon conversion process.

One optical element of particular significance is the bistable optical device<sup>(29)</sup>. This has an enormous range of optical signal processing capabilities, and could become a key component in future high-speed optical communication repeaters, terminal equipment, data communication systems, and systems for the direct optical processing of visual images. Such a device can be switched between two or more states of transmission of light by temporary changes in the level of light input, and could find applications in memory elements, differential amplifiers, pulse shapers and limiters, optical triodes, and logic elements etc.

In devices that employ waveguiding, several different types of structure can be envisaged, such as a linear guide on a non-linear substrate, or a non-linear guide on a non-linear substrate. Stripe waveguides fabricated by the in diffusion of titanium into a lithium niobate substrate have also been produced. However, an efficient non-linear optical device has yet to be realized using such structures, mainly due to the difficulty encountered in maintaining uniform guide dimensions over the length of the

waveguide (to maintain phase matching), as well as to scattering losses to the guide-substrate interface and to optical damage because of the high optical intensities employed<sup>(19)</sup>. The use of organic materials and lithographic techniques holds great promise for overcoming such problems.

Langmuir-Blodgett

Film Technology

### **3.0 LANGMUIR-BLODGETT FILM TECHNOLOGY.**

#### **3.1 Basic Concepts.**

##### **3.1.1 Historical introduction**

The effects of oil on the air/water interface have been known for centuries: there is even recorded evidence that the Babylonians in the eighteenth century BC practised divinity by observing such effects.

Scientific interest in monomolecular layers was first expressed in a communication to the Royal Society in 1774 by Benjamin Franklin, when he described the experiment that he carried out while at Clapham Common. Franklin did not try to quantify his observations; had he done so, he probably would have found that the thickness of the oil would have been approximately 1 nm. It was Lord Rayleigh who was the first to suspect that the maximum extension of an oil film on the water surface represents a layer one molecule thick. His early experiments were not definitive and he owed a lot to the work carried out by Agnes Pockels, whose apparatus was developed into the Langmuir trough.

It was Irving Langmuir who contributed the greatest advances, building on many of the ideas of Pockels and others and publishing 'The Constitution and Fundamental Properties of Solids and Liquids' in 1917 that described the 'new' surface effects. Langmuir studied the pressure-area relationship of molecules on an aqueous surface. He found that the areas occupied by molecules such as acids, alcohols, and esters were independent of the length of hydrocarbon chain, thus proving the theory that only the hydrophilic 'head' groups were immersed in the subphase.

Katherine Blodgett, who worked with Langmuir on the properties of floating monolayers, developed the technique of transferring the floating 'Langmuir' layers

onto solid substrates and therefore building up multilayer 'Langmuir-Blodgett' films.

### 3.1.2 Langmuir-Blodgett films

The Langmuir-Blodgett method is a fabrication technique appropriate for the formation of organic monolayers and multilayers that have a high degree of anisotropy and structural order, as well as a precise and uniform thickness<sup>(30)</sup>.

Langmuir-Blodgett films consist of monomolecular layers stacked sequentially onto a solid substrate. In order for a material to be suitable for deposition onto a substrate using the Langmuir-Blodgett technique it must first be able to form an insoluble monolayer at a gas-liquid interface; the liquid concerned is usually water. For this reason the molecules that can be incorporated into such films are usually long chain, amphiphilic (contain both a hydrophobic 'tail' group and a hydrophilic 'head' group), organic molecules. The material is first dissolved in a volatile organic solvent and the solution dispersed over the water surface; the solvent evaporates, leaving a layer of the material one molecule thick which does not dissolve in the water due to the nature of the tails. Solvation effects favour a molecular orientation within the monolayer such that the polar head groups and probably the first one or two methylene groups are in the water. The molecules in such a layer are disorganised, but if the layer is spread in an enclosed area which can be subsequently reduced, then as the surface area available to each molecule gets smaller, the arrangement becomes more ordered. If the monolayer is compressed sufficiently, it forms a quasi two dimensional solid, although if this process is taken too far the layer will buckle and eventually collapse. If a solid substrate is dipped through this compressed layer into the subphase, a monolayer of material will be transferred from the water surface onto the substrate. In the most common type of deposition, further traversal of the air-

molecule-subphase interface will result in subsequent transferral of a monolayer onto the substrate with each insertion or withdrawal.

### **3.1.3 Deposition principles**

There are several ways in which a floating monolayer may be transferred to a solid plate. This thesis is concerned only with the method reported by Langmuir, and extensively applied by Blodgett. A review of the other methods of transfer is found in a paper by Roberts<sup>(2)</sup> and the book by Gaines<sup>(31)</sup>.

Although the Langmuir-Blodgett method is a classical technique of surface chemistry, the detailed mechanisms by which floating monolayers are transferred to solid substrates are poorly understood. The molecular interactions involved in the deposition of the first layer may be quite different from those that are responsible for the transfer of subsequent layers. For example, in the former case a chemical reaction can take place between the monolayer and the substrate, resulting in a strongly bonded first layer. For some materials, film deposition also seems likely to be associated with a distinct phase change, from a two-dimensional liquid crystalline phase on the surface of the water to a closer packed solid crystalline phase on the substrate. Many phenomena noted by the original workers have never been explained completely, despite many experimental studies and several theoretical treatments of Langmuir-Blodgett deposition: the different modes of film transfer and the variation of the speed at which different materials can be deposited are two examples of this.

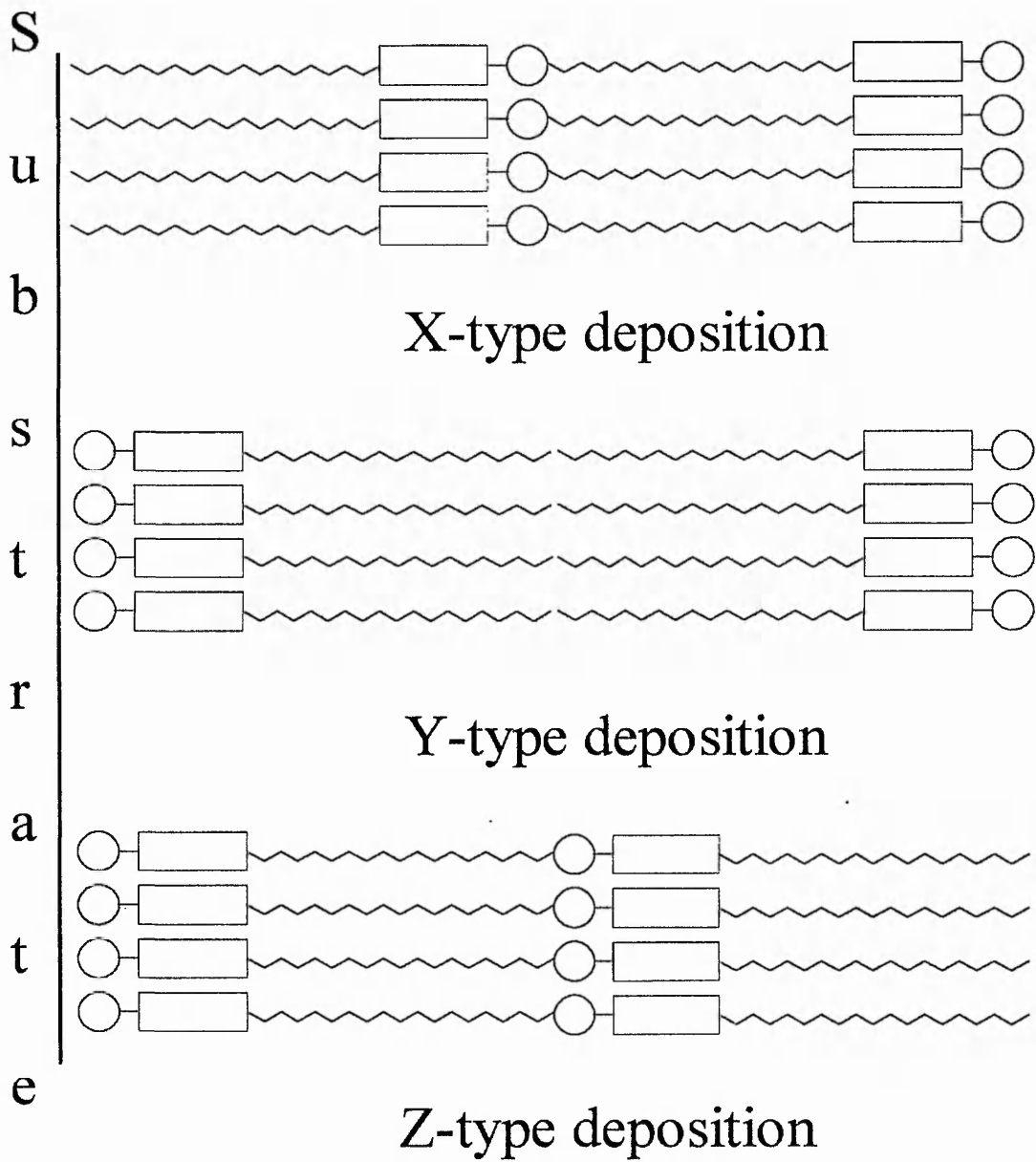


**Figure 3.1** The different modes of deposition.

Fig. 3.1 shows a schematic diagram illustrating the various possible forms of Langmuir-Blodgett film deposition. The first monolayer is transferred as the substrate is raised through the subphase if the substrate is hydrophilic, as shown in the diagrams for Y and Z type deposition. It is possible to place the substrate in the subphase before the monolayer is spread, or it may be lowered into the subphase through the compressed monolayer. The most common pattern of deposition is 'head-to-head' and 'tail-to-tail' as a monolayer is deposited on each traversal of the surface. This deposition mode is called Y-type. In this mode a multilayer containing an odd number of layers can be produced. However, if the substrate were hydrophobic, a multilayer with an even number of layers could be built up because it would pick up the first monolayer as it was lowered through the subphase.

Other types of deposition are known, but Y-type multilayers are the most common. Monolayers that only deposit as the substrate is inserted into the subphase are called X-type, whereas in Z-type deposition a monolayer is deposited only as the substrate is withdrawn. Mixed deposition modes have been observed; for instance XY deposition occurs when there is complete transfer when the substrate is lowered into the subphase and only partial transfer as the substrate is removed. Film deposition may usefully be characterized by reference to a deposition (transfer) ratio,  $\tau$ , given by Eqn 3.1:

$$\tau = A_L/A_S \quad (3.1)$$

Where  $A_L$  is the decrease in the area occupied by the monolayer on the water surface (held at constant pressure), and  $A_S$  is the coated area of the solid substrate. Honig *et al.* have suggested the use of another parameter,  $\phi$ , to help quantify the various deposition modes; this may be calculated from:



$$\phi = \tau_u / \tau_d \quad (3.2)$$

Where  $\tau_u$  and  $\tau_d$  are the deposition ratios on the upward and downward passages, respectively, of the substrate. Thus for pure Y-type  $\phi=1$ , for X-type deposition  $\phi=0$  and for Z-type deposition  $\phi$  is infinite. Care must be exercised in interpreting the measured deposition ratio if asymmetric substrates are used (eg a glass slide metallized on just one side); it is unlikely that  $\tau$  will be identical for the different surfaces. This, however, should be considered really as the apparent deposition ratio, because it is not known whether the transferred film has completely deposited on the solid substrate. Besides the additional monolayer losses arising from evaporation or collapse, some film molecules may dissolve in the subphase at the moment of transfer, or after deposition.

## **3.2 Materials**

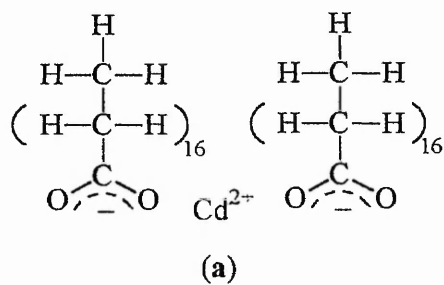
### **3.2.1 Introduction**

The materials used in Langmuir-Blodgett film formation can be classified as being either 'classical' or 'novel'. The classical materials are those such as the long chain fatty acids that form the basis of Langmuir-Blodgett film technology; the novel materials are taken to be those selected for study because they contain certain combinations of chemical groups within the molecules which are likely to impart specific properties to the films they form. In this discussion, the novel materials have been further subdivided into those reported by other workers in the field and those synthesised by the author at The Nottingham Trent University for their potentially large optical non-linearities.

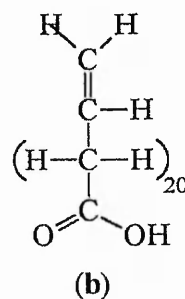
### **3.2.2 Classical materials**

Section 3.1.2 referred to the use of materials with hydrophilic head groups and

hydrophobic tails; perhaps the most commonly encountered molecule of this variety is stearic acid, which possesses a long hydrocarbon chain (hydrophobic) terminated by a carboxylic acid group (hydrophilic). For a homologous series of saturated aliphatic carboxylic acids, the solubility of the material is dependent on the length of the hydrocarbon chain, approximately 20 carbon atoms being required for negligible solubility. It is hardly surprising that solubility problems are encountered in this field, in view of the very large surface area to volume ratio of a monomolecular film. The stability and solubility of water surface monolayers, and the quality of the deposited films, are dependent on a wide range of inter-related variables, such as subphase pH, temperature, and the presence of counterions. For example, the solubility of stearic acid is reduced by the presence of divalent metal cations, such as  $\text{Cd}^{2+}$ , and control of pH is important in determining the extent of salt formation. Since such salt formation involves two stearic acid molecules for each cadmium ion (Fig. 3.2a), such a process improves the lateral cohesion of the layer and gives rise to superior film quality. The typical subphase conditions used for the deposition of cadmium stearate are a  $10^{-4}$  M cadmium chloride solution with  $\text{pH} = 5.6$ . A closely related material to this is  $\omega$ -tricosenoic acid<sup>(32)</sup> ( $\omega$ -TA), whose structural formula is given in Fig. 3.2b. The unsaturated terminal carbon-carbon bond renders the material susceptible to polymerisation by such means as an electron beam, and the resulting cross linking of bonds gives rise to a linear polymer. This feature had led to the proposed use of  $\omega$ -TA Langmuir-Blodgett films as electron beam resists<sup>(33)</sup>. The material has other advantages; in particular, well ordered films can be deposited at high speeds if the subphase does not contain divalent cations<sup>(34)</sup>.



Cadmium stearate,  
 $\text{Cd}(\text{C}_{17}\text{H}_{35}\text{CO}_2)_2$



$\omega$ -tricosenoic acid ( $\omega$ -TA),  
 $\text{CH}_2\text{CH}(\text{CH}_2)_{20}\text{CO}_2\text{H}$

**Figure 3.2** Structural formulae of some classical materials in the literature.

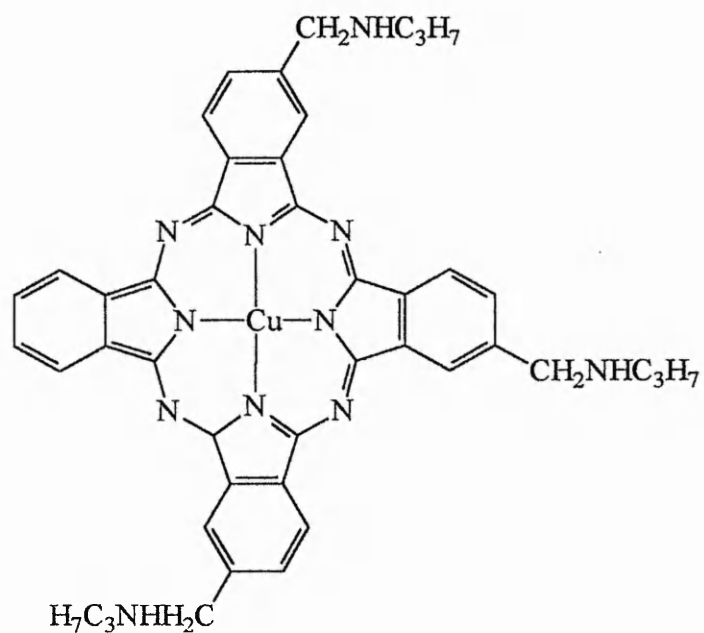
There have been a number of other materials investigated with structures related to those of the simple fatty acids. These include a range of polymerisable materials, the diacetylenes<sup>(35)</sup>, and some biologically important materials such as chlorophyll<sup>(36)</sup>, phospholipids<sup>(37)</sup> and cholesterol<sup>(38)</sup>.

### **3.2.3 Novel materials from the literature**

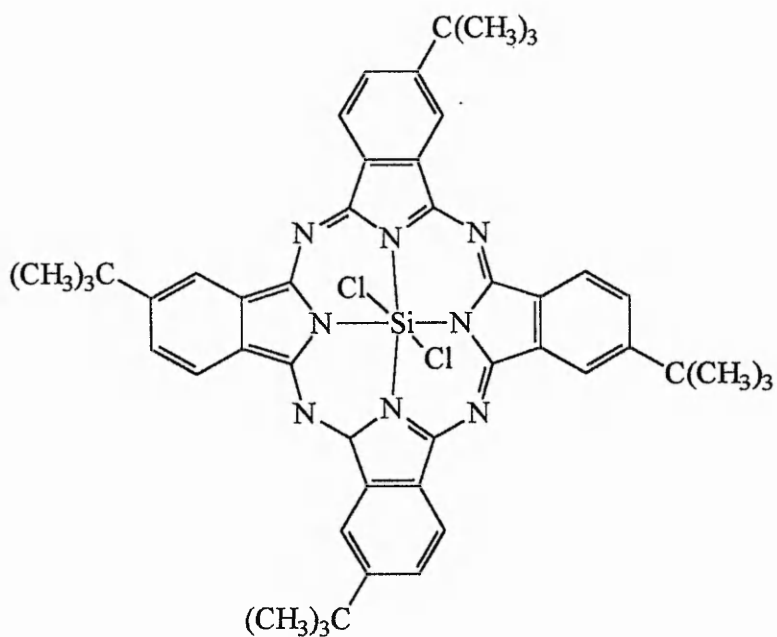
The current trend in Langmuir-Blodgett film technology is to custom synthesize materials incorporating chemical groups designed to impart specific physical properties to the films. In such materials the 'active' part of the molecule is usually the hydrophilic head group, and the hydrocarbon tail is passive in that it merely serves to render the molecule water insoluble (except when it contains unsaturated bonds for polymerisation). In many cases it is therefore desirable to reduce the length of the hydrocarbon chain to a minimum, since it effectively dilutes the useful electronic, optical, photoelectrical etc. properties of the head group. This is the origin of the interest in anthracene derivatives for applications involving charge transport. The anthracene derivative, 9-butyl-10-anthrylpropionic acid, can be made to form high quality multilayers providing the deposition conditions, particularly subphase pH, are very carefully controlled<sup>(39)</sup>. Another range of materials which have been studied extensively are phthalocyanine dyes. These compounds do not require hydrocarbon chains for insolubility and have exceptional thermal and chemical stabilities, as well as potentially useful electronic structures. Stable Langmuir-Blodgett films of metal free phthalocyanine and tetra-tert-butyl substituted phthalocyanine have been prepared<sup>(40)</sup> which are of a reproducible quality, but which are not composed of single monolayers. These films are polycrystalline, with no long range order; however, monomolecular or bimolecular layers of an asymmetrically substituted copper phthalocyanine (Fig.

3.3a) can be produced and have been built up into multilayer assemblies displaying interesting gas-sensitive properties<sup>(41)</sup>. A symmetrically substituted silicon phthalocyanine<sup>(42)</sup> (Fig. 3.3b) has shown improved water surface monolayer characteristics and deposition properties.

Many different substituted dyes have been deposited in Langmuir-Blodgett films, some as homogeneous layers, others as layers in which they are mixed with an inert fatty acid to provide a matrix which can confer desirable film-forming properties to the dye. The list of Langmuir-Blodgett film-forming chromophoric materials include merocyanine<sup>(43)</sup>, hemicyanine<sup>(44)</sup>, squarylium<sup>(45)</sup>, anthraquinone<sup>(46)</sup>, stilbene<sup>(47)</sup> and azo dyes<sup>(48)</sup>. In some cases the molecule contains more than one hydrocarbon chain in order to bring about a particular orientation of the chromophore.



(a)



(b)

**Figure 3.3** (a) Asymmetric Copper Phthalocyanine,  
 (b) Symmetric Silicon Phthalocyanine

### **3.2.4 Novel materials used in this project.**

There were two types of novel material investigated in this project. The first type of molecule was a basic amphiphile like stearic acid, but incorporated in the aliphatic carbon chain at various positions was a thiophene moiety. These materials were investigated in order to ascertain what effects the thiophene moiety had upon the stability and film forming capabilities of the fatty acids. The second type of molecule was designed according to the guidelines discussed in chapter 2 for producing molecules with a high second-order hyperpolarizability (ie molecules containing donor and acceptor groups separated by a conjugated system), their water solubility being reduced by the addition of hydrocarbon chains. These molecules were analogues of stilbene molecules but with one of the benzene moieties being replaced by a thiophene moiety. It was planned to replace both benzene groups but due to synthetic difficulties (described in chapter 4) this was not possible. Thiophene was chosen because it is a  $\pi$ -excessive aromatic compound that possesses a dipole moment, and it was thought that this would increase the non-linear optical effects as compared to the benzene analogue.

## **3.3 Hardware**

### **3.3.1 Mechanical Construction of the Langmuir Trough**

There have been many modifications made to the original trough used by Langmuir and Blodgett. Variations have been made with a single movable barrier or a constant perimeter barrier, or with a circular construction employing radial compression barriers. A constant perimeter barrier type trough, as illustrated in Fig. 3.4, was used in the initial studies, but subsequently a Nima Technology circular design trough was employed and gave comparable results. The results that are quoted

in this thesis are from the Nima trough.

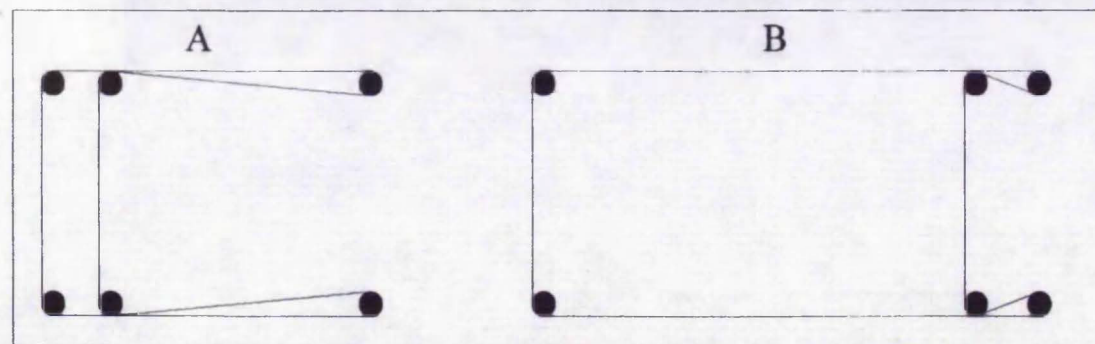
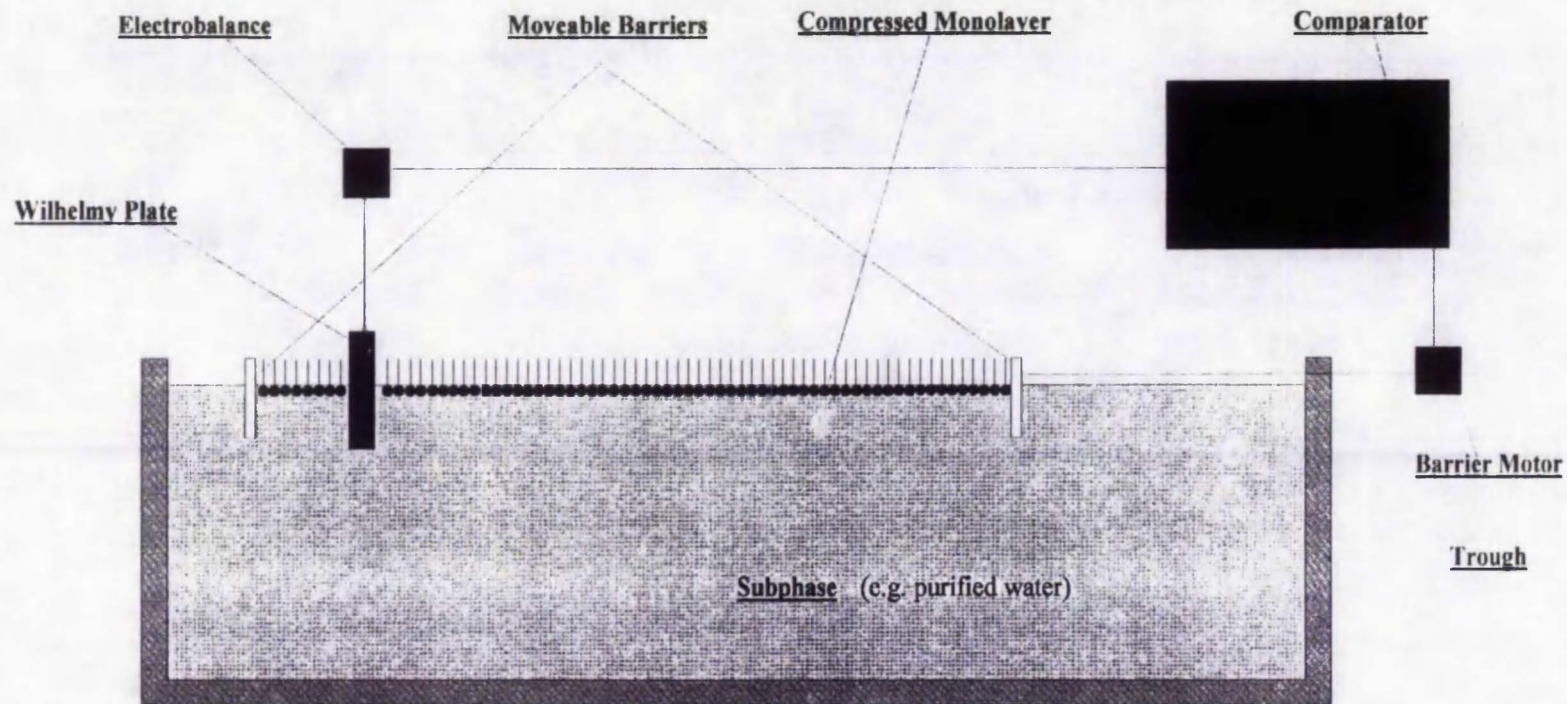
The Nima Technology trough is fabricated from polytetrafluoroethylene (P.T.F.E.), a material that will not contaminate the subphase. The polymer is essentially chemically inert, it will not leach plasticiser, and is the most hydrophobic of the known polymers. P.T.F.E. can be subjected to very rigorous cleaning procedures.

The trough is milled from a single block of P.T.F.E. and is then bolted to a rigid aluminium metal block to prevent any distortion to the trough dimensions. This base has channels milled into it to enable thermostatically controlled water to be circulated for trough temperature control. A steel base that can be levelled by use of three bolts is used to support the trough. Vibration isolation is achieved by a pneumatic support between the base and the trough, the best results being obtained from only partial inflation, which just raises the trough from the base.

This trough can be set up to facilitate either 'Langmuir-Blodgett' mode for conventional LB deposition (see Fig 3.5) or 'AB' mode for alternate layer LB deposition (see Fig. 3.6)



# Langmuir-Blodgett Trough



This is a constant perimeter barrier trough:

- A) Barriers are fully closed
- B) Barriers are fully open.

**Figure 3.4** Schematic diagram of the constant perimeter barrier langmuir trough.

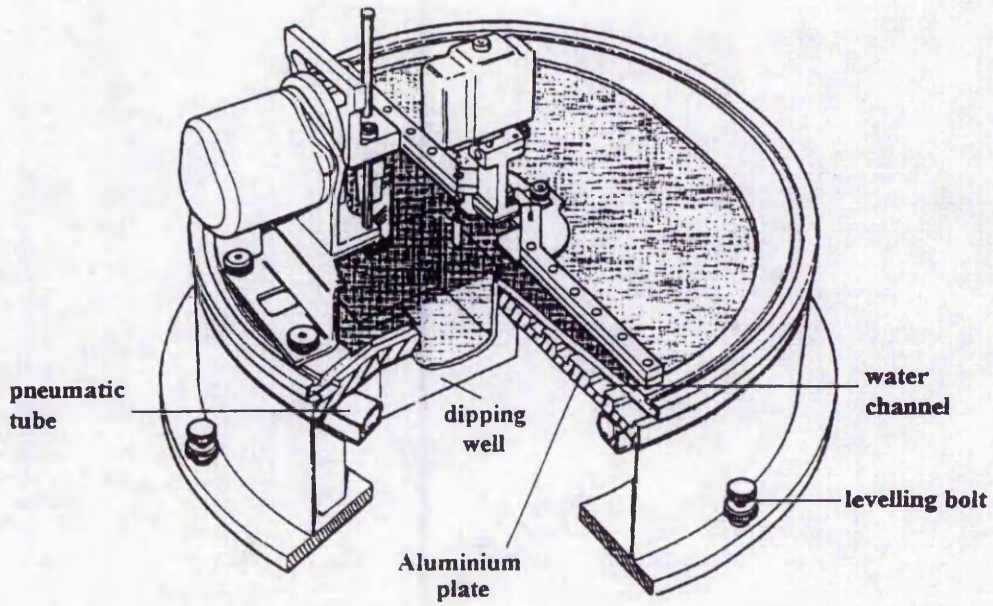


**Figure 3.5** Cut away showing Nima Technology PTFE trough in conventional deposition mode.

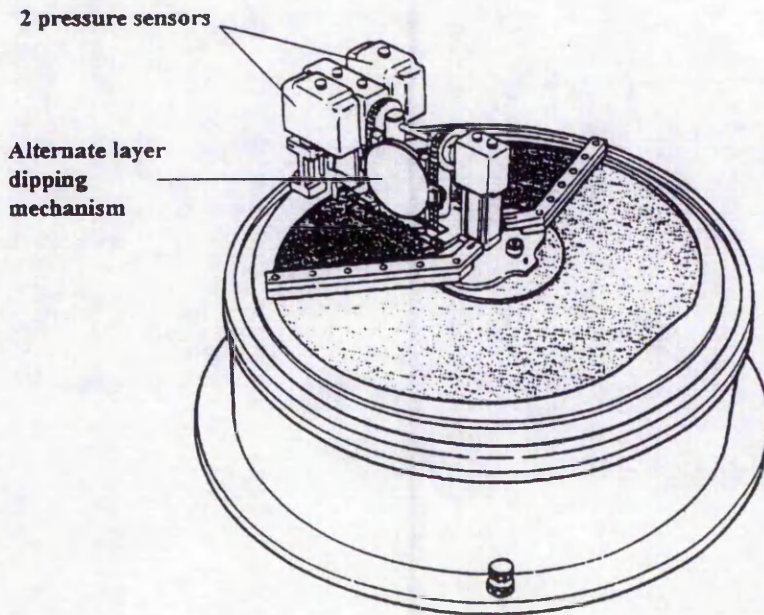


**Figure 3.6** Nima Technology trough in 'AB' mode for alternate layer deposition.

### **3.3.2 Pressure sensors.**

When a plate is suspended across the air-water interface, the surface tension of the water acts to pull the plate downwards into the water to minimise the free energy of the surface. Spreading a contaminant on the surface reduces the surface tension, and this change in tension is called the surface pressure. International Standard I.S.O. 304 recommends that the surface pressure be measured by a Wilhelmy plate. This is the method used in the Nima system (See Fig. 3.7).

A 10mm wide piece of filter paper [1] is suspended at the end of the arm of a galvanometer movement [2 and 3] and serves as the Wilhelmy plate. Optical feedback [4 and 5] keeps the arm in a fixed position; the current required to keep the arm in the same position is a measure of the force on the plate. This method is extremely sensitive while also being highly stable and mechanically reliable. The Wilhelmy plate can be raised or lowered by means of a screw [8]. This mechanism can be calibrated by attaching the weighing pan [6 and 7] to the galvanometer movement and placing standard weights into the pan.

### **3.3.3 Barriers**

An aluminium bar is attached to the barriers, which are also made of solid blocks of P.T.F.E. to prevent distortion. The barriers are attached to the barrier gearboxes, which consist of a specially designed reduction gearbox with anti backlash cogs that are driven by a dc motor and a standard gearbox. The amount of backlash is reduced from 3° to about 0.3°. Non corroding materials are used to make the gearbox and all other parts.

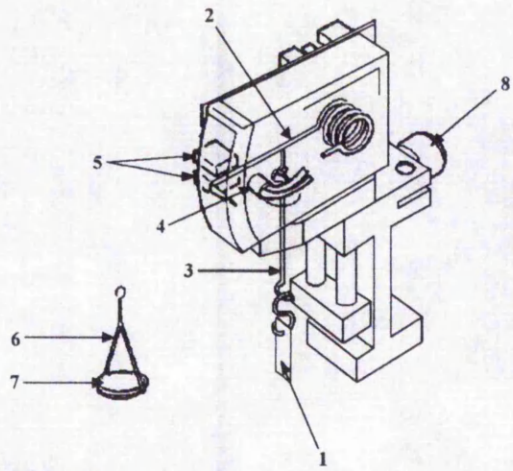
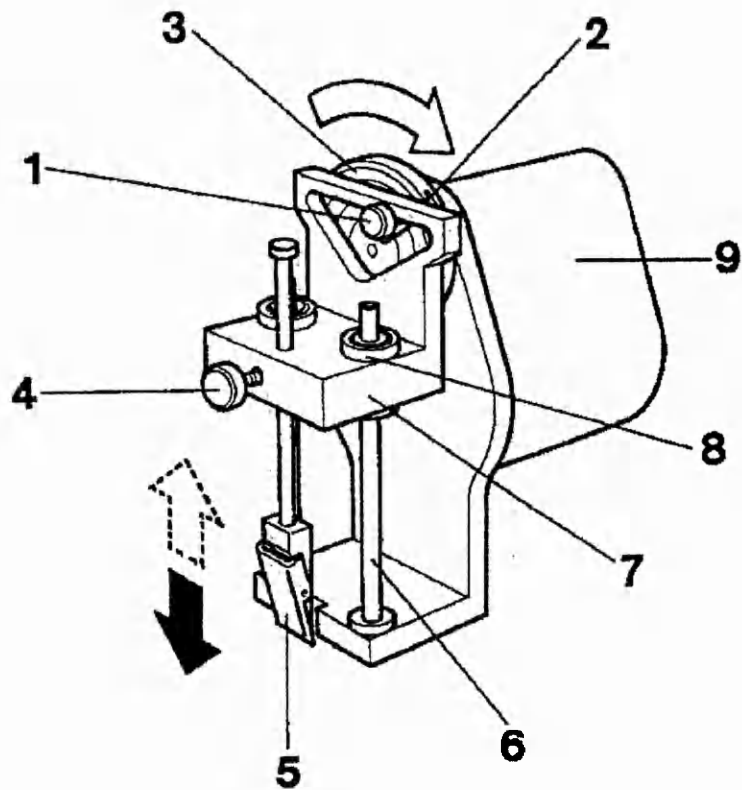


Figure 3.7 Pressure sensor.

### 3.3.4 Dipper Mechanisms

Two different dipper mechanisms can be used in conjunction with the Nima trough, as shown in figures 3.8 and 3.9. Figure 3.8 is a diagram of the dipper mechanism used for the production of multilayer structures in which each layer has the same composition. The substrate velocity is varied sinusoidally during deposition to ensure a smooth transition between up and down strokes. The stroke is infinitely variable between 1 cm and 5 cm by adjusting the bolt [1] sited in the radial slot [2] of the driving disc [3]. Bolt [4] is used to lock the rod that holds the substrate clamp. This sets the absolute height of the substrate.

Figure 3.9 is a diagram of an alternate layer dipper mechanism. The alternate layer dipper mechanism consists of a dc motor and gearbox [1] driving a pair of sprockets [2] that in turn drive a pair of belts [3]. The substrate carrier [4] is mechanically clamped to the belt and the substrate [5] is either mechanically clamped or chemically bound to the carrier. Belt guards that consist of a rigid P.T.F.E. arm [6] and a flexible P.T.F.E. tape [7] are used to protect the belts from the monolayers. This eliminates cross-contamination between compartments as the flexible guard is pressed tight against the P.T.F.E. back plate [8]. The backplate also prevents deposition of molecules onto the back of the substrate carrier, effectively doubling the area of the trough as compared with deposition onto both sides of the substrate.



**Figure 3.8** Single molecule dipper mechanism

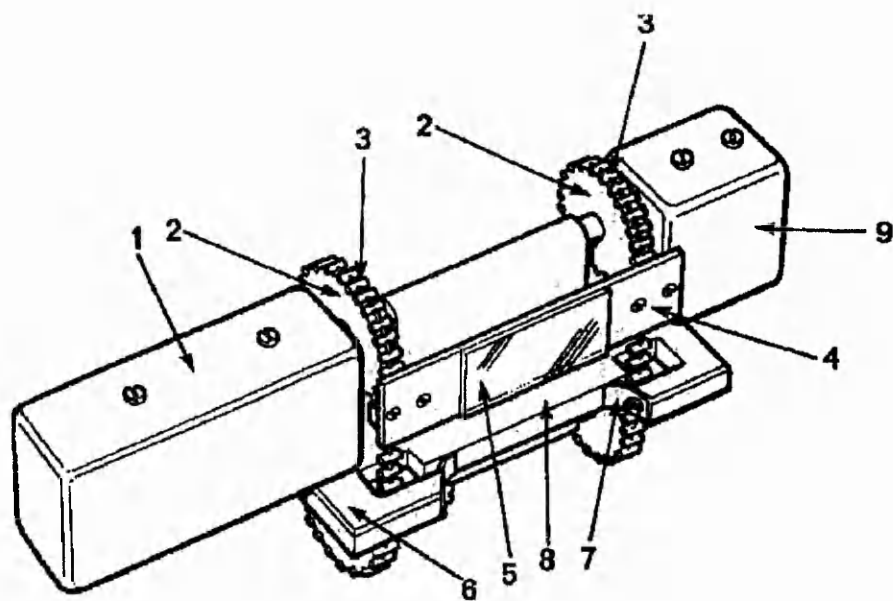


**Figure 3.9** Alternating layer dipper mechanism.

### **3.3.5 Trough control**

The trough is controlled via an external interface unit by a microcomputer. An interface unit houses the electronic interface between the Amstrad PC 2286/40 microcomputer and the trough. It consists of amplifiers and filters for the sensors and the motor potentiometers, the outputs of which are fed into an 8 channel, 12 bit analogue-to-digital converter card slotted into the PC. The trough is a computer automated system allowing easy user-friendly operation. It can generate, display, store and plot pressure-area isotherms as well as pressure-time graphs and transfer ratio bar charts. The software allows automatic deposition of Y-type multilayers at preset pressures and dipping speeds; transfer ratios are generated during this process and sets of conditions and notes can be saved and retrieved from disc. With the alternate dipping mechanism, alternate, X and Z-type multilayers can also be fabricated and the order of the compartments used to deposit from is fully programmable. The pH of the water subphase is detected by an RS Components Limited pH probe.

### **3.3.6 Reduction of contamination**

A dust free environment is essential for the production of good quality Langmuir-Blodgett films. Consequently the trough is housed in a clean laboratory with an air filtration system producing a slight positive pressure inside the room thus reducing the amount of dust from entering the room when the air lock doors are opened. The trough itself is fitted with a clear plastic cover ensuring even more protection from airborne contaminants. Pure water for the subphase is produced by an ELGA® ELGASTAT® SPECTRUM REVERSE OSMOSIS water purification system. This system consists of a Mixed-Bed Deionisation - Nuclear grade cartridge, an Organic Removal - Activated Carbon cartridge and a Reverse Osmosis cartridge

delivering water at 18 MΩcm at a rate of approximately 2 litres hr<sup>-1</sup>. High purity subphase water is vital, since impure water can be a major source of ionic and organic contaminants, resulting in excessive monolayer dissolution and poor deposition. All the solvents and other chemicals used in the preparation of spreading solutions, or as additives to the subphase, are of the highest available commercial grade of purity.

A rigorous cleaning procedure is regularly undertaken in which the P.T.F.E. trough and barriers are cleaned with chloroform, propan-2-ol and water. On reassembly of the trough, the subphase and the Wilhelmy plates are replaced and the trough instrumentation is recalibrated. Before spreading the monolayers, the surface of the water is cleaned by closing the barriers and sweeping the surface of the water with a fine glass tube connected to a water driven pump. This process is repeated until no change in surface pressure is detected, from the fully opened to the fully closed barrier position.

### **3.4 Quality Assessment**

A great deal of effort has been devoted to the determination of the molecular order (crystalline or not) observed in both the hydrophobic and hydrophilic regions of Langmuir-Blodgett films. This is the most interesting property of these films considering that the relationship between molecular structure and molecular functions governs most of the specific properties of these films and their potential applications<sup>(49)</sup>.

At least three major aspects pertaining to the quality of Langmuir-Blodgett films can be identified. Firstly, it is important to know whether the same amount of material is being deposited in each monolayer. Although this information can be deduced from the deposition ratios calculated for each monolayer from the dipping



record (plot of area against time), the accuracy given by this technique is very low (particularly with small samples whose areas are almost insignificant compared to the trough area and/or with water surface monolayers which collapse or dissolve at appreciable rates). Further problems with this method arise when mixed (heterogeneous) monolayers are being deposited, since the pick up of the different components cannot be distinguished. The second major point in assessing film quality is the determination of the degree of crystalline order in the films. A further consideration concerns the nature and number of any defects in the film; for instance, pinholes might occur between crystalline regions and lead to undesirable effects.

A number of assessment techniques described in the literature will now be summarised:

### **Capacitance**

A common method for checking the consistency of deposition and for finding any major defects is to plot reciprocal capacitance against the number of layers in a metal-insulator-metal structure<sup>(50)</sup>. A linear plot would demonstrate the repeatability of dielectric thickness of each monolayer; however, if the film is badly pinholed then all the devices will be short circuited and no meaningful values of capacitance will be observed.

### **Optical Spectra**

Optical spectra in the visible and ultraviolet spectral regions are easily measured on thin films, even down to monolayer thickness, if the materials used are highly coloured. Linear plots of optical absorption (measured at a fixed wavelength - usually the absorption maximum) as a function of film thickness can be used to determine the quality of the multilayers, provided that the interference effects are

small. This is particularly useful when looking at mixed layers as any one of the components can be studied at a time.

### **Infra-red Spectroscopy**

Analogous linear plots can be made using data from infra-red reflectance spectra<sup>(51)</sup>. Infra-red spectroscopy measures molecular vibrations that are predominantly localized on specific functional groups. It can determine the orientation of selected functional groups by observing the intensity differences between the absorption in plane and that normal to the plane.

### **Brillouin Spectroscopy**

Brillouin scattering experiments on Langmuir-Blodgett films have shown that these films are easily deformed by shear motion and behave a little like liquids; the layers most closely attached to the substrate are the most difficult to shear<sup>(52)</sup>. The elastic constant for shear has been found to be two orders of magnitude less than other elastic constants<sup>(53-55)</sup>.

### **Raman Spectroscopy**

Like Infra-red spectroscopy, raman spectroscopy measures vibrational modes of molecules by raman scattering visible radiation. The sensitivity of this technique tends to be, in general, less than infra-red methods. The additional information obtained can help to solve the complex structure in films.

### **Electron Spin Resonance**

This method, albeit limited, is used to determine the orientation of molecules or molecular groups from an ESR spectrum for molecules in thin films with unpaired spins.

## **Diffraction and Reflectivity**

Another method is to plot film thickness against results from the attenuation of the X-ray photoemission signal<sup>(56)</sup> from a metal substrate onto which the Langmuir-Blodgett film has been deposited. Another technique in this class is to label the molecules with <sup>14</sup>C and examine the autoradiographs to obtain a plot of count rate against number of monolayers<sup>(57)</sup>.

Various diffraction techniques can be used to determine the degree of crystalline order in a Langmuir-Blodgett film. For a complete structural assessment, transmission electron<sup>(58,59)</sup>, X-ray<sup>(60-67)</sup> diffraction and reflectivity, low energy electron diffraction (LEED), reflection high energy diffraction (RHEED)<sup>(63,68)</sup>, neutron reflectivity<sup>(69-72)</sup>, and helium scattering<sup>(73)</sup> have all been used to measure such properties as film thickness, lattice spacing, coherence length, and the presence and amount of defects. RHEED is a very convenient technique in that it is non-destructive, and requires minimal sample preparation.

## **XPS and NEXAFS**

X-ray photoelectron spectroscopy (XPS) is a powerful method for identifying and determining the concentration of various elemental species in a film. Near-edge X-ray fine structure, measured with a beam from a synchrotron source, has been shown to give detailed information about the orientation of groups in films from the angular dependence of the signal. This method is very sensitive to very thin films, that is, monolayer or submonolayer coverages. Cadmium arachidate Langmuir-Blodgett films were found to be in agreement with infra-red results, oriented almost perpendicular to the film surface. Other films showed an angular tilt or disorder<sup>(74)</sup>.

## Scanning Tunnelling Microscopy and Atomic Force Microscopy

A related technique to XPS and NEXAFS is scanning tunnelling microscopy (STM) and the related technique of atomic force microscopy (AFM). The AFM technique avoids the electron tunnelling problem in very insulating thick organic films and gives much useful information. There have been many systems examined by STM; however, few have been seen at molecular resolution. A review of thin films at molecular resolution is given by Rabe<sup>(75)</sup>. There have been a few STM<sup>(76,77)</sup> and AFM<sup>(78,79)</sup> molecular images of Langmuir-Blodgett films on various substrates.

### 3.5 Possible applications for Langmuir-Blodgett films.

Initial applications that were proposed for Langmuir-Blodgett films were very simple (eg. soft X-ray gratings, anti-reflection gratings and step thickness gauges).

With the introduction of multilayer assemblies and alternate layer systems researchers have proposed much more subtle and complex uses; such asymmetric assemblies may be employed as active layers in pyroelectric devices as well as the non-linear optical ones. A comprehensive list of possible applications for Langmuir-Blodgett films is given in a review by Roberts<sup>(80)</sup>, and includes the following:

- **Pyroelectric devices** A thin film geometry is preferred because a large area imaging device can be formed directly on microelectronic amplifying circuits.
- **Optoelectronic devices** Devices based on nonlinear optical effects, such as second harmonic generation and parametric amplification are perceived as being most exciting. Similarly, cubic effects such as four wave mixing, phase conjugation, and optical bistability are important.
- **Enhanced device processing** Langmuir-Blodgett films are not likely to have any conventional role in semiconductor circuits or devices but they could have

a part to play as passive layers, as they are invariably insulating in nature.

- **Electron beam Lithography** The quest for faster speed and larger memory in computing has led to circuits with smaller and more closely packed elements. Conventional photolithography cannot produce the sub-micron resolution required. Certain materials (eg  $\omega$ -tricosenoic acid) can be used as electron beam resists. These polymerisable materials have a great advantage over conventional spin coated photoresists, in that they can be laid down with precise thickness control and refractive index. This controllability gives a line resolution down to 60 nm, which is far in excess of other methods because of less scattering of the beam.
- **Semiconductor barrier height modification** Changing the effective barrier height at a semiconductor surface has beneficial effects (eg increased efficiency in an electroluminescent diode)
- **Tunnelling devices** Langmuir-Blodgett films could be used to control the critical current, switching speeds, and energy gap parameters in superconducting quantum interference devices.
- **Semiconductor devices** Langmuir blodgett films have been employed to form an insulating layer on semiconductors that do not possess native oxide layer with good insulating properties, such as InP. This has been of great interest in the formation of metal-insulator-semiconductor (MIS) structures for applications in integrated circuits and planar electronic devices.
- **Optical sensors** If a metal is sandwiched between two materials of different dielectric constants, then a type of resonance can occur. This is called surface plasmon resonance (SPR). This is extremely sensitive to changes in the

refractive index of the medium next to the metal. These changes can be caused by gas in concentrations down as low as parts per billion absorbing in the organic film. A large interest has arisen in trying to incorporate biological molecules in order to produce biosensors.

- **Quartz oscillator, surface acoustic wave oscillator and acoustoelectrical devices**

The resonant frequency of a body is altered when material is either added or removed. Gas absorption into Langmuir-Blodgett films coated onto quartz produces minute changes, thus forming the basis of gas detectors.

- **Optical waveguides and switches** The very nature of the Langmuir-Blodgett technique for thin layer fabrication makes them ideal for the manufacture of optical waveguides. There are still some problems to be overcome, for example the ability to produce a couple of hundred high quality layers of materials with high optical power density thresholds. This must also be fabricated in a reasonable time period.

### **3.5.1 Devices that have been demonstrated.**

#### **Gas Sensors**

Langmuir-Blodgett films, being extremely thin, have a very large surface area to volume ratio. Any gas molecule that is adsorbed onto the film will therefore cause a chemical or physical effect, which results in a large and rapid modulation of the chemical or physical quantities in the underlying volume. The sensors now used for gas detection are made of inorganic semiconductor polycrystals (usually ceramics). They are so porous that their response times are usually long at room temperature, though the pores effectively give the large surface area to volume ratios. If Langmuir-Blodgett films with good molecular packing and with gas-sensitive molecular groups

aligned at or near the surface are employed can obtain efficient and quick response gas sensors.

Adsorbed gases influence the electrical conductivity of various organic solids, including aromatic hydrocarbons, phthalocyanines and  $\beta$ -carotene. Phthalocyanine has been widely studied for gas sensor applications. An asymmetrically substituted copper phthalocyanine Langmuir-Blodgett deposited film has been shown to detect  $\text{NO}_2$  molecules in  $\text{N}_2$  down to a few ppm<sup>(81)</sup>. A device of 45 layers of a 1:1 mixture of copper tetracumylphenoxyphthalocyanine and stearyl alcohol on a gold interdigital electrode was able to detect  $\text{NH}_3$  down to 0.5 ppm in about 30 seconds. This also gave a sensitivity of about 1 ppm for  $\text{NO}_2$ <sup>(82)</sup>. There have also been some reports of unsymmetrical axially substituted phthalocyanines which are sensitive to  $\text{O}_2$ ,  $\text{NH}_3$ ,  $\text{NO}_2$  and  $\text{Cl}_2$  gases by Fu *et al*<sup>(83)</sup>.

### **Ion sensors**

A mixed Langmuir-Blodgett film of cadmium arachidate and valinomycin on an  $\text{Al}_2\text{O}_3/\text{Al}/\text{glass}$ <sup>(84)</sup> substrate has been shown to complex selectively with  $\text{K}^+$  ions in a hydrocarbon environment although the sensitivity is not as great as the conventional type of sensor. A highly sensitive pH ion selective field effect transistor has been reported that uses a Langmuir-Blodgett film of arachidic acid which coats the gate insulator<sup>(85)</sup>.

### **Biosensors**

Moriizumi<sup>(86)</sup> has been developing biosensors using solid state device technology, referring to them as 'solid state biosensors'<sup>(87)</sup>. Those that have been developed are a urea sensor<sup>(88)</sup> and several types of glucose sensors. These sensors were developed using an ISFET<sup>(89)</sup> and thin film  $\text{H}_2\text{O}_2$  electrodes with photosensitive

polyvinyl alcohol (PVA) for enzyme immobilization<sup>(90)</sup>. Moriizumi made glucose sensors using 2 and 10 Langmuir-Blodgett layers, reporting that the 10 layer sensor showed high sensitivity but became saturated at glucose concentrations higher than 500 mg dl<sup>-1</sup> and that the 2 layer sensor, however, gave an unsaturated output for concentrations as high as 5000 mg dl<sup>-1</sup>, although the sensitivity was reduced.

### **Immunosensors**

Katsube *et al*<sup>(91)</sup> have adsorbed immunoglobulin G (IgG) antigen onto stearic acid monolayers on a FET, making an immuno field effect transistor (IMFET). This was reported to measure solutions of concentrations of between  $5 \times 10^{-8}$  and  $1 \times 10^{-6}$  M. Immunosensors using AT-cut oscillators have been shown to have a greater sensitivity<sup>(92)</sup> than those for immunoelectrodes or IMFETs.



# Discussion

## 4.0 DISCUSSION OF THE CHEMISTRY.

### 4.1 Introduction.

For a compound to be suitable for Langmuir-Blodgett film formation it must exist as an amphiphile<sup>(31)</sup>. An amphiphile is a molecule that possesses both a hydrophilic (water loving) 'head' group and a hydrophobic (water hating) 'tail' group. A typical example of an amphiphile is stearic acid (see Fig. 4.1).

Stearic acid, when it is compressed into a '2-D solid' on the subphase, forms an ordered molecular array, something akin to soldiers on a parade ground all standing to attention. This is a very simplified view of things, and not all molecules will be aligned correctly. There will be some molecules at a different angle, and even some that are completely inverted. However, the molecules will be essentially perpendicular to the subphase. This is not true of all materials: in some materials all the molecules may be aligned with a definite 'tilt', at an average angle  $\theta$  to the vertical. It can also be safely assumed that the first one or two methylene groups are also immersed in the subphase along with the carboxyl 'head' group<sup>(93)</sup>. This can be justified in terms of the water solubility of the lower members of the homologous series (i.e. ethanoic and propanoic acid).

The first half of the research was to synthesize a variety of amphiphiles that contained the thiophene molecule, and then to obtain the area per molecule for each one by means of the pressure/area isotherms. It was also intended to determine monolayer stability on the subphase, and to investigate how the films behaved during transfer to a substrate. Atomic Force Micrographs of monolayers of these materials deposited on a silicon substrate were obtained. Attempts were also made to take Scanning Tunnelling Micrographs of some films, but the films proved to be too

insulating to allow a tunnelling current to form, and hence it was not possible to obtain images by this technique.

Thiophene was chosen as the basic central aromatic moiety for the synthesis of novel amphiphiles for use as Langmuir-Blodgett film materials because it is a  $\pi$ -excessive aromatic compound (i.e. it has a greater electron density per carbon atom in the ring than benzene) and the delocalisation energy of thiophene is lower than that of benzene, therefore its substitution in donor-acceptor compounds should be expected to result in enhanced charge transfer properties and nonlinear responses relative to benzenoid rings. Rao<sup>(27)</sup> *et al* have shown dramatic enhancement of  $\beta\mu$  values by using thiophene as a conjugated moiety in a series of dialkylamino-nitro substituted stilbenes (see Chapter 2 Section 2.5)

#### 4.2 Structure of Thiophene.

The fact that thiophene has a planar structure is widely accepted. Using electron diffraction, Schomaker and Pauling established the bond lengths and angles of thiophene in 1939<sup>(94)</sup> (See Figs. 4.2 and 4.3).

The electronic structure of thiophene has been the subject of debate for several decades. It was thought to be analogous to that of furan. In this approach the 3s, 3p<sub>x</sub> and 3p<sub>y</sub> orbitals of the sulphur form three sp<sup>2</sup> hybrid orbitals, two of which form  $\sigma$ -bonds with the ring carbon atoms while the third, non-bonding, hybrid contains a lone pair. The remaining two electrons in the 3p<sub>z</sub> orbital can then enter into conjugation with the 2p<sub>z</sub> electrons of the carbon atoms of the heterocycle<sup>(95)</sup>. In an alternative treatment of the structure of thiophene the sulphur d orbitals are brought into consideration.

- a) Two of the 3p orbitals and the 3s orbital hybridise in the usual way to

give three  $sp^2$  orbitals; two overlap with the neighbouring carbon atom  $sp^2$  orbitals to complete the strong  $\sigma$ -bonded framework of the molecule, and the third contains the unshared pair of electrons. Thus 4 of the sulphur outer electrons are involved in these  $sp^2$  orbitals.

- b) The remaining  $3p_z$  orbital, and two of the 3d orbitals (the  $3d_{xz}$  and  $3d_{yz}$ ) hybridise to form three hybrid orbitals, of correct energy and symmetry to overlap with the carbon 2p orbitals. Two of the pd hybrids are able to do so; the third lies at right angles to them. Each of the overlapping pd hybrids contains one electron, so that the thiophene aromatic sextet is still composed of two electrons from sulphur, and four from carbon. The difference now is that the thiophene molecular orbital system is constructed from six atomic orbitals instead of five, and it is thus nearer to the situation with benzene.

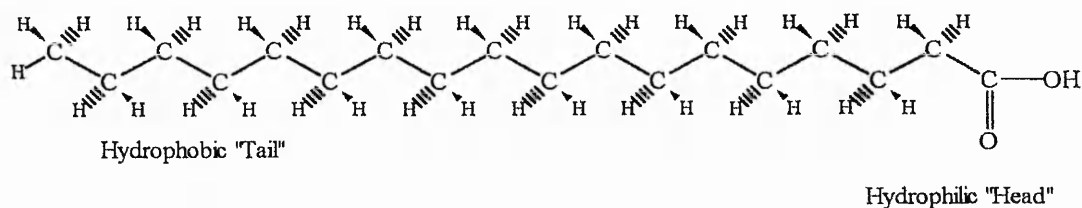


**Figure 4.1** Structural formula of stearic acid.



**Figure 4.2** The structure of thiophene (after Schomaker).

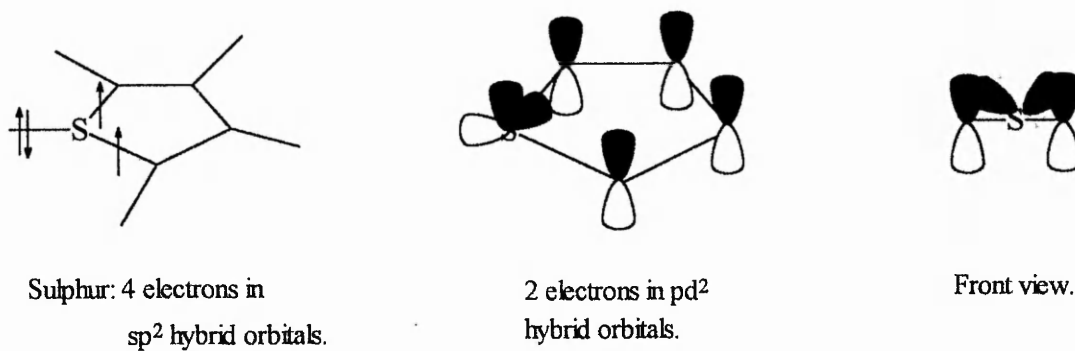


**Figure 4.3** Molecular orbital picture of thiophene.

This picture of thiophene is in accord with some of its properties (eg its uv spectrum is very similar to that of benzene) but not of others; at present the question of d orbital participation is still open.

The reactions of thiophene are very similar to benzene; however, thiophene is more reactive than benzene and undergoes reactions that fail when attempted with benzene. For example, thiophene rings that are suitably activated by substituents will undergo the Diels-Alder reaction under ordinary conditions. The first reported example, discovered at Trent Polytechnic, is the reaction of 2,5-dimethoxythiophene with maleic anhydride in boiling xylene. The adduct produced spontaneously loses sulphur, to give a new diene which, in turn, reacts with more of the anhydride<sup>(96)</sup>.

The main reactions, however, are those associated with aromatic compounds like benzene, the electrophilic substitution reactions, (eg Friedel-Crafts acylation, nitration and Vilsmier-Haack formylation), a general mechanism is shown in Fig 4.4.

### **4.3 Reactions.**

#### **4.3.1 Friedel-Crafts Acylation.**

The essential reaction in this process is between an acylating agent (such as an acid chloride) and an aromatic substrate, in the presence of a catalyst, to yield an aromatic ketone (See Fig 4.5).

##### **4.3.1.1 Catalysts.**

The reaction is very dependent upon the choice of catalyst, the ratio of catalyst to substrate, and the choice of solvent. Metallic halides that are used with acyl halides include aluminium(III) chloride, aluminium(III) bromide, iron(III) chloride and titanium(IV) chloride.

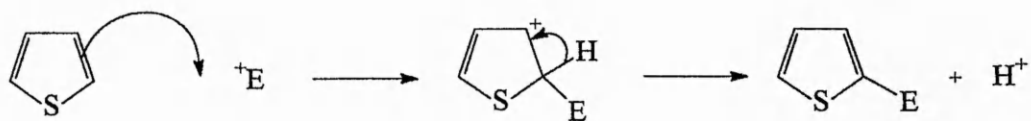


**Figure 4.4** The general mechanism for electrophilic substitution.

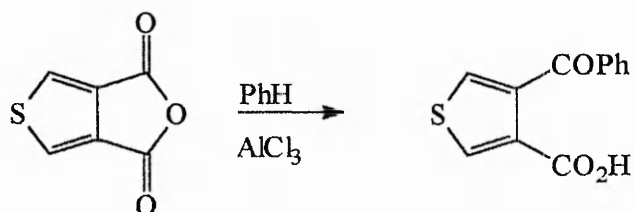
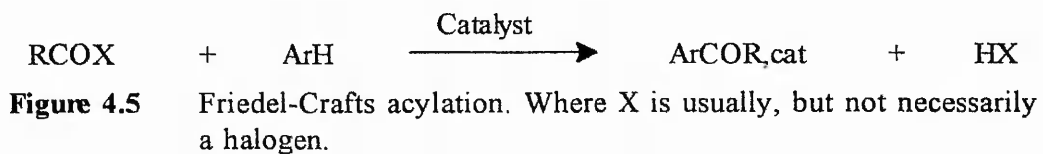


**Figure 4.6**

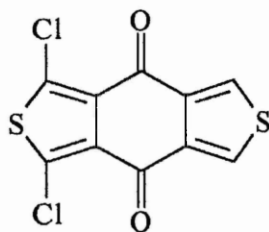
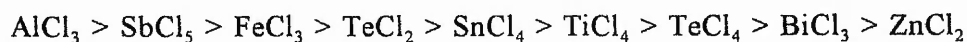


**Figure 4.7**

The high catalytic activity of aluminium(III) chloride, i.e. its high Lewis acid strength<sup>(97,98,99,100)</sup> can also bring with it certain disadvantages. The catalyst cannot be used, for example, with several heterocyclic systems because decomposition occurs even in the presence of moderating solvents. The use of aluminium(III) chloride also can cause side reactions such as intra- and inter-molecular migration of alkyl groups<sup>(101,102,103)</sup> and the removal of alkyl groups (especially tertiary) preceding or accompanying acylation<sup>(104-110)</sup>; furthermore, the splitting of *ortho*-alkoxy groups, both with the acyl halide<sup>(111-113)</sup> and, more often, on the substrate<sup>(114,115)</sup>, can also occur. These effects are minimised by using a solvent such as nitrobenzene with which the catalyst is complexed. Tin(IV) chloride, first employed by Stadinkoff<sup>(116)</sup>, is especially valuable as a catalyst for use with highly reactive substrates such as oxygen or sulphur heterocycles, which may be unstable in the presence of aluminium(III) chloride. Dermer<sup>(117,118)</sup> found that the relative activities of halide Lewis acid catalysts for the acylation of toluene are in the following order:



Marked success has been achieved when certain mineral acids have been employed in certain cases. Phosphoric acid is a very effective catalyst for use with anhydrides, especially in the thiophene series<sup>(119,120)</sup>, whilst polyphosphoric acid, first used for cyclizations, has found use in intermolecular acylations.

Boron trifluoride and its complexes with diethyl ether, methanol and acetic acid are pre-eminent among non-metallic halides capable of catalysing acylations<sup>(121)</sup>. Boron trifluoride and phosphorus pentachloride have also been used as acylation catalysts<sup>(122,123)</sup>. In almost all cases the optimum amount of catalyst employed is found to be up to, or just over, the calculated stoichiometric amount.



#### 4.3.1.2 Choice of Solvent.

A variety of solvents have been employed in Friedel-Crafts aromatic ketone synthesis. Nitrobenzene and carbon disulphide are the most commonly used solvents that simultaneously govern the type of acylation reaction: essentially homogeneous and essentially heterogeneous acylations, respectively. Polar solvents such as nitrobenzene dissolve (and solvate) both aluminium(III) chloride and the acyl-aluminium-chlorine complex, and frequently the aluminium(IV) chloride complex of the resulting ketone<sup>(124,125)</sup> as well. In nonpolar solvents such as carbon disulphide or petroleum ether neither aluminium(III) chloride nor any complexes with the acyl halide are appreciably soluble and the reaction is heterogeneous throughout its course.

Intermediate to these are chlorinated solvents such as dichloroethane and dichloromethane that do not appreciably dissolve aluminium(III) chloride but are excellent solvents for the final complex. The main influence of the solvent in acylations of benzenoid or heterocyclic systems is on the yield of ketone obtained. There are also few significant differences between solvents with respect to acylation rates<sup>(126,127)</sup> and orientation of substitution<sup>(128-131)</sup>.

#### 4.3.1.3 The Friedel-Crafts Acylation of Thiophene.

Acylation of thiophene leads almost exclusively to monosubstitution. It can be effected by a variety of catalysts. Anhydrous aluminium(III) chloride and to a lesser extent tin(IV) chloride react with thiophene to yield intractable tars. However, this undesirable resinification is largely avoided by adding the catalyst gradually to a mixture of the thiophene and the acylating agent, when the catalyst reacts preferentially with the acylating agent to give the electrophile. In the presence of tin(IV) chloride or titanium(IV) chloride, benzene can be used as the solvent, since

these inorganic chlorides do not initiate reaction between benzene and the acid chloride.

It has been found that the acylation of thiophene with acetic anhydride or benzoyl chloride is promoted by catalytic amounts of iodine and hydroiodic acid<sup>(132)</sup> or boron trifluoride complexes<sup>(133)</sup>. Thiophene, 3-methyl-dichlorothiophene, and 2,5-dichlorothiophene react with acid anhydrides or acid chlorides in the presence of orthophosphoric acid, to form acyl derivatives in very good yields<sup>(134)</sup>. Thiophene is acylated by aliphatic or aromatic acid when phosphorus pentoxide<sup>(135)</sup> is the catalyst.

Friedel-Crafts acylation can be successful with deactivated thiophene rings, although yields are often poor. Ethyl thiophene-2-carboxylate gives the 5-acetyl derivative with acetic anhydride and zinc chloride<sup>(136)</sup>; acylation at C<sub>5</sub><sup>(137,138)</sup> occurs with the esters of thiophene-3-carboxylic acid. In a reversal of this approach, a thiophene dicarboxylic acid anhydride will act as a monoacylating agent. The reaction of thiophene-3,4-dicarboxylic acid anhydride with benzene-aluminium(III) chloride complex<sup>(139,140)</sup> and with dimethylcadmium<sup>(141)</sup> (which gave 4-benzoyl- and 4-acetyl-thiophene-3-carboxylic acids in 66% and 32% yields, respectively), illustrates the possibilities, as in the equation shown in Fig 4.6.

Thiophenecarboxylic acid chlorides derived from all types of acids behave quite normally as Friedel-Crafts acylating agents. Reactions have been carried out with many of benzene derivatives: biphenyl and fluorene<sup>(142)</sup>, 2- and 3-methoxy benzo (b) thiophenes and a wide range of other heterocyclic systems have been substrates for thenoylation. Aluminium(III) chloride catalysed the acylation of 2,5-dichlorothiophene by thiophene-3,4-dicarboxylic acid chloride leading to an excellent yield of the quinone<sup>(143)</sup>, shown in Fig 4.7.

#### 4.3.2 Reduction of the carbonyl function to methylene (CH<sub>2</sub>) in ketones.

There are various ways of reducing the carbonyl group of ketones to CH<sub>2</sub><sup>(144)</sup>. The two oldest methods are the Clemmensen reduction and the still very popular Wolff-Kishner reduction. The Clemmensen reduction consists of heating the ketone with zinc amalgam and aqueous HCl<sup>(145)</sup>. In the Wolff-Kishner reduction<sup>(146)</sup> the ketone is heated with hydrazine hydrate and a base (usually NaOH or KOH). The Huang-Minlon modification<sup>(147)</sup> of the Wolff-Kishner reaction, in which the reaction is carried out in boiling diethylene glycol, has completely replaced the original procedure. The reaction can also be carried out under more moderate conditions (room temperature) in dimethyl sulphoxide with potassium *t*-butoxide as the base<sup>(148)</sup>. The Clemmensen reduction fails for acid sensitive and high molecular weight substrates. For these cases the Wolff-Kishner reduction is quite useful. A modified Clemmensen reduction, using activated zinc and gaseous HCl in an organic solvent such as diethyl ether or acetic anhydride, has proved successful in high molecular weight substrates<sup>(149)</sup>. The Clemmensen and Wolff-Kishner reactions are complementary, since the former uses acidic and the latter basic conditions. These methods are fairly specific for ketones or aldehydes and can be carried out with many other functional groups present. These reactions do not work for all ketones such as sterically hindered ketones and  $\alpha,\beta$ -unsaturated ketones. The mechanism for the Wolff-Kishner reduction is shown in Fig 4.8.

Not much is known about the mechanism of the Clemmensen reduction, but it is known for certain that it does not proceed via the corresponding alcohol because alcohols prepared by different means fail to give the reaction<sup>(150)</sup>.

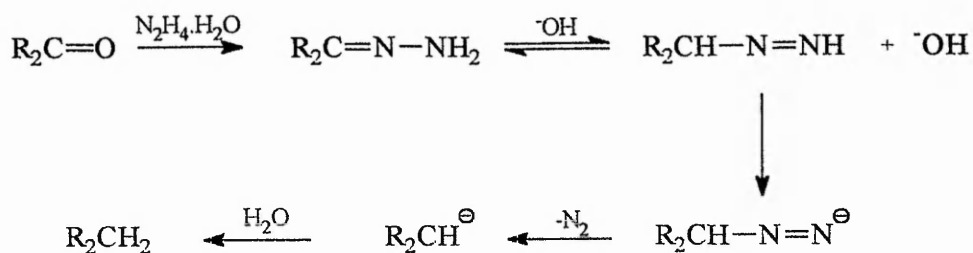


**Figure 4.8** Mechanism of the Wolf-Kishner reduction.

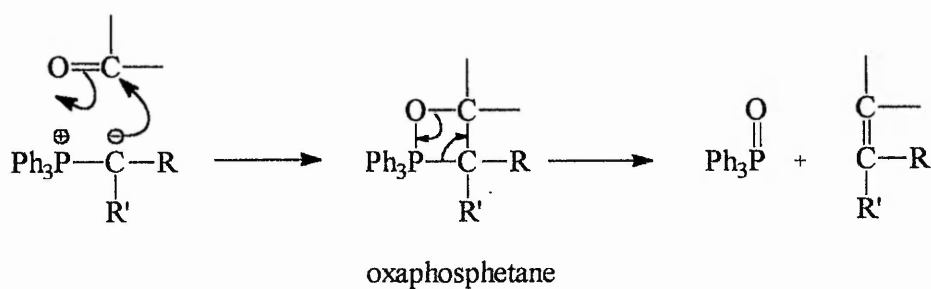
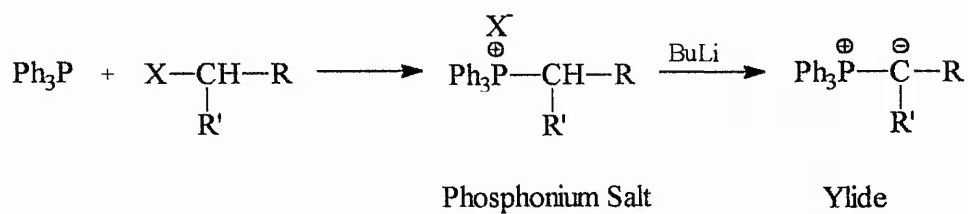


**Figure 4.9** The mechanism for the Wittig Reaction.

### 4.3.3 The Wittig Reaction<sup>(151)</sup>

In 1953 Wittig and Geissler observed that, when methyltriphenylphosphonium bromide was treated with phenyllithium, an ylide was formed which could react with benzophenone to give triphenylphosphine oxide and 1,1-diphenylethylene in 84% yield. This discovery led to the development of a new method for the preparation of alkenes which has since found widespread application in synthetic organic chemistry and is now universally known as the Wittig reaction. One of the main virtues of the Wittig reaction, in marked contrast to other alkene syntheses, is the fact that no ambiguity exists concerning the position of the newly formed carbon-carbon double bond, even in cases of energetically unfavourable sites. The scope of the Wittig reaction is extremely wide because of the wide variety of the carbonyl compounds that can be used; moreover, the mildness of the reaction conditions allows the inclusions of delicate groups such as esters and acetals.

The preparation of an alkene by the Wittig reaction involves three stages<sup>(152)</sup>. First, the phosphonium salt must be prepared, usually from triphenylphosphine<sup>(153)</sup>. In the second stage of the reaction the salt is treated with a base to convert it into an ylide which is then, in the third stage, allowed to react with the carbonyl compound to give the alkene and triphenylphosphine oxide via the intermediate betaine. Groups that are strongly electron withdrawing will stabilize and consequently reduce the reactivity (nucleophilicity) of the ylide and hence reduce the ease of formation of the betaine. Replacing the phenyl groups on the phosphorus with electron withdrawing groups such as alkyl will increase the reactivity of the ylide. The phosphorus ylides are prepared from the reaction of a phosphonium salt with a base, and the choice of base depends upon the nature of the groups attached to the  $\alpha$ -carbon. Electron

withdrawing groups on the  $\alpha$ -carbon can be deprotonated using dilute aqueous alkalis or by neat amines. If the groups are electron donating, for example alkyl groups, then metal alkyls or hydrides will be required to remove the  $\alpha$ -proton. In the intermediate case where the  $\alpha$ -proton is allylic or benzylic then alcoholic alkoxides are employed. For  $(\text{Ph}_3\text{P}^+)\text{CH}_2$ , sodium carbonate is a strong enough base<sup>(154)</sup>.

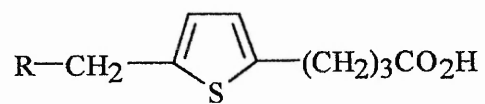
The reaction is also very general. The aldehyde or ketone can be aliphatic, alicyclic, or aromatic, and the compound can also contain double or triple bonds, -OH, -OR, -NR<sub>2</sub>, aromatic nitro or halo, acetal and ester groups. The mechanism of the Wittig reaction is shown by Fig. 4.9.

#### 4.3.4 Reduction of nitro groups.

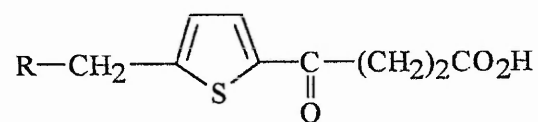
For a complete review of the methods and conditions of nitrating thiophene see Hartough. Many reducing agents have been used to reduce aromatic nitro compounds, the most common being Zn, Fe, or Sn and an acid, and catalytic hydrogenation. Free amino thiophene compounds are unstable unless they are stabilised by functional groups that have a strong -M effect such as esters and acids and therefore it is necessary to react the resulting amine with acetic anhydride to produce the corresponding acetamide *in situ*.

#### 4.4 Synthesis of Thiophenes for Study.

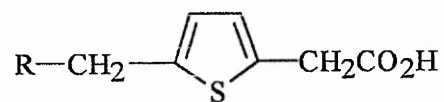
The structures of the series of compounds required for study are shown in Fig 4.10. An account of the synthetic approaches adopted for each group will now be given, beginning, in each case, with a scheme showing the retrosynthetic analyses.



(1)



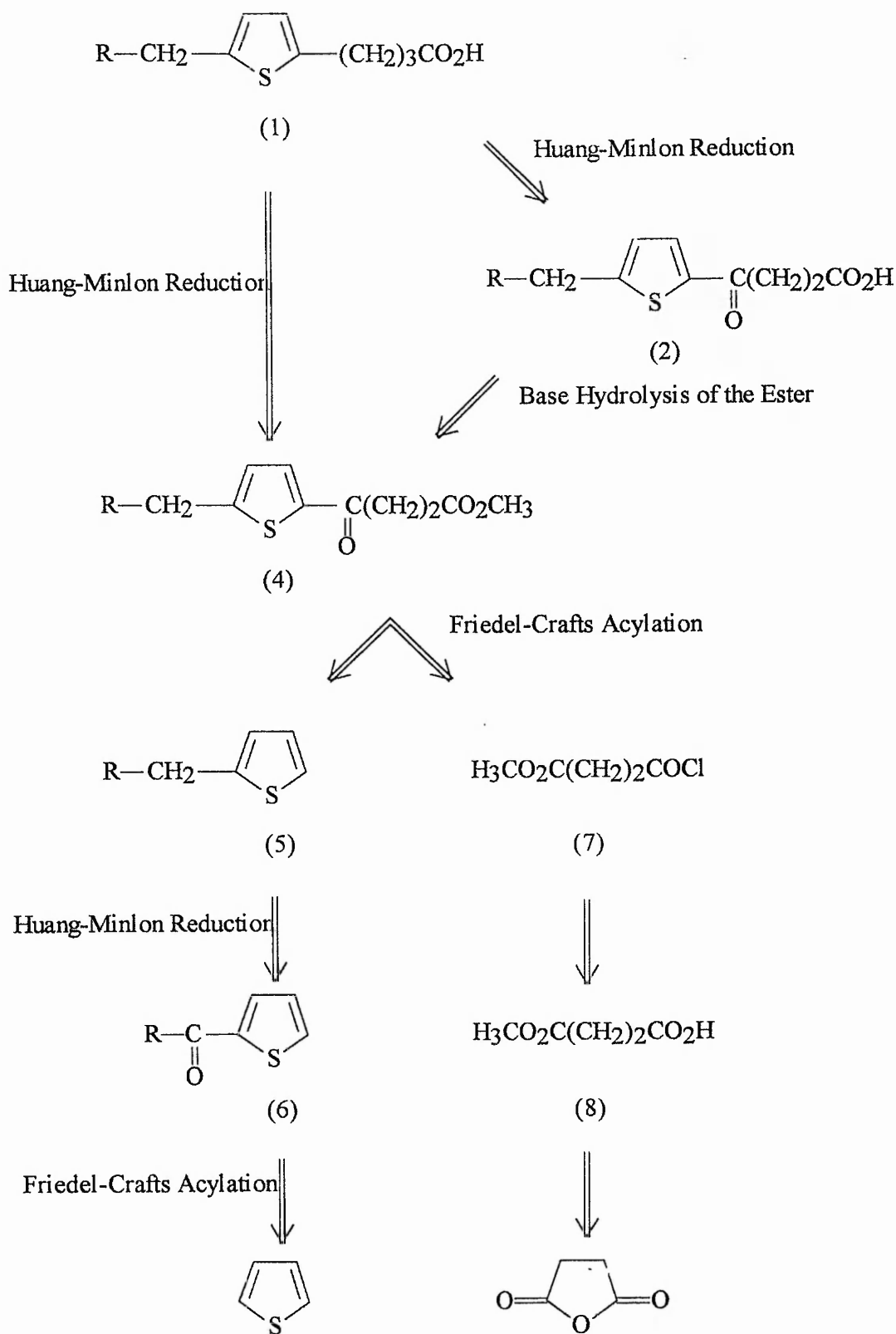
(2)



(3)

**Figure 4.10** The series of thiophene compounds that were synthesised.

4.4.1 Retrosynthetic analysis of compounds 1. and 2.





#### 4.4.2 Synthesis of compounds 1 and 2.

The first step in the synthesis of compounds 1 and 2 was to acylate thiophene by the Friedel-Crafts method using either

- a) a carboxylic acid and phosphoric acid catalyst
- or b) an acid chloride and tin(IV) or titanium(IV) chloride as the catalyst.

The second method was preferred, although the starting materials and reactants were more expensive. This was because much higher yields of a purer product were obtained. The first method gave approximately 55% pure product and the second gave about 80%. It is also not advisable to use aluminium trichloride as the catalyst in these acylations (see Section on Friedel-Crafts Acylations). Thiophene, because it is more susceptible to electrophilic substitution on the two and five positions, acylates exclusively in those positions. Ketones (6) were then reduced to the hydrocarbons by the Huang-Minlon modification of the Wolff-Kishner reduction. This used hydrazine hydrate and potassium hydroxide in diethylene glycol at approximately 190-200°C for two hours. This reaction works well, giving about 70% yield for the alkylthiophenes (5).

It is necessary to synthesize alkylthiophenes by this two-step process rather than the one step alkylation reaction, because once the thiophene ring has been alkylated, it is more susceptible than the original thiophene molecule to further alkylation, producing polyalkylated thiophenes. This does not occur with the two-step process because the acylated thiophene is deactivated and is not susceptible to further attack.

The next stage is to perform a second Friedel-Crafts reaction using  $\text{H}_3\text{CO}_2\text{C}(\text{CH}_2)_2\text{COCl}$ ; the latter is synthesized from succinic anhydride by heating it

at reflux temperatures in methanol for 30 minutes to make the half ester  $\text{H}_3\text{CO}_2\text{C}(\text{CH}_2)_2\text{CO}_2\text{H}$ , followed by reaction of this intermediate with thionyl chloride or oxalyl chloride at approximately 30-40°C for 3 hours. This sequence provides an almost quantitative yield of the acid chloride required for the second acylation reaction. The substitution product is then subjected to either a second Huang-Minlon reaction (giving compound (1) in approximately 65% yield) or saponification to the free acid (2). This hydrolysis can be performed in various ways, but the method preferred by the author was to heat the compound under reflux for 2 hours with 10% w/w alcoholic potassium hydroxide, followed by acidification, giving a greater than 90% yield of the ketoacid.

### 4.4.3 Retrosynthetic analysis of compound 3.

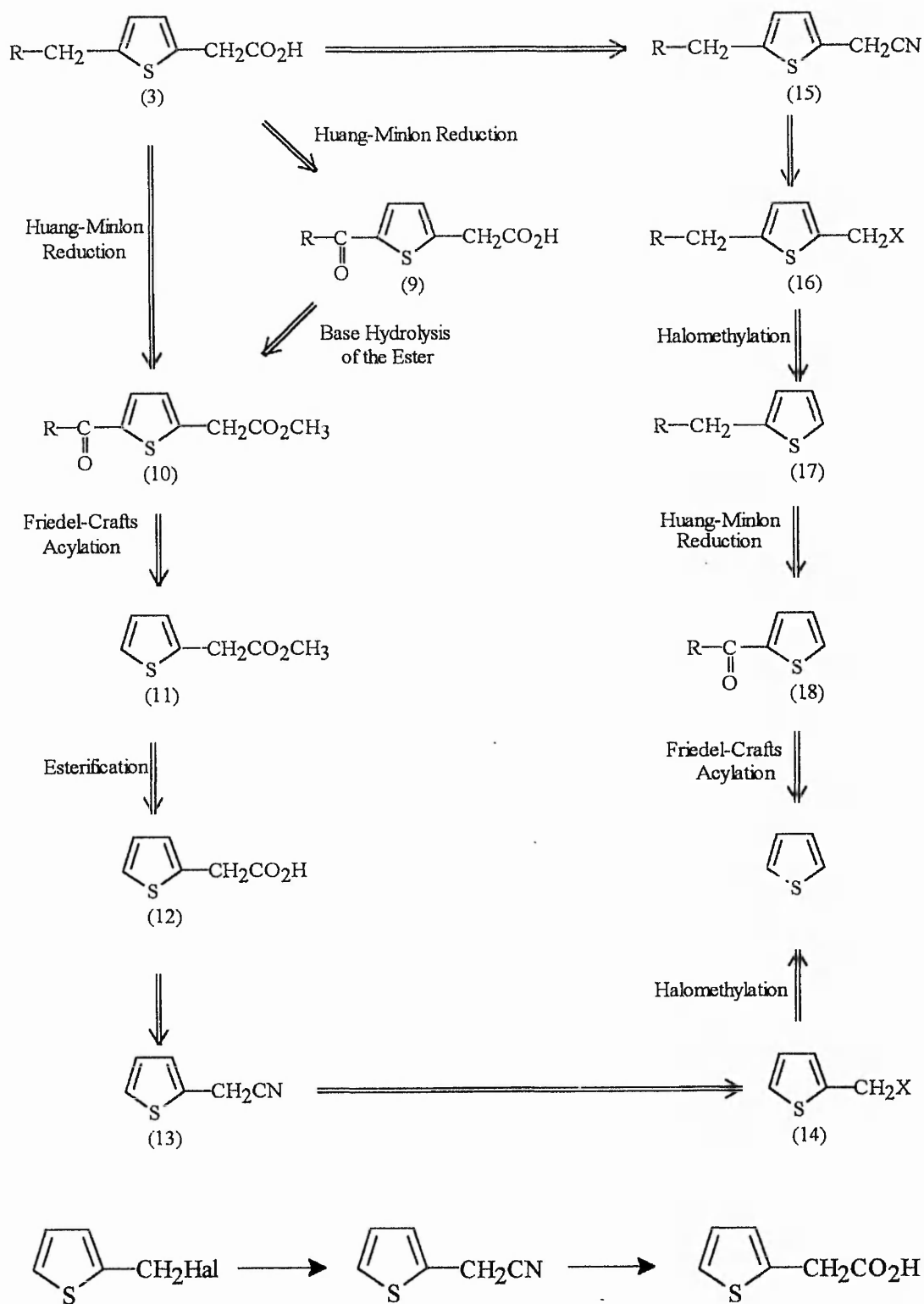


Figure 4.11 Synthetic route to thiophene-2-acetic acid.

#### 4.4.4 Synthesis of compound 3.

The fairly obvious route to thiophene-2-acetic acid is shown in Fig. 4.11.

The required 2-halomethylthiophenes could possibly be prepared by two routes

- (a) from 2-methylthiophenes by reaction with N-bromosuccinimide or sulphuryl chloride
- (b) from thiophene by reaction with HCHO/HCl

Both methods were tried, and both methods were unsuccessful

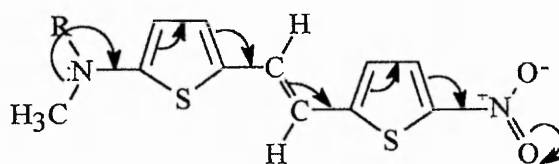
Route (a) was not successful with 5-n-alkyl-2-methylthiophenes because the alkyl chain was halogenated as well as the methyl group, whilst route (b) gave products that polymerised to dithienylmethane and higher self-condensation products.

A sample of the simplest member of the series, thiophene-2-acetic acid, was donated by Synthetic Chemicals Ltd., and this was used to carry out exploratory work. It was necessary first to esterify the acid to reduce the possibility of an anhydride being formed with the acid chloride in the Friedel-Crafts reaction. The acid was esterified using either one of two methods. In the first case the acid was boiled under reflux in methanol for 5 hours with concentrated sulphuric acid as the catalyst. The second method was to stir a solution of the acid in dry diethyl ether with methanol and N,N-dicyclohexylcarbodiimide, for 30-40 minutes with 4-pyrrolidinopyridine as a catalyst. This compound was then acylated in a Friedel-Crafts reaction and reduced to give compound (3) by the Huang-Minlon procedure. These reactions were performed in the same way, and gave similar yields to those used in the synthesis of compounds (1) and (2).

The types of molecules discussed in section 4.4 will not show any second

harmonic generation or non-linear optical effects; for these effects to be observed it is necessary to modify the structures. The hydrophilic group and hydrophobic group in the molecule are still essential, but besides these it is also necessary to have an extended area of  $\pi$ -electrons that is bounded at one end by an electron donor group and at the other by an electron acceptor group, this being called a D- $\pi$ -A system. Several molecules have already been studied for these effects, but the author wished to use substances containing five membered heterocycles, because they are  $\pi$ -excessive in character and give a bigger net dipole moment along the molecule from donor to acceptor. A consequence is that larger beta values should be observed in measurements of second order Non-linear Optical properties, compared with the analogous benzene derivatives. With all these items in mind attempts were made to synthesize compounds with general structure (19) as shown in Fig. 4.12.

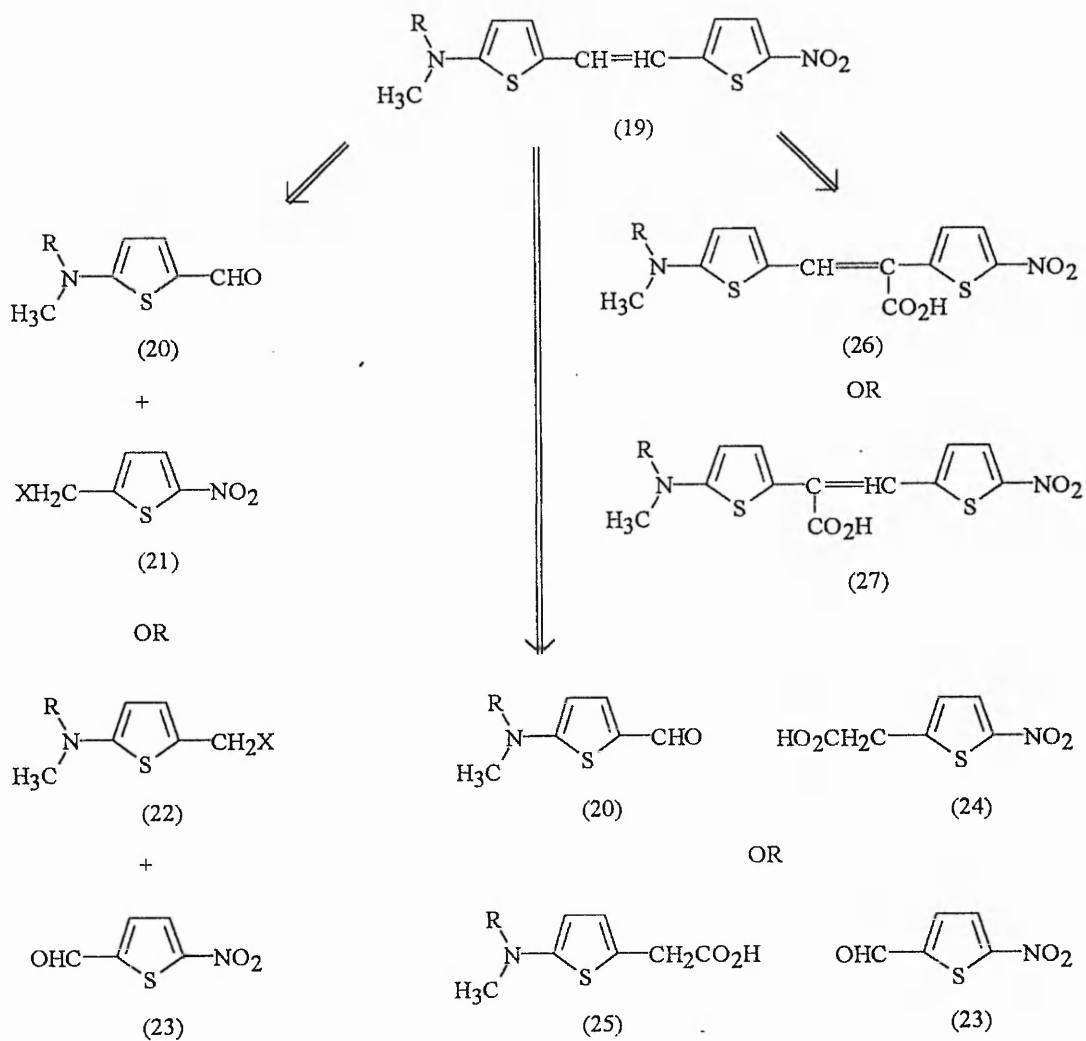
#### 4.5 Synthesis of Materials for Non-linear Optics.



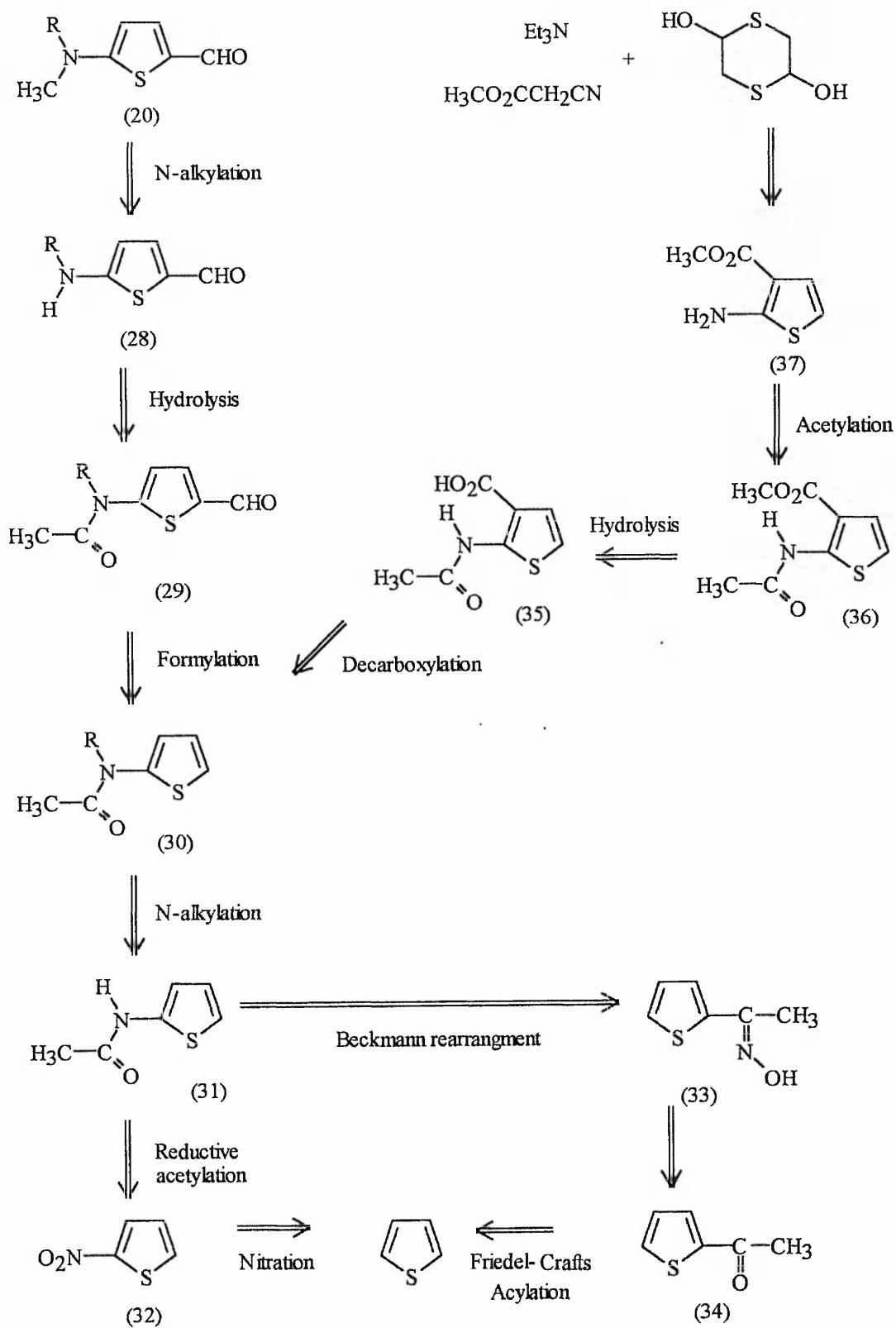
(19)

**Figure 4.12** 1-(5-N-alkyl-N-methylamino-2-thienyl)-2-(5-nitro-2-thienyl) ethene.

##### 4.5.1 Retrosynthetic analysis of compounds 19.



4.5.2 Retrosynthetic analysis of compounds 20. (see section 4.5.1)



### 4.5.3 Synthesis of compounds 20.

The first route that was tried employed methyl 2-aminothiophene-3-carboxylate, which was already available in the laboratory; it was prepared from the reaction of p-dithiane-2,5-diol, methyl cyanoacetate and triethylamine in methanol in a one pot reaction that goes well, giving approximately 70% yield (see Fig. 4.13). Normally simple 2-aminothiophenes are not stable, but those with adjacent ester (and other -M groups) are exceptions.

The next stage was to react the amino ester with acetic anhydride or acetyl chloride in the presence of triethylamine to produce the amide, The reaction went very readily and gave almost quantitative yields of the amide. The next step was to hydrolyse selectively the ester group, and for this was necessary to use basic conditions. This was achieved satisfactorily (yields approximately 90%). Decarboxylation of the acid proved to be a considerable problem, and, under a variety of conditions, high yields of the decarboxylated product were not obtained. The majority of the effort involved treatment of the acid with copper in high boiling bases such as quinoline; complete removal of the solvent was not the least of the difficulties encountered.

The second approach to 2-acetylaminothiophene was *via* the Beckmann rearrangement of the oxime of 2-acetylthiophene by reaction with phosphorus pentachloride in dry diethyl ether heated at reflux temperatures. Although this route has fewer steps than the one just described, it proved to be no more satisfactory. A mixture of the desired product with an undesired one is obtained, the latter arising from the Z-oxime (see Fig. 4.14).



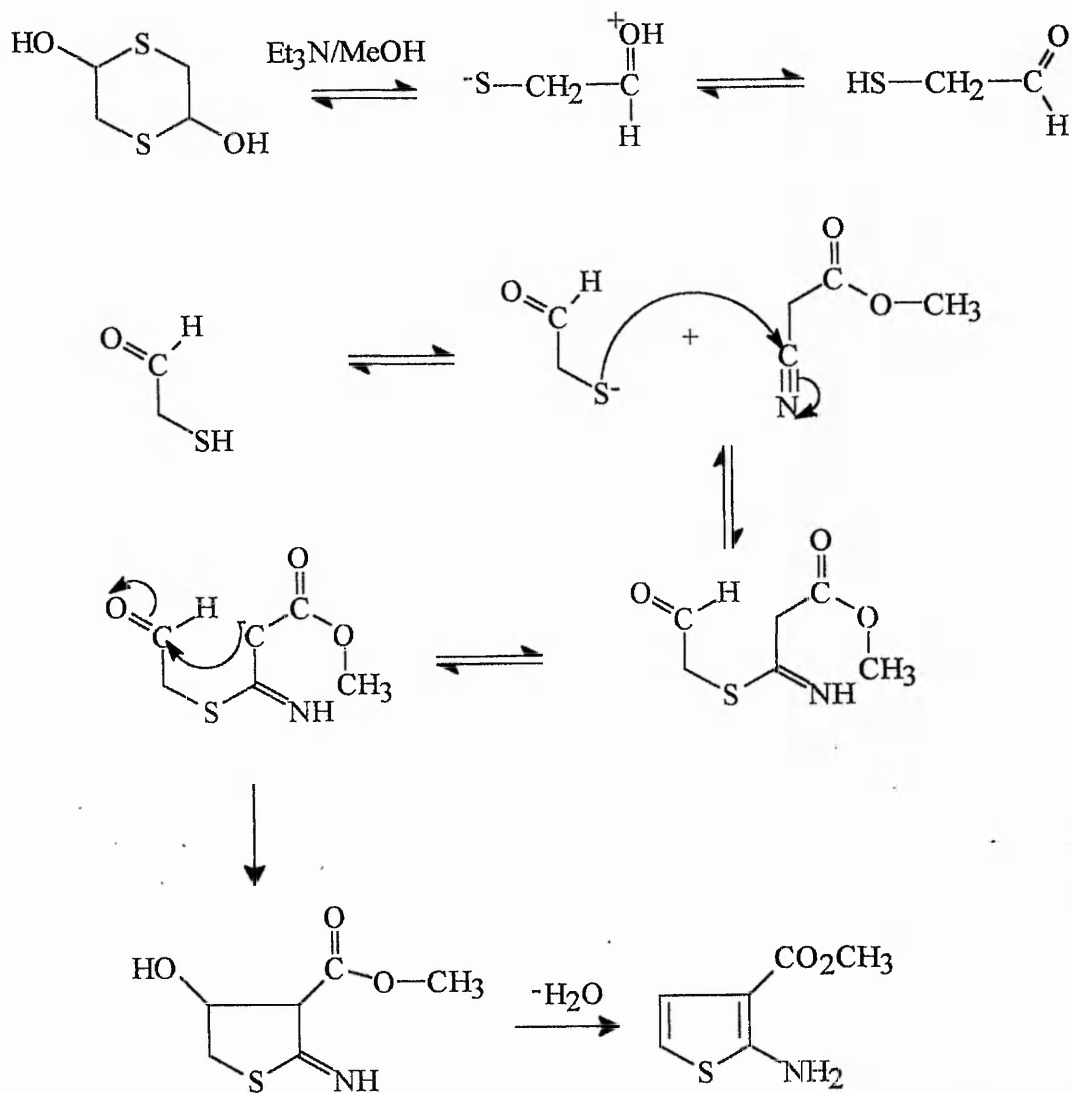


**Figure 4.13** The reaction mechanism for the synthesis of methyl 2-aminothiophene-3-carboxylate.

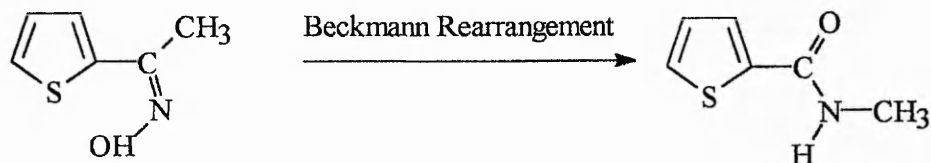
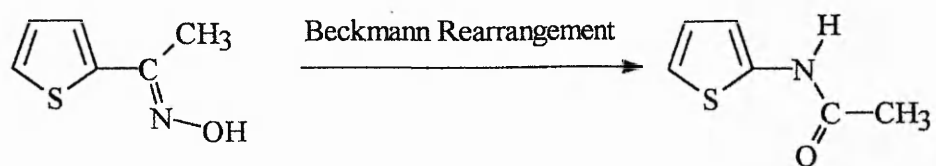
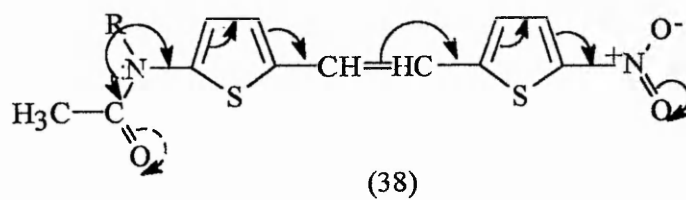


**Figure 4.14** The Beckmann Rearrangement



- > Movement of electrons.  
 - - - - -> Competing movement of electrons.

**Figure 4.15**

Eventually an excellent route to the required product was developed, based on 2-nitrothiophene. The first stage was to nitrate thiophene, either with a mixture of nitric and sulphuric acids or with copper nitrate in acetic anhydride. Whenever nitration of thiophene occurs there is at best 85% of the 2-nitrothiophene in the product, 15% of the 3-nitrothiophene also being formed. The 3-nitrothiophene is not required and must be removed; this, however, is quite difficult to achieve, because both compounds have very similar properties. For example, they cannot be separated by either recrystallisation or chromatography. Use is made of their different behaviour towards chlorosulphonic acid<sup>(172)</sup>, with which the 2-nitrothiophene does not react but the 3-nitrothiophene yields 3-nitrothiophene-2-sulphonic acid. The 3-nitrothiophene-2-sulphonic acid is then easily separated from the 2-nitrothiophene because it is soluble in water.

The next stage was to reduce the nitro group to the amine with an iron and acetic acid mixture in the presence of acetic anhydride, which immediately converts the amine into the amide before it has a chance to decompose. This reaction also proceeded very well, giving yields over 90%. Vilsmier-Haack formylation of 2-acetamidothiophenes leads to thieno[2,3-b]pyridines; however, this does not occur with a tertiary amide-thus it is essential to carry out the sequence in the correct order. Alkylation<sup>(155)</sup> of the amide was achieved by heating it in benzene with the appropriate alkyl bromide and potassium carbonate, in the presence of the phase transfer catalyst myristyltrimethylammonium bromide. The alkyl halides chosen had chain lengths designed to give the hydrophobic character required in the final product.

The next step was to formylate<sup>(156)</sup> the thiophene ring in the 5 position; this was accomplished in good yields using dimethylformamide and phosphorus oxychloride.

The aim of next stage, hydrolysis of the amide to give the free amine, was not achieved because the product decomposed under all the conditions that were tried. It was then decided to use the amides themselves in the final step to produce the modified product of the form (38) shown in Fig. 4.15 (i.e. stopping at compound (28) in section 4.5.2, retrosynthetic analysis of compounds (20)).

It would be expected that the amide (38) would not show such a marked D- $\pi$ -A effect as the free amine (19) since electron release from the nitrogen atom to the conjugated system in the former will be considerably reduced.

4.5.4 **Retrosynthetic analysis of compound 21.** (see section 4.5.1)

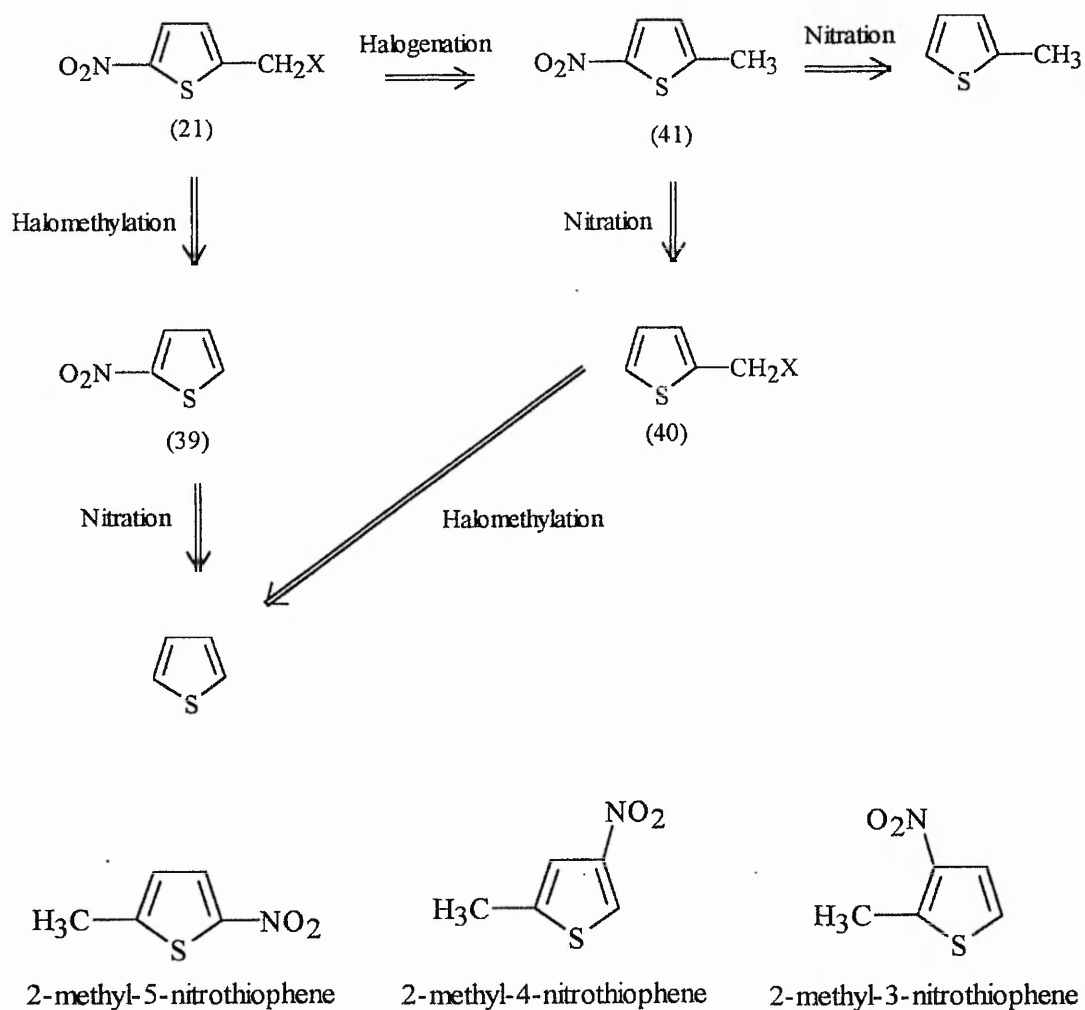


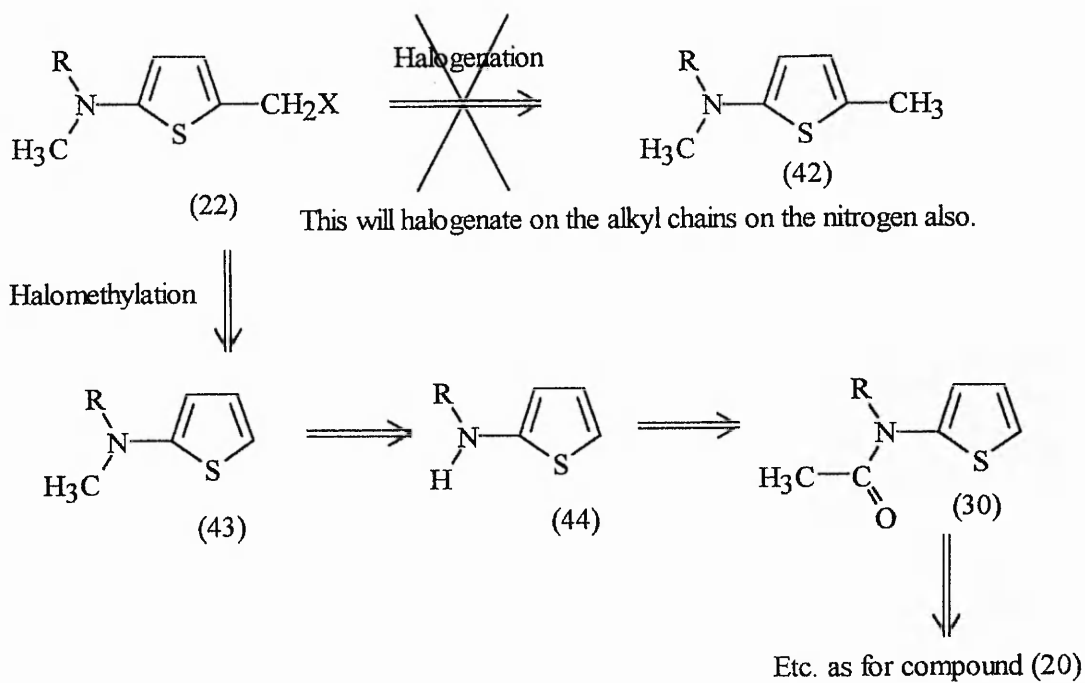
**Figure 4.16** The three different possible 2-methyl-nitrothiophenes.

#### 4.5.5 Synthesis of compound 21.

The first route was to nitrate 2-methylthiophene by the procedures that were outlined earlier. This reaction could produce three products, illustrated in Fig 4.16.

The second and third compounds were removed by washing with water after reaction with chlorosulphonic acid. The next stage was to halogenate the methyl group by either using N-bromosuccinimide or sulphuryl chloride. This proved to be very unsatisfactory, due to the extremely low yields obtained. The other two routes were unsuccessful because the halomethylation step invariably either gave intractable tars or dithienylmethanes.

4.5.6 Retrosynthetic analysis of compounds 22. (see section 4.5.1)



#### 4.5.7 Synthesis of compounds 22.

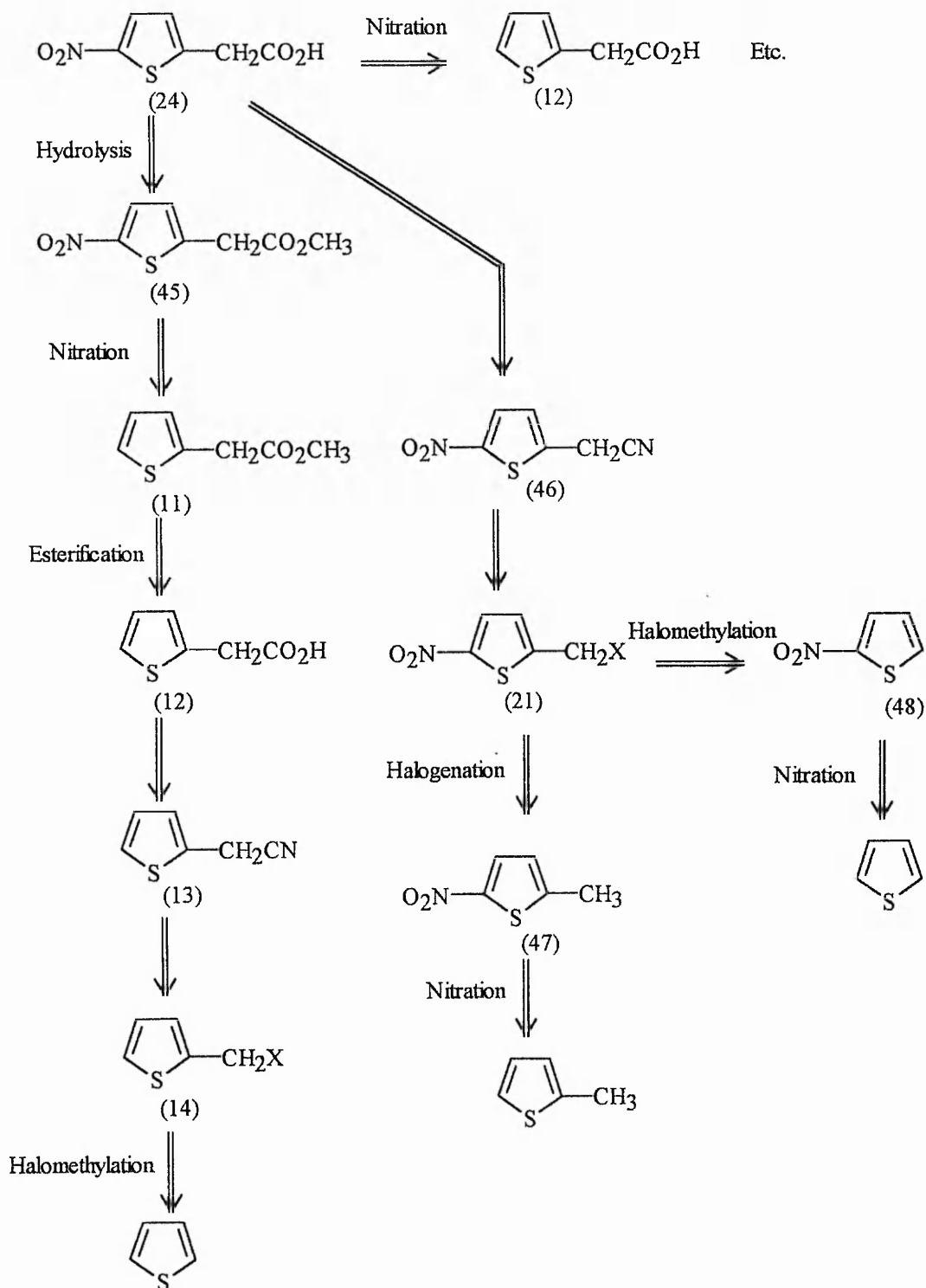
There was no attempt to synthesize this compound because it can clearly be seen from the retrosynthetic analysis that the problems that were encountered and described in the synthesis of compounds (20) are still present. It was then decided to try to make the halomethyl compound of the secondary amide (compounds (28)) to synthesize compounds (36). This again proved to be unfruitful either because of

a) the failure of the halomethylation step

or b) halogenation of the N-alkyl side chains when using N-bromosuccinimide or sulphuryl chloride when trying to halogenate the methyl group if the 2-methylthiophene is used as the starting material, (this would interfere with the Wittig reaction producing multiple products). It is also not possible to perform the halogenation stage before both N-alkylation steps because of the probability that the halomethyl compounds would interfere in the N-alkylation reaction and produce dimers, trimers, etc.



4.5.8 Retrosynthetic analysis of compound 24. (see section 4.5.1)



#### 4.5.9 Synthesis of compound 24.

The first method was to attempt to nitrate thiophene-2-acetic acid directly; this, however, only produced a polymeric tar by any of the nitration methods employed. The next route was to form the methyl ester of the acid and then nitrate that. The ester was formed by either heating to reflux in methanol for five hours with a small catalytic amount of concentrated sulphuric acid or by stirring for 30 minutes in dry diethyl ether with methanol, N,N-dicyclohexylcarbodiimide (D.C.C.) and the catalyst 4-pyrrolidinopyridine (both methods giving the desired product in excess of 95%). The nitration of the ester proceeded smoothly and in high yields similar to that of thiophene. The next stage was to attempt to hydrolyse the ester to the acid. Many methods were attempted, but in no case was a satisfactory result achieved. The problems that were encountered were either that an intractable tar was produced or that the compound was left unchanged. Compound (24) could not be synthesized by the halogenation or halomethylation methods because of the problems that were outlined earlier.

4.5.10 Retrosynthetic analysis of compound 25. (see section 4.5.1)

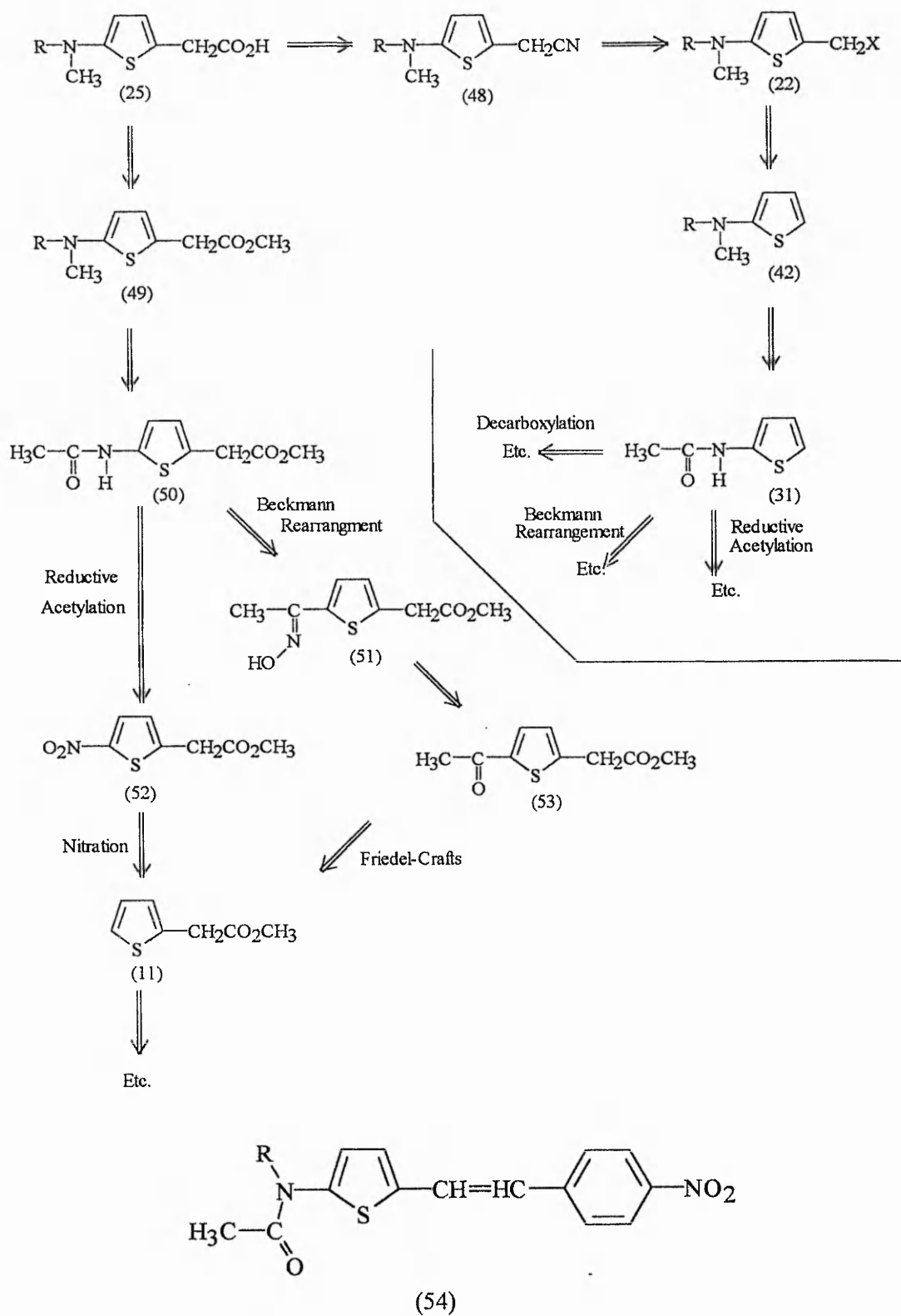


Figure 4.17

#### **4.5.11 Synthesis of compound 25.**

The synthesis of compound (25) had all the problems that were encountered in the synthesis of compounds (20-24) and was therefore discounted.

Since the author had been unsuccessful in synthesising one of the building blocks necessary for producing the final molecules, ie. compounds (36), it was then decided to replace one of the troublesome thiophene moieties with its benzene analogue, so as to obtain compounds (54) (see Fig. 4.17).

One of the building blocks, 4-nitrobenzyl bromide, is available from the Aldrich Chemical Company.

#### **4.5.12 Synthesis of compound 54.**

This compound was synthesized by the Wittig reaction using 4-nitrobenzyl-triphenylphosphonium bromide and compound (29). The 4-nitrobenzyl-triphenylphosphonium bromide was synthesized by dissolving 4-nitrobenzyl bromide in dry diethyl ether and adding an equimolar amount of triphenylphosphine and warming gently. The 4-nitrobenzyltriphenylphosphonium bromide precipitated out and was then filtered off and stored in a vacuum desiccator.

The Wittig reaction was performed by suspending the triphenylphosphonium salt in dry T.H.F. and adding a slight molar excess of butyl lithium, dropwise. This gave a blood red suspension of the ylide. Then compounds (29) were added and the reaction was complete almost immediately. The product was purified by repeated column chromatography, giving pure compounds (54) in slightly less than 50% yield.

The possible future of this work could be to synthesize a compound with the benzene and thiophene moieties transposed, as in compounds (55) in Fig. 4.18. This would probably be better because the free amine would be on the benzene ring and

therefore more stable. This could be made from the building blocks shown in Fig. 4.18.

It might also be an idea to increase the electron density in the  $\pi$ -system by replacing the thiophene ring by a 2,2'-bithiophene system. This would have the further beneficial effect that the alkyl chain would not have to be as long to provide insolubility. Thus the dilution of the non-linear optical effect due to the relatively large spacing of the  $\pi$ -systems in the molecular lattices of the Langmuir-Blodgett multilayers would be reduced.

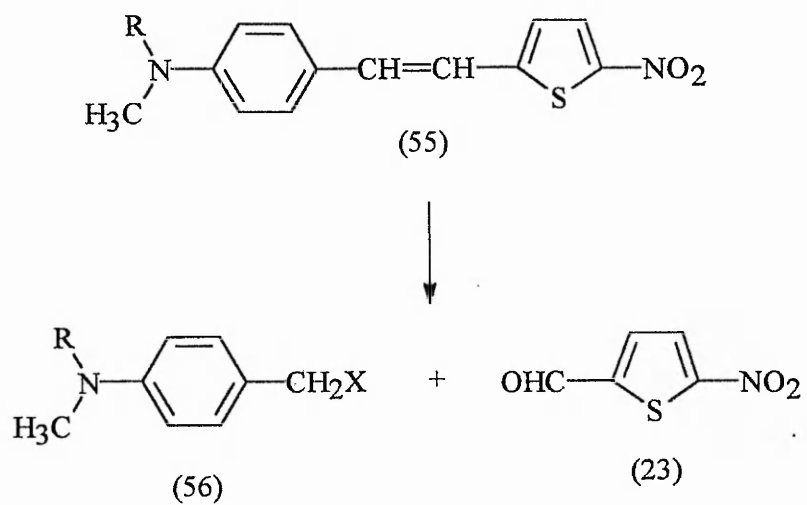


**Figure 4.18**

#### 4.6 Langmuir-Blodgett discussion.

Table 4.1 summarizes the results obtained for the simple amphiphilic thiophenes that were prepared for preliminary study. For each individual molecule it can be seen that the pH of the subphase has very little effect on the area per molecule. If anything the area per molecule at pH = 9.0 is slightly larger than that observed at pH = 4.0, which could be accounted for by the association of the acid groups into dimers with a large cadmium ion in the middle. The area per molecule for the molecules in group two are larger than those in groups one and three. This is probably a consequence of the carbonyl group next to the thiophene moiety in the group two molecules preventing the molecules from packing as close together as those in groups one and three, which do not have this carbonyl group. It can be seen from the time stability experiments that the longer the hydrophobic hydrocarbon 'tail', the more stable the molecules are to dissolution and/or collapse; furthermore, the molecules in group two are less stable than those of corresponding length in group three. This is again probably due the lower packing density, and hence reduced intermolecular interactions, relative to the group three molecules. When comparing molecules of the same overall length but with the thiophene moiety in a different position along the carbon chain (cf. 1h with 3j), it can be seen that there is very little difference in monolayer stability.

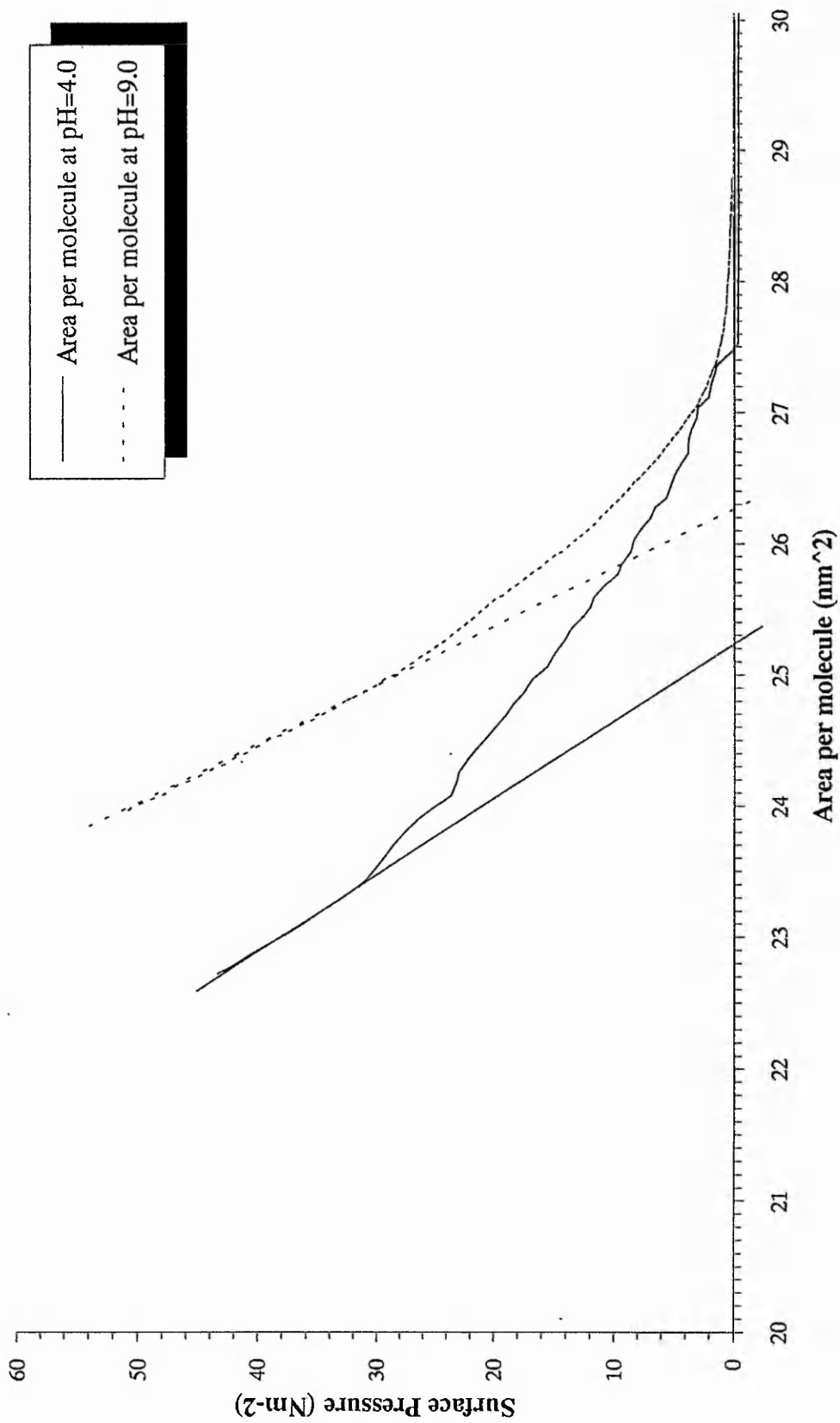


**Figure B.1** Area-Pressure Isotherm of 4'-(5-tetradecyl-2-thienyl)-butanoic acid (compound Ig).



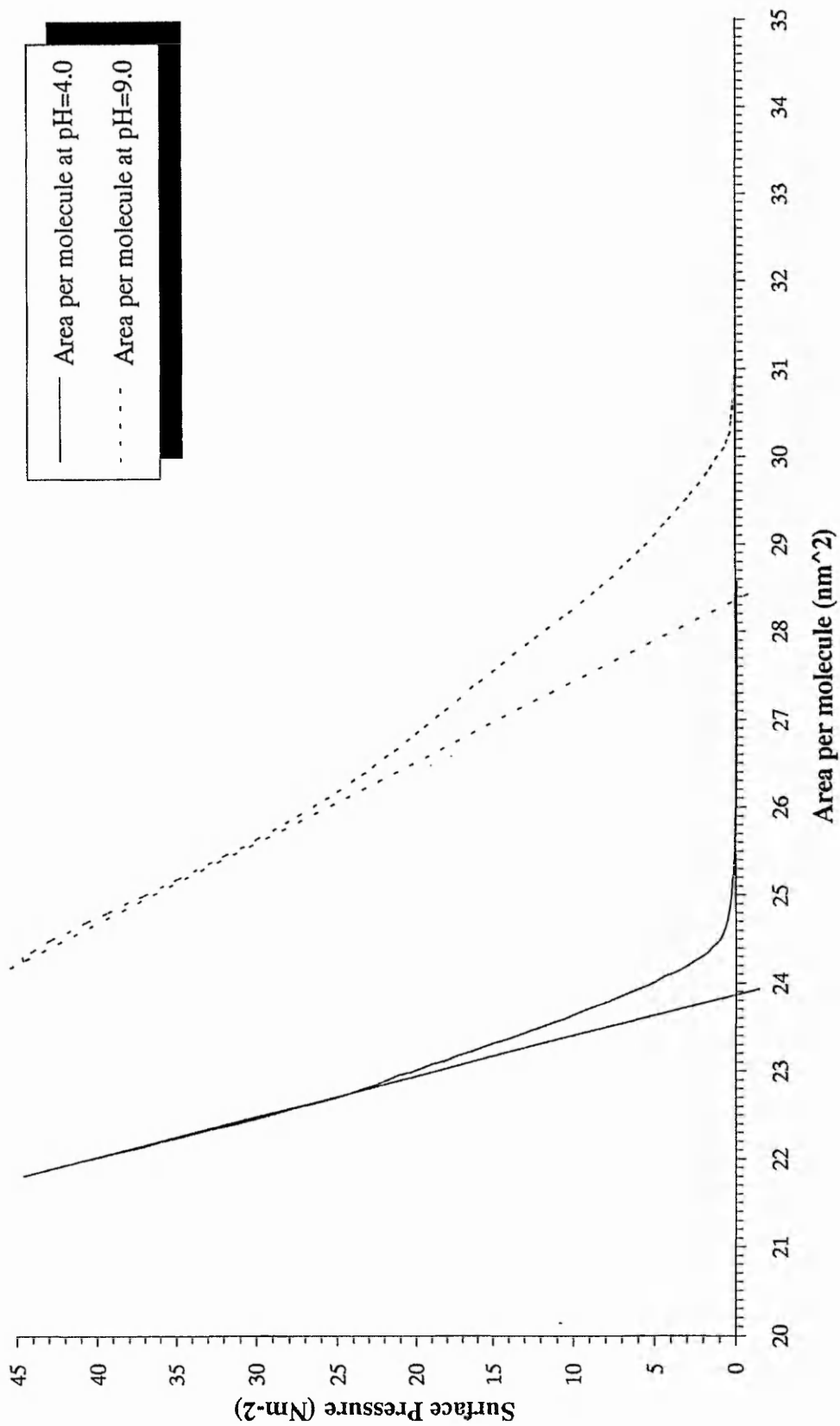


Figure B.2 Area-Pressure Isotherms of 4'-(5-hexadecyl-2-thienyl)-butanoic acid (compound 1h).

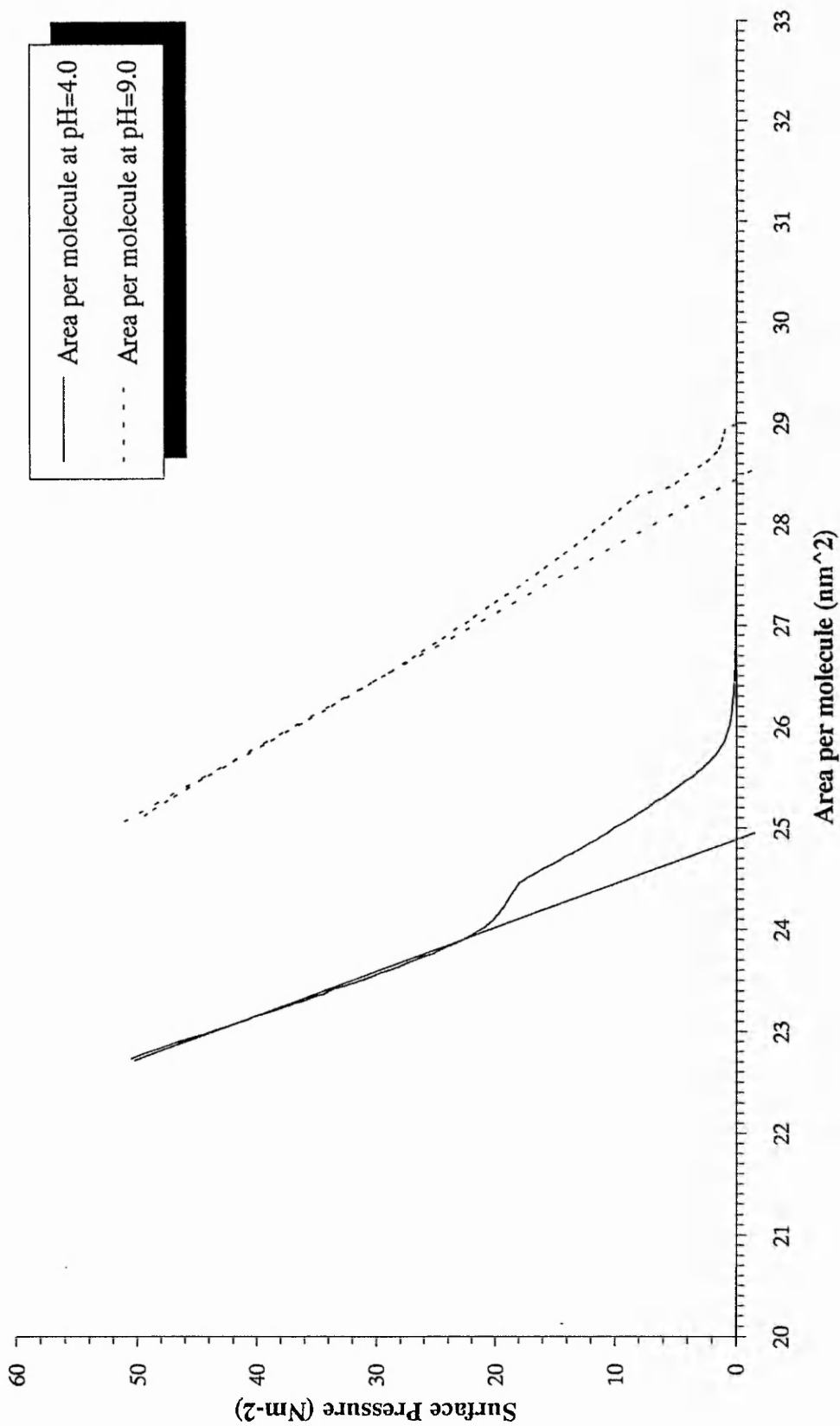


Figure B.3 Area-Pressure Isotherm of 4'-(5-heptadecyl-2-thienyl)-butanoic acid (compound Ii).

From the representative selection of isotherms (Figs. B.1 to B.15), it can be seen that these compounds do not produce the type of isotherm that is obtained from a classical compound such as stearic acid, ie they do not have the three distinct phases of 2-dimensional 'gases', 'liquids' and 'solids'. These compounds give an isotherm that is somewhat expanded in nature, some more than others (eg. Figs. B.6 and B.8). The expanded nature is more pronounced in the isotherms of monolayers spread on a subphase with a pH = 9.0 as opposed to a subphase of pH = 4.0 (eg. Fig. B.5). It can be seen in some of the isotherms that there are various phase changes occurring in the isotherm; these probably correspond to some of the phase changes that are described by Stenhagen<sup>(157)</sup> it would be necessary to do more experimentation in order to ascertain which phase they corresponded to.

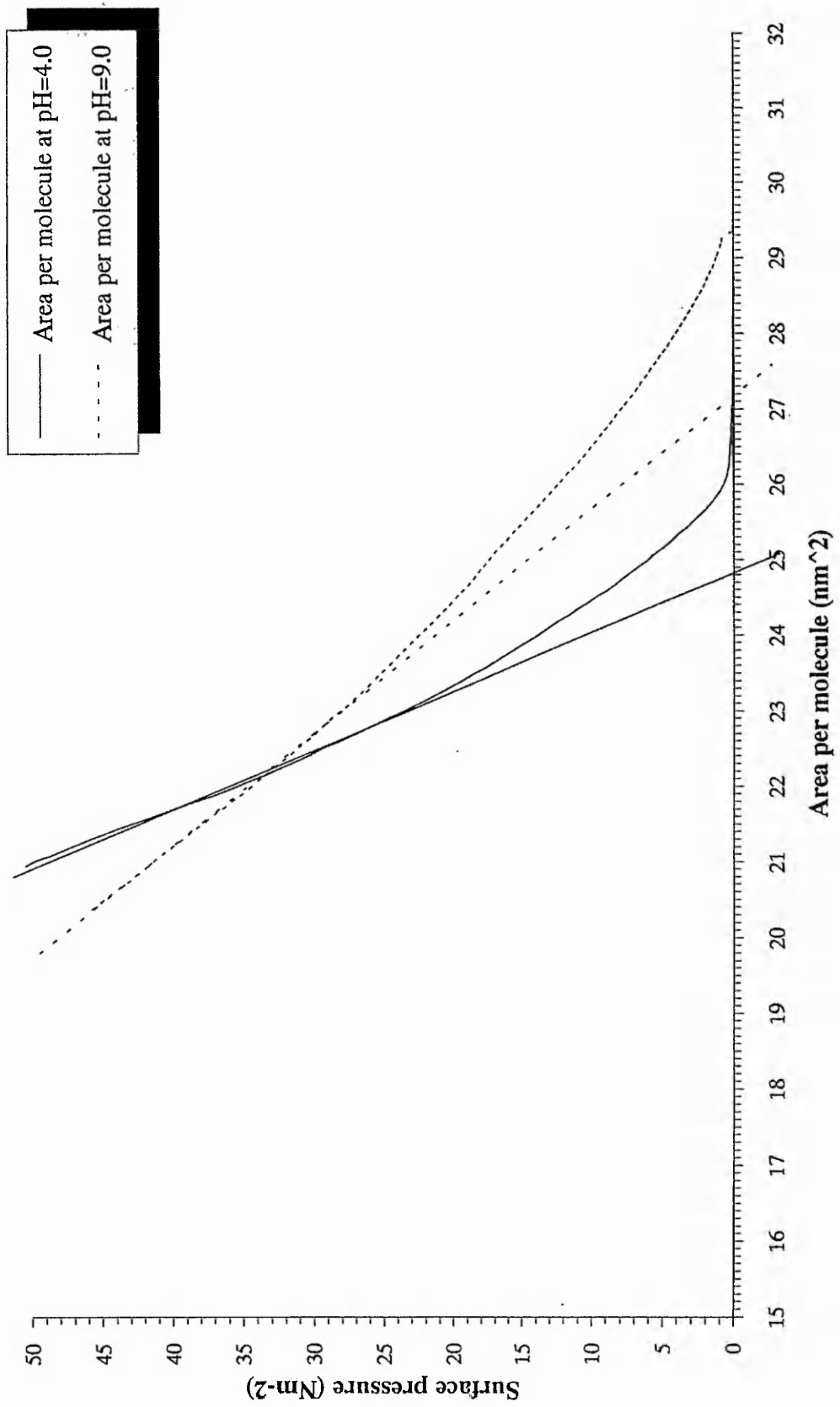


Figure B.4 Area-Pressure Isotherm of 4'-(5-octadecyl-2-thienyl)-butanoic acid (compound 1j).

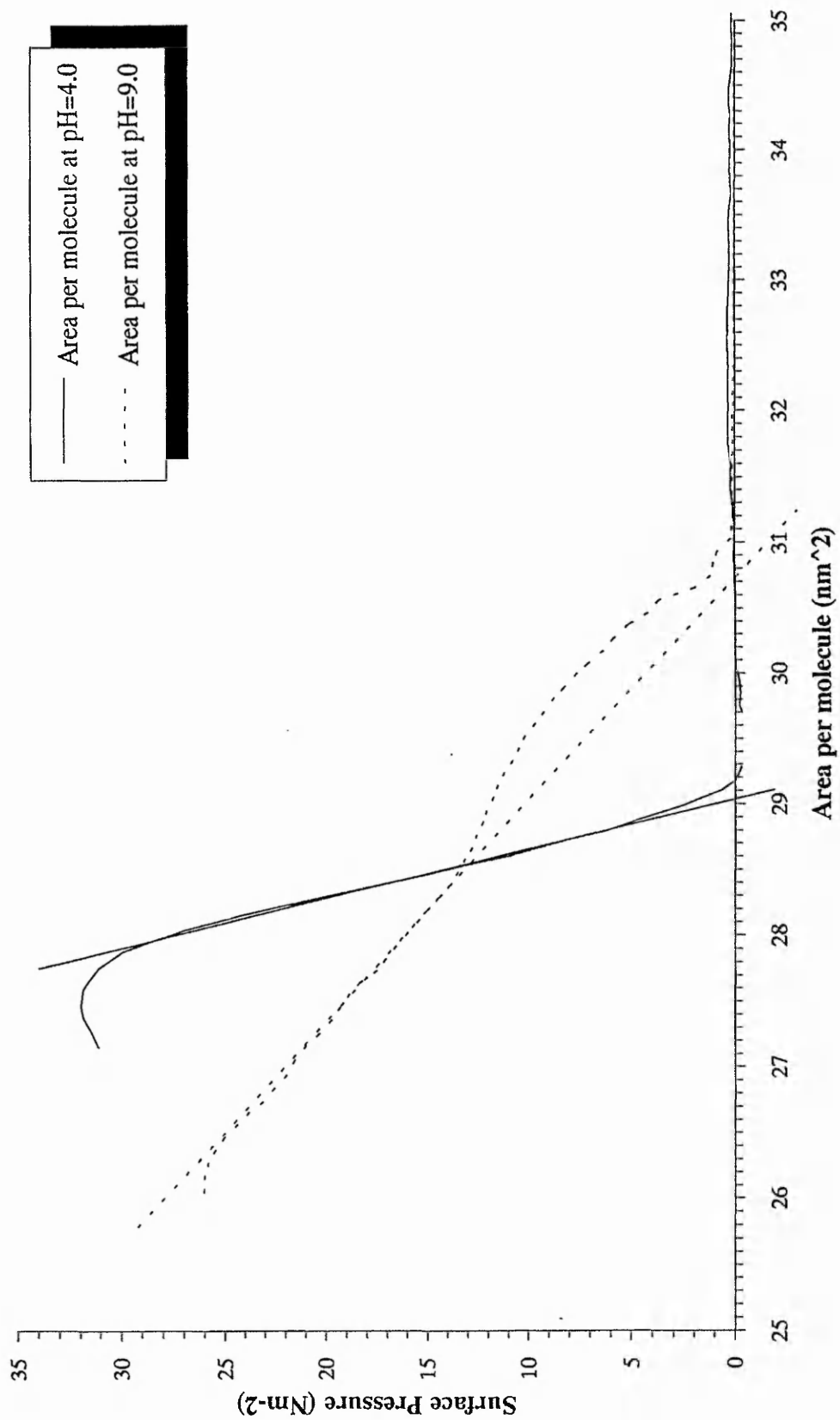


Figure B.5 Area-Pressure Isotherm of 3'-(5-tetradecyl-2-thienoyl)-propanoic acid (compound 2g).

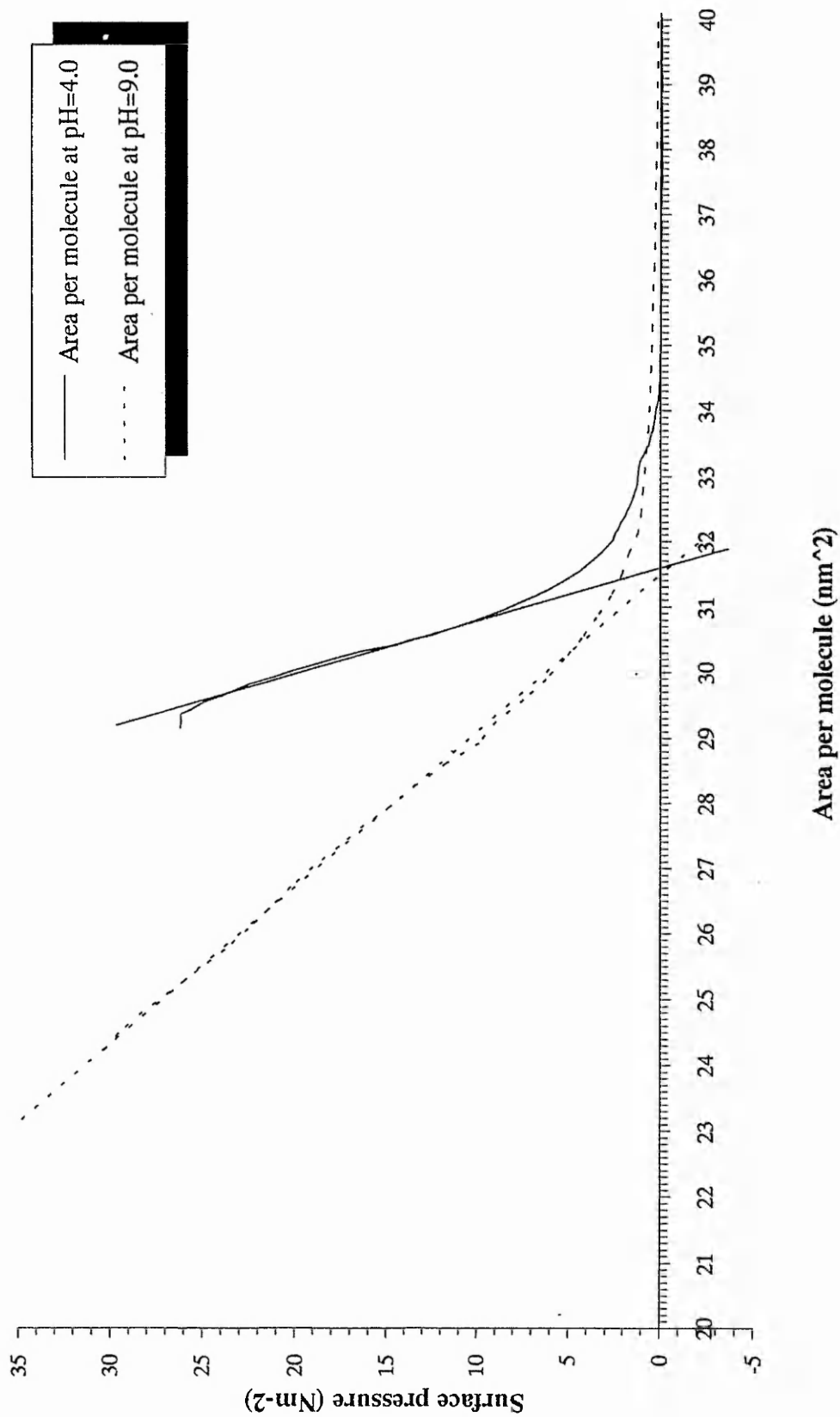


Figure B.6 Area-Pressure Isotherm of 3'-(5-hexadecyl-2-thenoyl)-propanoic acid (compound 2h).

Table 4.1

|   | Compound | Area/Molecule (nm <sup>2</sup> )                                      |      | Time Stability (cm <sup>2</sup> min <sup>-1</sup> ) |       | Transfer Ratio (%) |       |       |
|---|----------|-----------------------------------------------------------------------|------|-----------------------------------------------------|-------|--------------------|-------|-------|
|   |          | pH=4                                                                  | pH=9 | pH=4                                                | pH=9  | pH=4               | pH=9  |       |
| 1 | g        | c <sub>14</sub> Th(CH <sub>2</sub> ) <sub>3</sub> CO <sub>2</sub> H   | 25.3 | 26.3                                                | 0.25* | 0.057              | 93.2  | 99.6  |
|   | h        | c <sub>16</sub> Th(CH <sub>2</sub> ) <sub>3</sub> CO <sub>2</sub> H   | 23.9 | 28.4                                                | 0.019 | 0.12               | 96.8  | -     |
|   | i        | c <sub>17</sub> Th(CH <sub>2</sub> ) <sub>3</sub> CO <sub>2</sub> H   | 24.9 | 28.5                                                | 0.019 | 0.028              | 97.5  | -     |
|   | j        | c <sub>18</sub> Th(CH <sub>2</sub> ) <sub>3</sub> CO <sub>2</sub> H   | 24.9 | 27.2                                                | 0.013 | 0.018              | 99.8  | -     |
| 2 | g        | c <sub>14</sub> ThCO(CH <sub>2</sub> ) <sub>2</sub> CO <sub>2</sub> H | 29.1 | 30.8                                                | 4.56  | 1.55               | -     | 110.9 |
|   | h        | c <sub>16</sub> ThCO(CH <sub>2</sub> ) <sub>2</sub> CO <sub>2</sub> H | 31.6 | 31.5                                                | 0.42  | 0.39               | -     | 103.3 |
|   | i        | c <sub>17</sub> ThCO(CH <sub>2</sub> ) <sub>2</sub> CO <sub>2</sub> H | 31.5 | 31.1                                                | 0.055 | 0.059              | -     | 96.1  |
|   | j        | c <sub>18</sub> ThCO(CH <sub>2</sub> ) <sub>2</sub> CO <sub>2</sub> H | 31.6 | 31.1                                                | 0.042 | 0.074              | 95.7  | -     |
| 3 | g        | c <sub>14</sub> ThCH <sub>2</sub> CO <sub>2</sub> H                   | 26.4 | 26.6                                                | 0.13  | 0.39               | 109.7 | -     |
|   | h        | c <sub>16</sub> ThCH <sub>2</sub> CO <sub>2</sub> H                   | 26.2 | 27.6                                                | 0.06  | 0.097              | 95.6  | 104.5 |
|   | i        | c <sub>17</sub> ThCH <sub>2</sub> CO <sub>2</sub> H                   | 25.6 | 29.5                                                | 0.073 | 0.078              | 93.3  | -     |
|   | j        | c <sub>18</sub> ThCH <sub>2</sub> CO <sub>2</sub> H                   | 27.4 | 27.7                                                | 0.029 | 0.07               | 94.2  | -     |
| 4 |          | C <sub>9</sub> COTh(CH <sub>2</sub> ) <sub>3</sub> CO <sub>2</sub> H  | 27.5 | -                                                   | 2.83  | -                  | -     | -     |

\* This is not taken from an actual time stability study, but the beginning of a dipping record and therefore is probably not a true reflection of the stability of the compound.

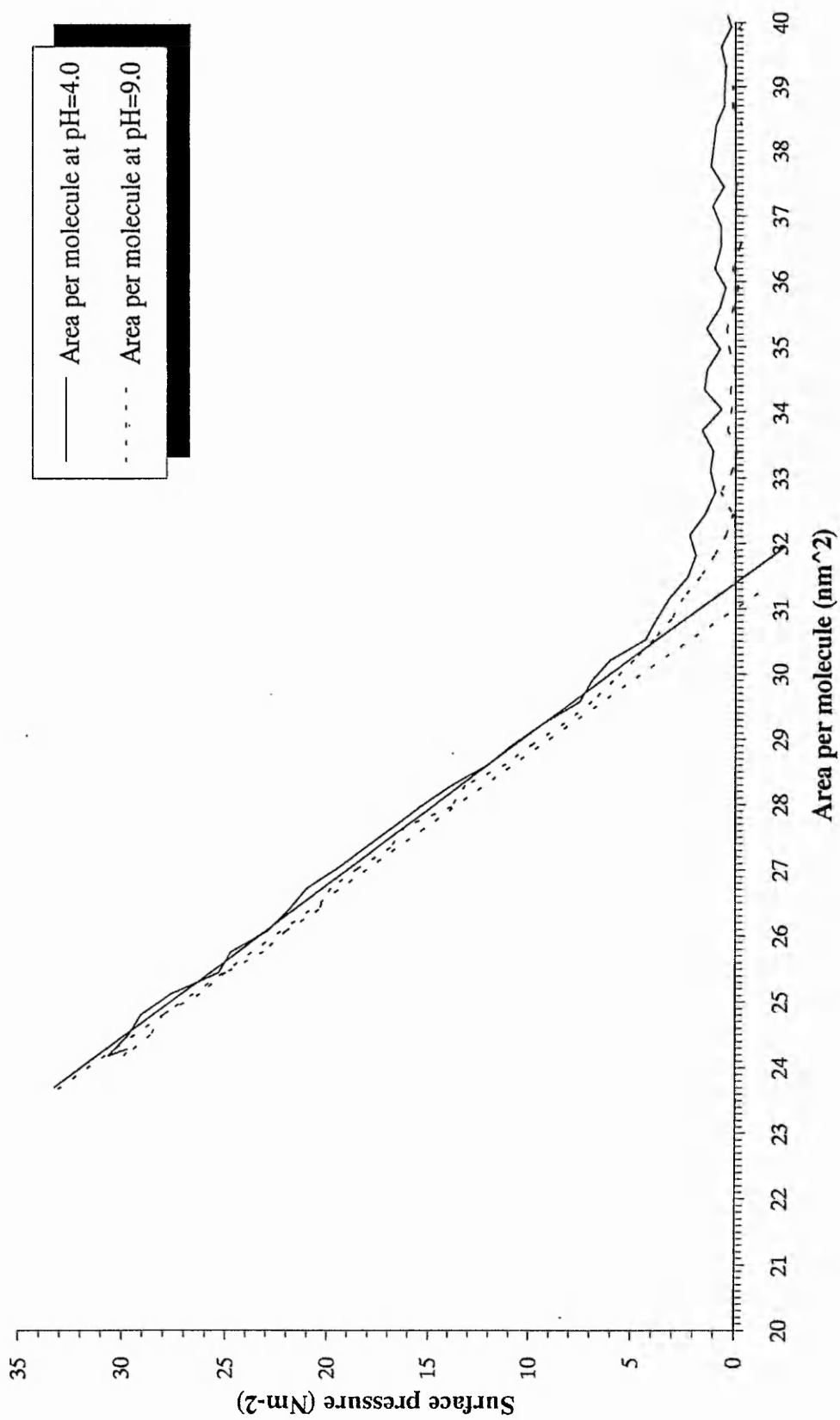


Figure B.7 Area-Pressure Isotherm of 3'-(5-heptadecyl-2-thenoyl)-propanoic acid (compound 2i).



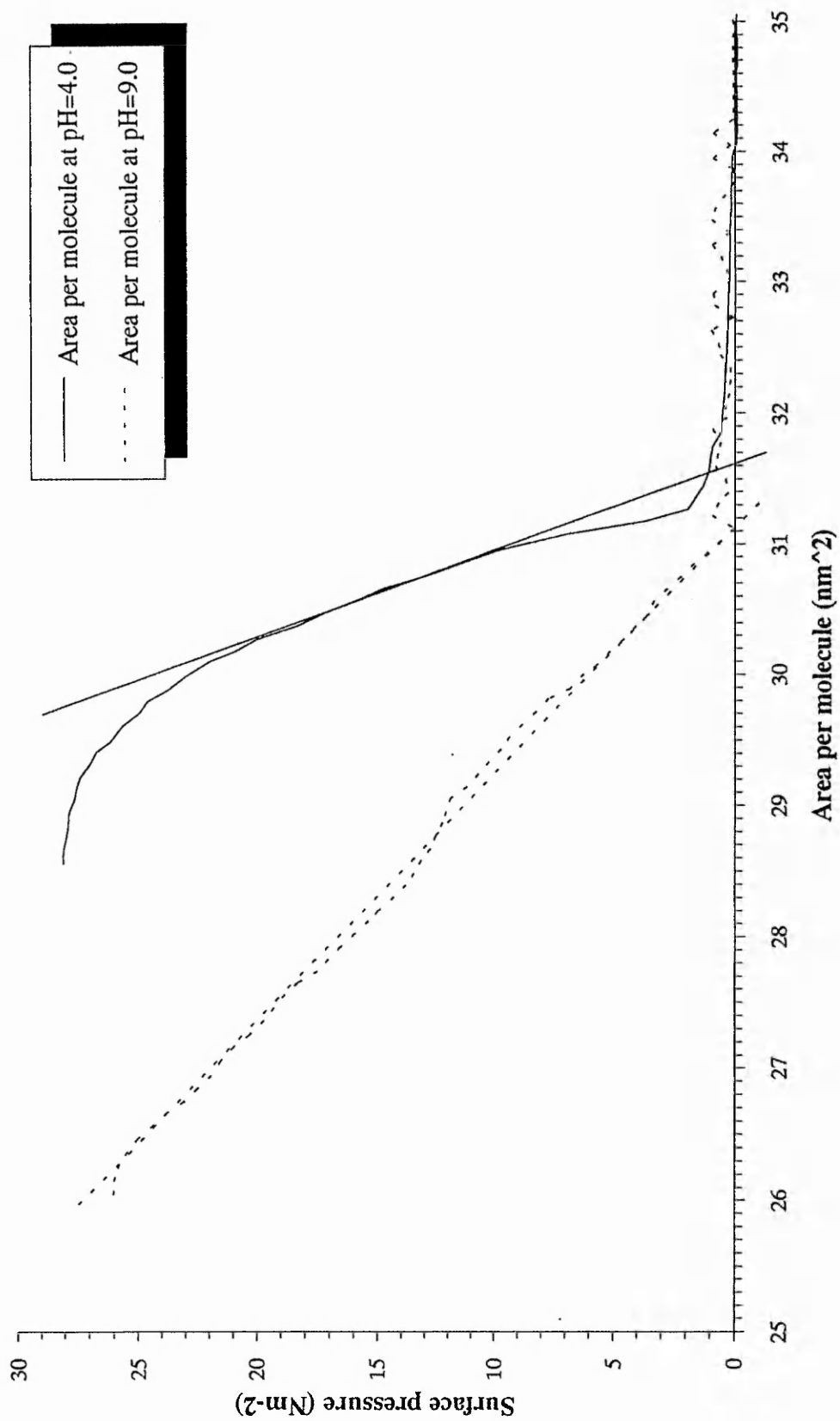


Figure B.8 Area-Pressure Isotherm of 3'-(5-octadecyl-2-thienoyl)-propanoic acid (compound 2j).

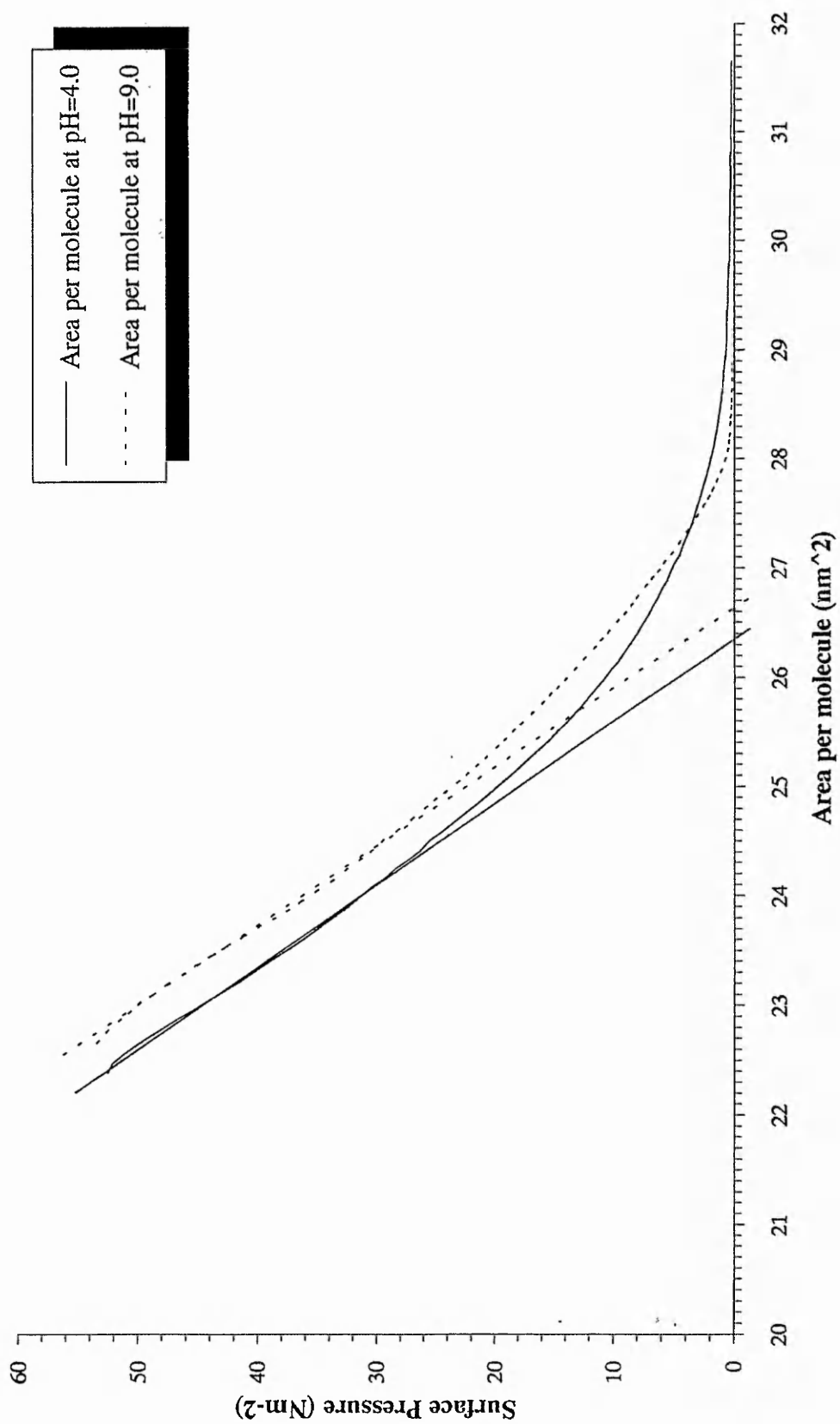


Figure B.9 Area-Pressure Isotherm of 2-tetradecylthiophene-5-ethanoic acid (compound 3g).

The transfer ratio of the monolayers is almost the same for all the compounds studied in this manner; any discrepancies are probably due to one or more of the following factors:

- A) Factors decreasing apparent film transfer.
  - i) Incomplete cleansing of the substrate.
  - ii) Minor surface defects on the substrate.
- B) Factors increasing apparent film transfer.
  - i) Vibration of the trough during deposition.
  - iii) The fracture of rigid monolayers as the substrate traverses the air-monolayer-subphase interface can cause a small amount of monolayer collapse in less stable films. This is most likely the cause of the greater than 100% transfer ratio of the films made from the compounds with the shorter 'tail'.

Compound 54 k (Fig. B.14) behaves in a similar manner to types 1-4 in that its isotherm does not exhibit distinct 'gas', 'Liquid' and 'solid' phases; however, it does show a steady increase in area per molecule as the pH of the subphase increases, which is probably due to the higher pH resulting in a greater tendency for the molecules to associate with the large cadmium ions in the subphase, causing them to have greater stability and slightly larger area per molecule. The isotherms of the mixtures of compound 54 k and arachidic acid (Fig. B.15) show a phase change that exhibits a progressively greater similarity to that of 'the ideal' stearic acid as the percentage of arachidic acid in the mixture is increased, culminating with the 30% of compound 54 k isotherm showing three very distinct regions. In the isotherms of compound 54 k at pH = 5.0 (Fig. B.14) it can be seen that there is a further phase

change whereby the surface pressure reached a local maximum at an area per molecule of approximately  $47\text{nm}^2$ . This could be due to the monolayer being initially compressed to a state where the region of conjugation, being fairly rigid due to the aromatic rings, is lying flat on the surface of the subphase; further compression may lead this region of conjugation to reorientate, resulting in a fall in the surface pressure, until the monolayer eventually adopts a more ordered packing arrangement. In the mixed monolayers there is also a decrease in the average area per molecule, towards that of pure arachidic acid, with an increase in the percentage of arachidic acid in the mixture, as would be expected.

It can be seen in the pure compound 54 k that the higher the pH of the subphase the more stable the monolayer is on the subphase, which leads to a better transfer ratio from the subphase to the substrate. As with the higher area per molecule reported earlier this is probably due to the association of a large cadmium ion with each pair of molecules of 54 k, as the cadmium chloride in the subphase should be totally dissociated in the aqueous medium will therefore be free to stabilise the compound on the subphase, resulting in a dimer structure consisting of one cadmium ion and two molecules of compound 54 k associating through the  $-\text{NO}_2^\ominus$  'head' group in a similar way to the carboxylic acid group in cadmium stearate.

The mixtures of compound 54 k and arachidic acid were prepared in order to convey some stability to the monolayers of compound 54 k and to aid the transfer from the subphase to the substrate. The transfer ratios of the mixtures of arachidic acid and compound 54 k were all approximately the same and therefore the 67:33 of compound 54 k to arachidic acid was chosen for subsequent experiments on alternate layer structures, since it contained the highest concentration of active material. The

alternating layer deposition had to be performed at  $\text{pH} = 8$  because films of arachidic acid are unstable at higher values of subphase  $\text{pH}$ . The superior transfer ratio of the mixtures when forming the alternating structures rather than monolayer films may be due to the arachidic acid component being more stable at the slightly lower  $\text{pH}$  employed in this set of studies; however, more experiments will have to be performed in order to confirm this.

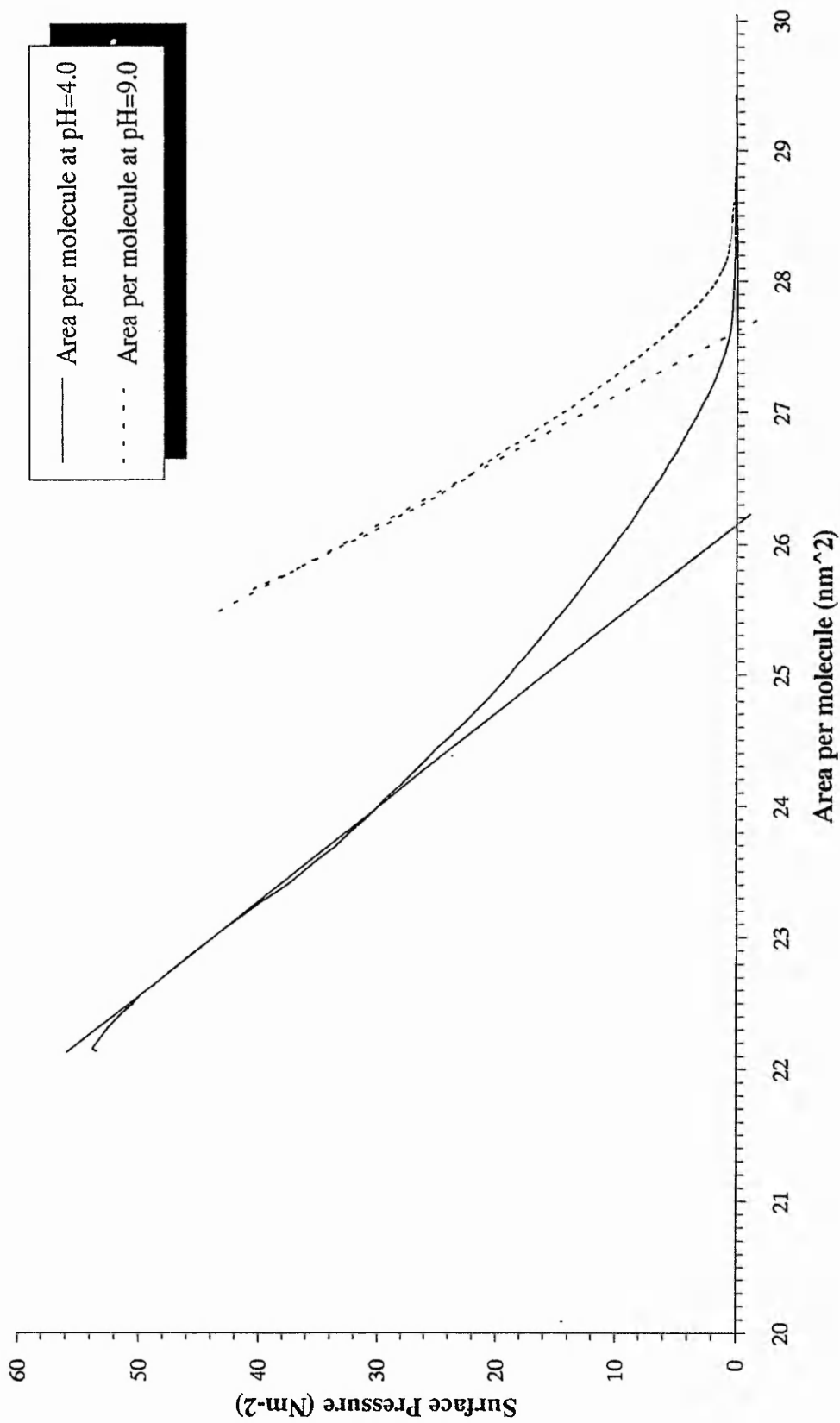


Figure B.10 Area-Pressure Isotherm of 2-hexadecylthiophene-5-ethanoic acid (compound 3h).

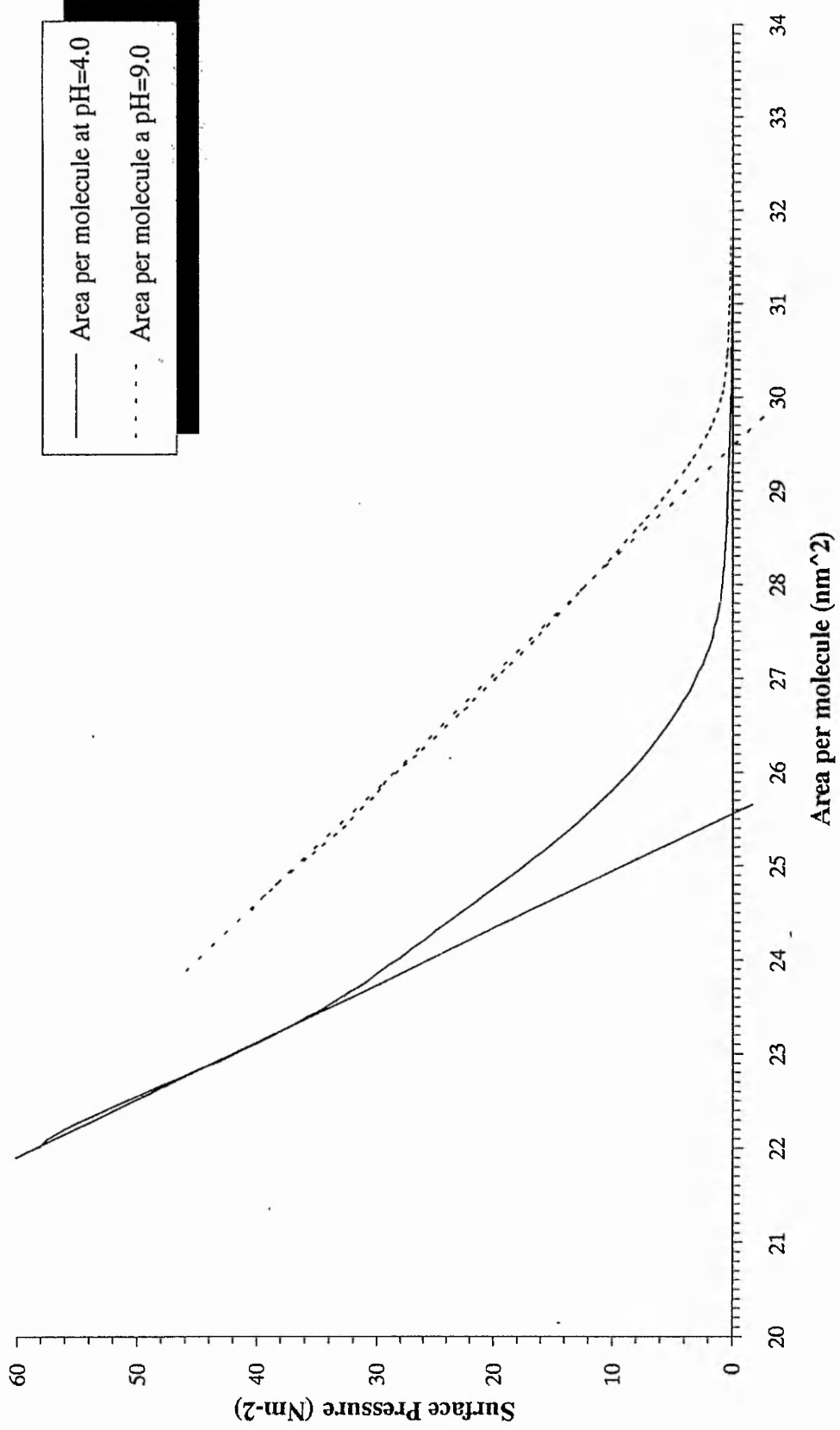


Figure B.11 Area-Pressure Isotherm of 2-heptadecylthiophene-5-ethanoic acid (compound 3i).

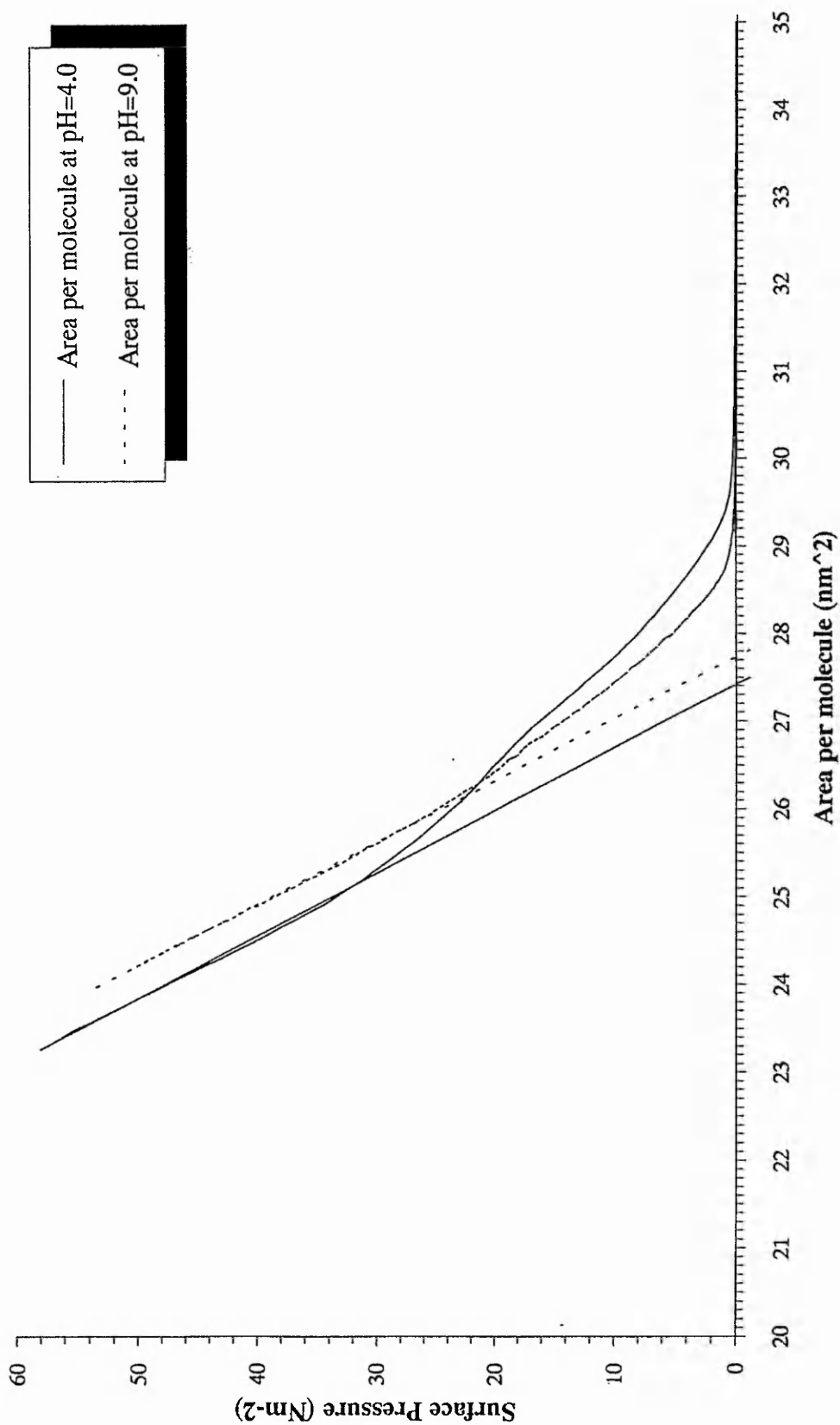


Figure B.12 Area-Pressure Isotherm of 2-octadecylthiophene-5-ethanoic acid (compound 3j).



**Table 4.2**

| Compound           | Area per Molecule (nm <sup>2</sup> ) |      |      | Decay Rate (cm <sup>2</sup> min <sup>-1</sup> ) |      |      | Transfer Ratio (%) |      |      | S.H.G Average* |
|--------------------|--------------------------------------|------|------|-------------------------------------------------|------|------|--------------------|------|------|----------------|
|                    | pH=5                                 | pH=7 | pH=9 | pH=5                                            | pH=7 | pH=9 | pH=5               | pH=7 | pH=9 |                |
| pure 54k           | 19.5                                 | 22.0 | 24.0 | 1.15                                            | 0.32 | 0.17 | 48.4               | 54.7 | 70.9 | 1.000          |
| 30:70 <sup>‡</sup> | 19.8                                 |      |      | -                                               |      |      | 77.1               |      |      | 0.113          |
| 50:50 <sup>‡</sup> | 23.2                                 |      |      | -                                               |      |      | 75.3               |      |      | 0.397          |
| 67:33 <sup>‡</sup> | 23.6                                 |      |      | -                                               |      |      | 76.3               |      |      | 1.059          |
| Alt 3 <sup>†</sup> | 39.5                                 |      |      | 0.13                                            |      |      | 103.5 <sup>§</sup> |      |      |                |
| Alt 5 <sup>†</sup> | 35.5                                 |      |      | 0.09                                            |      |      | 98.4 <sup>§</sup>  |      |      |                |
| Alt 7 <sup>†</sup> | 39.5                                 |      |      | 0.16                                            |      |      | 97.7 <sup>§</sup>  |      |      |                |
| Alt 9 <sup>†</sup> | 38.6                                 |      |      | 0.15                                            |      |      | 103.1 <sup>§</sup> |      |      |                |

54k E-1-(N'-docosyl-5'-acetamido-2'-thienyl)-2-(4''-nitrophenyl)-ethene

‡ These are mixtures of 54k to arachidic acid in the ratios shown. Experiments carried out at pH = 9.0 and between 18-20°C.

† These are alternate layers of arachidic acid and the 67:33 mixture deposited on three layers of arachidic acid on glass. Experiments carried out at pH = 8.0 and between 18-20°C. § These are average transfer ratios.

\* These are p→p SHG measurements. (see experimental), normalised relative to the figures for the pure monolayer.

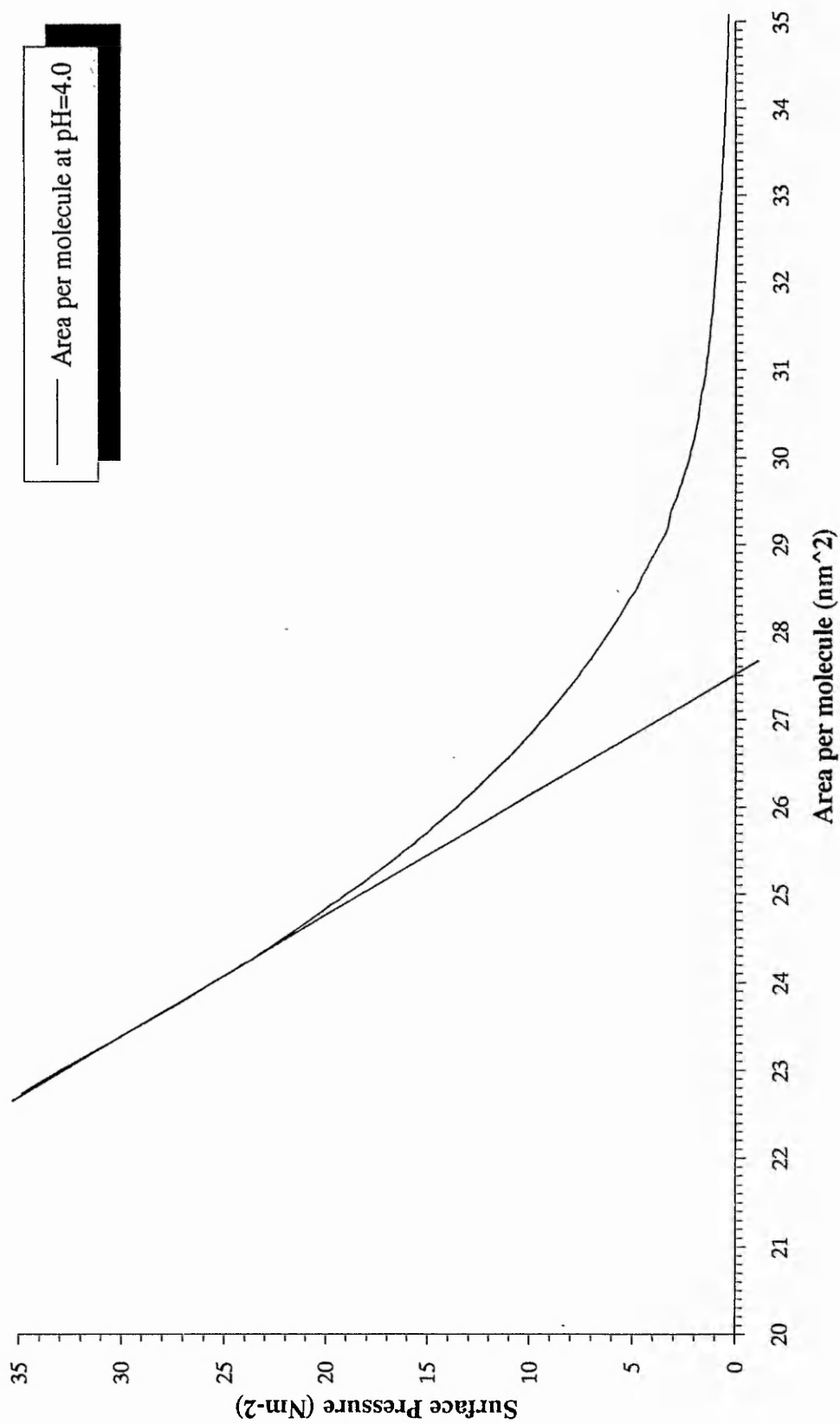
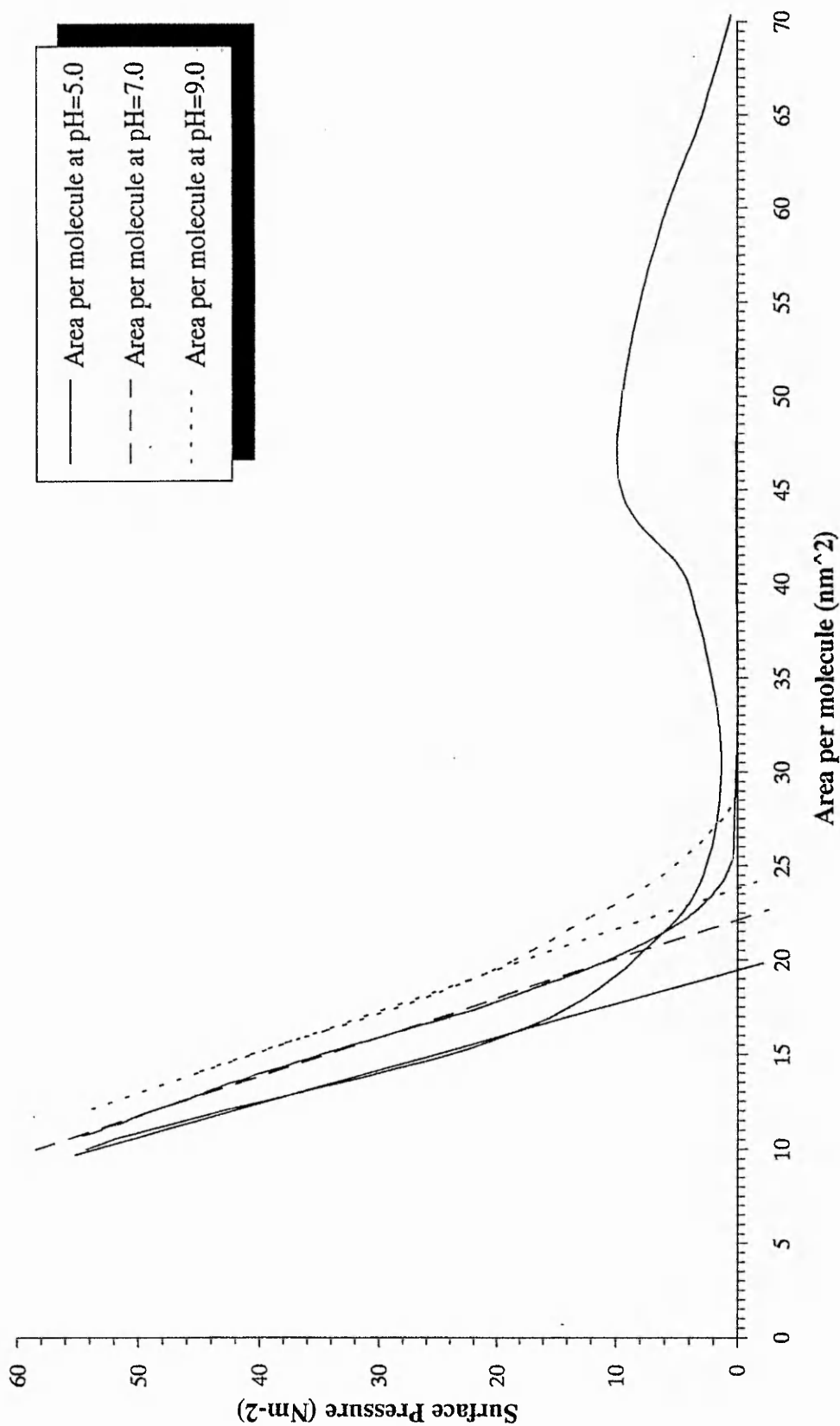


Figure B.13 Area-Pressure Isotherm of 6'-(5-decanoyl-2-thienyl)-hexanoic acid.



**Figure B.14** Area-Pressure Isotherm of E-1-(N-docosyl-5'-acetamido-2'-thienyl)-2-(4''-nitrophenyl)-ethene (compound 54k).

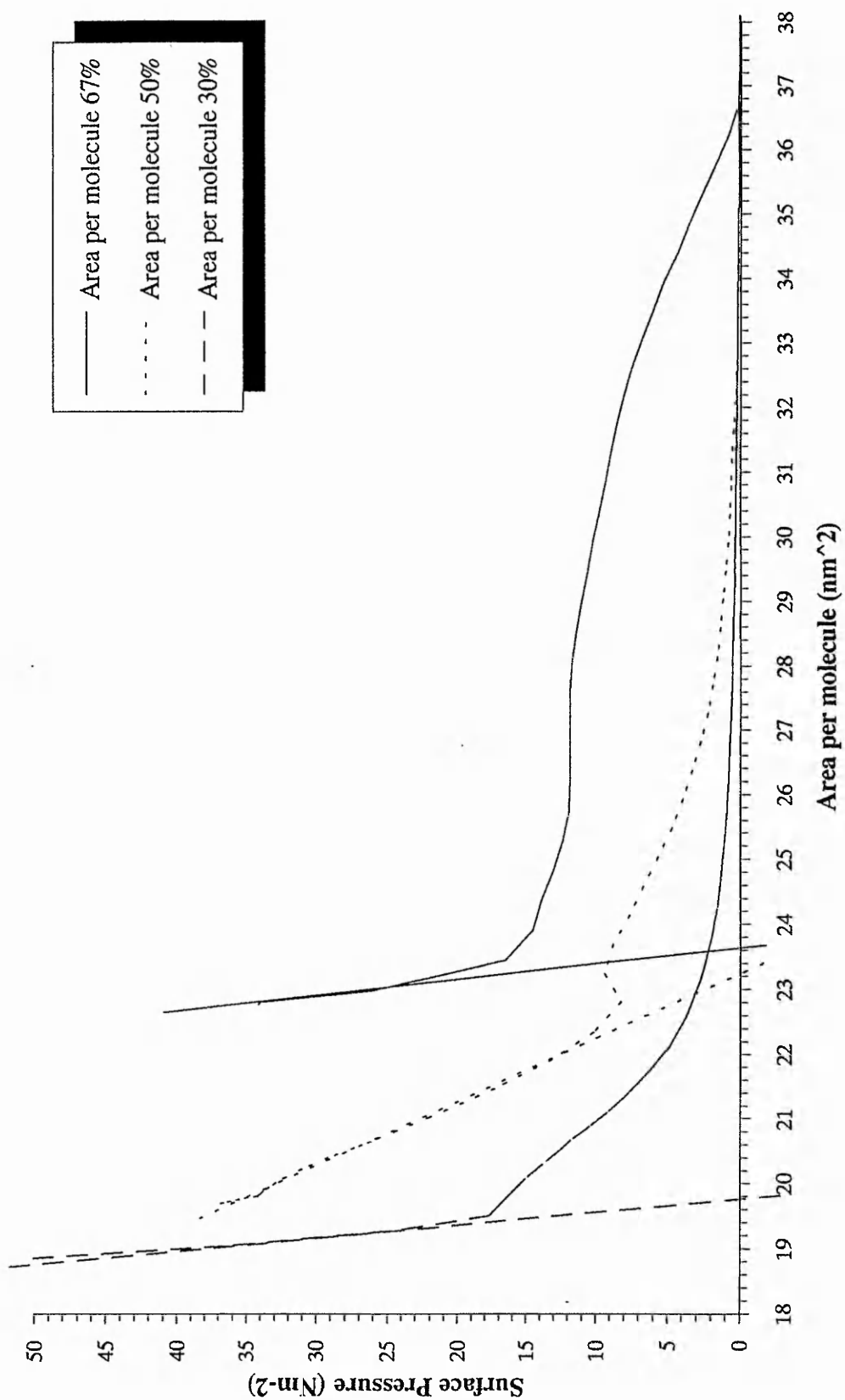


Figure B.15 Area-Pressure Isotherm of various mixtures of compound 5Ak and arachidic acid.

SHG studies were performed on structures consisting of  $n$  pairs of alternate layers of a 67% 54 k : 33% cadmium arachidate  $((C_{19}H_{39}CO_2)_2Cd)$  mixture and cadmium arachidate deposited on top of three layers of cadmium arachidate, where  $n=3,5,7,9$ . The results obtained were inconsistent, the greatest SHG being obtained from the  $n=7$  structure, but with values that varied by up to 30% from one region of the specimen to another. Although most of the data did reflect an increase in SHG with increasing  $n$  ( $n=3 < n=5 < n=9$ ), a single monolayer of the mixture deposited directly onto a glass substrate gave greater SHG than did the  $n=9$  film. The apparently anomalous result for the monolayer was probably due to a more favourable orientation of the chromophore in a monolayer bonded directly to the substrate compared with that adopted in subsequent layers. In addition, the slightly lower pH used in the formation of alternate layer structures may have been unfavourable to the deposition of the active component; the resulting poor quality may account for the scatter of the data, including the erroneous position in the sequence for  $n=7$ .

It can be seen from the SHG results of the monolayer mixtures of compound 54 k and cadmium arachidate that the higher the concentration of compound 54 k the greater the amount of SHG, up to a certain point (around the 70% active molecules). More experiments will have to be carried out to ascertain the best possible ratio. This result is in full agreement with the results on stilbene molecules found by Neal *et al*<sup>(158)</sup>. It is likely that the optimum conditions result from a trade off between having the maximum possible amount of compound 54 k and improving:-

- (a) the quality of deposition,
- (b) the molecular orientation within the film, and
- (c) the dielectric environment of the active species.

(d) the possible stabilisation of the layers by the possible interdigitation of the spacer molecule with the active molecules<sup>(159)</sup>.

In Fig. B. 16 a decay rate isotherm of 4'-(5-octadecyl-2-thienyl)-butanoic acid at pH 9.0 is shown, it also shows an example calculation of how the decay rate for a given compound at a particular pH is derived. It is worked out by drawing a best fit straight line through the decay curve ignoring the initial period when the film is settling down. The gradient of the slope is then calculated giving the average decay rate of the compound under these specific conditions. Fig. B. 17 shows a dipping record of 9 alternate layers of compound 54k and arachidic acid. The percentage compound transferred to the substrate is determined by subtracting the amount of compound that would be lost due to normal film decay from the total amount of compound removed from the surface and then dividing the result by the the surface area of the substrate.

Two energy minimised molecular models of compound 54 k, which were produced using the Chem-X molecular modelling computer program. Fig. 18 shows the *E* or *Trans* configuration and Fig. 19 shows the *Z* or *Cis* configuration.

A few atomic force microscope pictures are shown (Figs. 20 and 21). These show the packing arrangement of the molecules taken from different sites on the same sample of compound 54 k on the surface of silicon. It can be seen from the photographs that there is approximately 16 peaks in a 3.5 nm range which gives approximately 0.21 nm per peak giving an area of 0,0376 nm<sup>2</sup> (using the formula for a circle). This could be the effect produced by the hydrogen atoms at the end of the long alkyl chain.

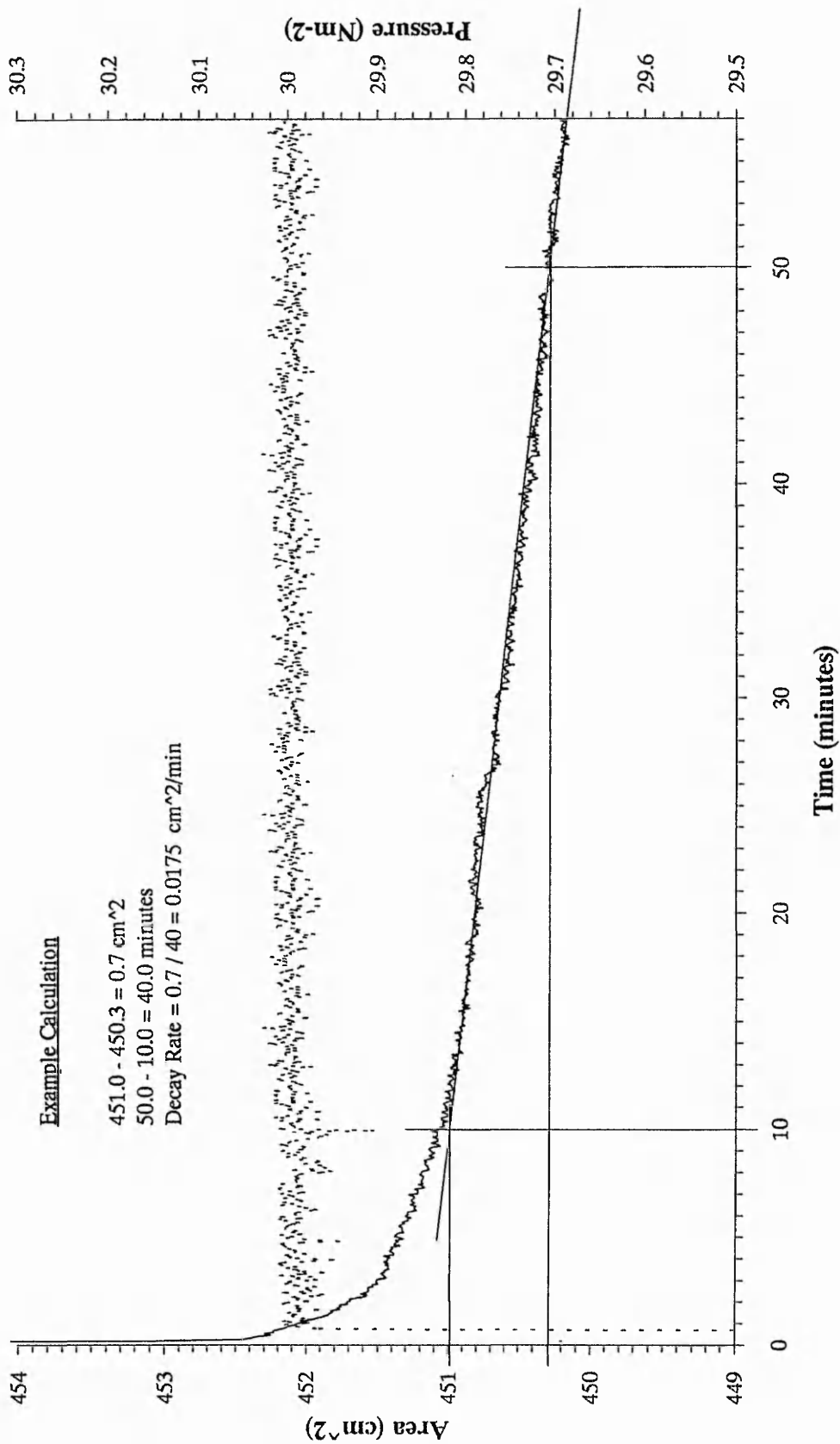


**Figure B.16** Decay Rate Isotherm of 4'-(5-octadecyl-2-thienyl)-butanoic acid at pH=9.0. The method and an example calculation for the determination of the decay rate is given.

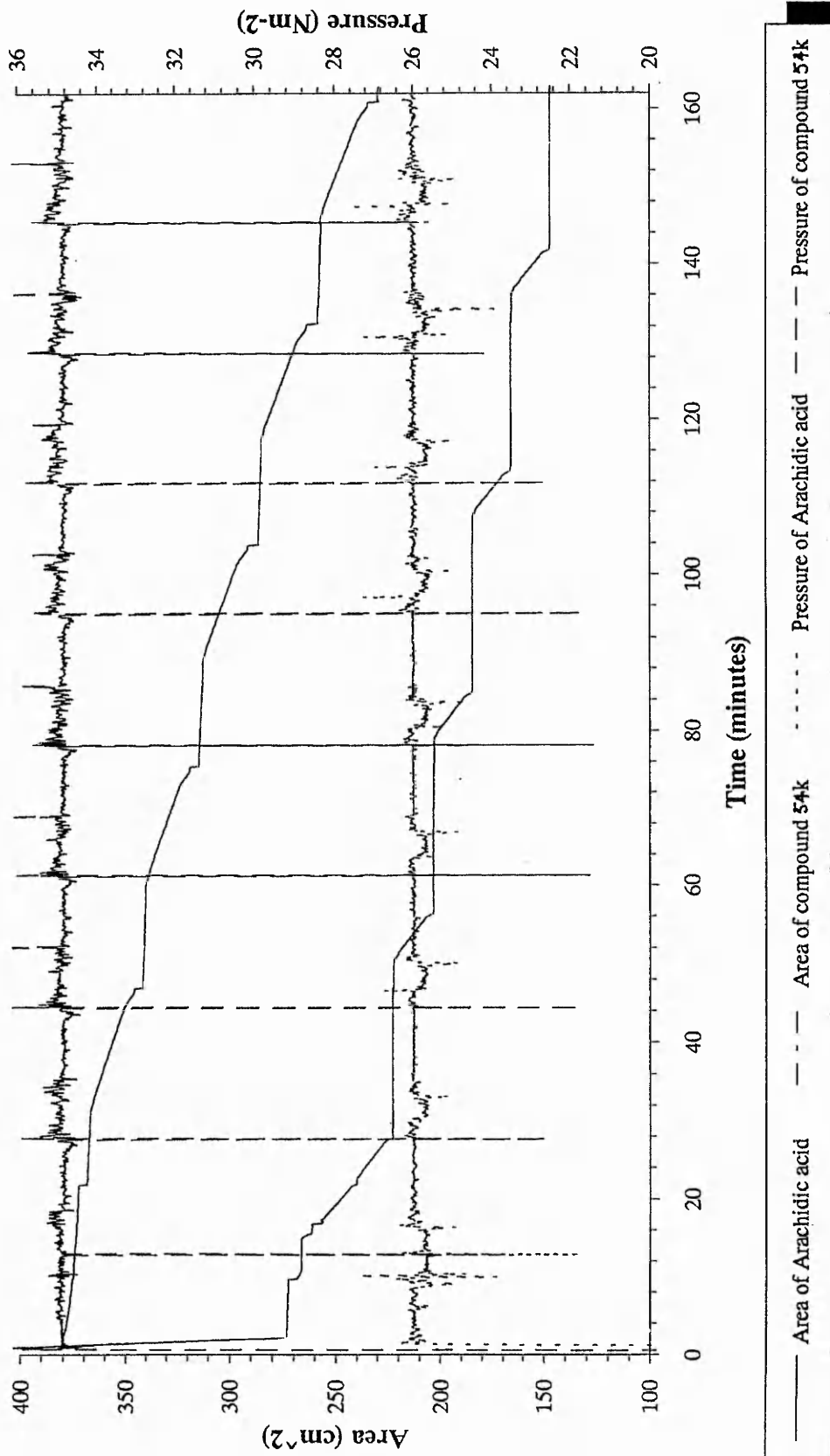


Figure B.17 Dipping Record of the 9 layers of compound 54k and arachidic acid.



# Experimental

## 5.0 LANGMUIR-BLODGETT MATERIAL SYNTHESIS EXPERIMENTAL

$^1\text{H}$  Nuclear Magnetic Resonance spectrographs were performed on a 60 MHz Perkin Elmer R24B instrument and a 270 MHz JEOL EX270,  $^{13}\text{C}$  Nuclear Magnetic Resonance spectrographs were performed on the 270 MHz JEOL machine. The infrared spectrographs were performed on a Perkin Elmer 1605 FT-IR spectrophotometer. The progress of most of the reactions were monitored by using Thin Layer Chromatography on silica gel plates.

Diethyl ether was dried over sodium metal. Tetrahydrofuran was dried by continuous heating under reflux with sodium metal and benzophenone, which turned the solution blue when the tetrahydrofuran was dry.

### 5.1 Preparation of mono methyl succinate.

Succinic anhydride (200 g, 2 moles) and absolute methanol (97 ml) were heated under reflux on a steam bath for 35 minutes. The mixture was swirled frequently by hand until it became homogeneous; it was then heated for a further 25 minutes. After removal of the excess of methanol by evaporation, the liquid was allowed to cool then dried in a vacuum desiccator to yield a white solid, (262.4 g, 99%), Mp. = 56-58°C.  $\nu_{\text{max}}$  (KBr) ( $\text{cm}^{-1}$ ) 3500-2500br (OHstr), 2960st (aliphatic C-Hstr), 1760st (C=Ostr from carboxylic acid), 1700st (C=Ostr from carboxylic ester), 1450-1150v (C-Hdef), 1170st (C-Ostr from carboxylic ester)  $\text{cm}^{-1}$ .  $\delta_{\text{H}}$ (DMSO) (ppm) 2.55 (4H, t,  $2\text{CH}_2$ ), 3.60 (3 H, s,  $\text{OCH}_3$ ) and 11.2 (1 H, br, s,  $\text{CO}_2\text{H}$ , disappears on  $\text{D}_2\text{O}$  shake).

### 5.2 Preparation of methyl half ester succinyl chloride.

Mono methyl succinate (69 g, 0.52 moles) was stirred with thionyl chloride for 3-4 hours, then the excess of thionyl chloride was removed by vacuum distillation.

The crude product was then distilled to give a colourless oil of the pure methyl half ester succinyl chloride, (71 g, 90%), Bp. = 75-80°C @ 1.5 mm Hg.  $\nu_{\max}$  (film) ( $\text{cm}^{-1}$ ) 2980st (aliphatic C-Hstr), 1800st (acid chloride C=Ostr), 1750st (ester C=Ostr), 1215m (C-Ostr)  $\text{cm}^{-1}$ .  $\delta_{\text{H}}$ ( $\text{CDCl}_3$ ) (ppm) 2.45 (2 H, t,  $\text{CH}_2$ ), 3.05 (2 H, t,  $\text{CH}_2$ ) and 3.45 (3 H, s,  $\text{OCH}_3$ ).

### 5.3 Preparation of compounds 1 and 2. (via compounds 3-6)

#### 5.3.1 Step 1: Friedel-Crafts acylation.

##### Method 1.

The carboxylic acid chloride (0.1 moles) was added dropwise to a well stirred solution of tin(IV) chloride (12 ml) and thiophene (0.1 moles) in dry 1,2 dichloroethane (100 ml) cooled to 0°C and protected by calcium chloride guard tubes. When all the additions had been made the mixture was stirred at room temperature for a further hour. The mixture was cooled to 0°C and washed with 10% hydrochloric acid solution (50 ml); the aqueous layer was then separated and extracted with 1,2 dichloroethane. The combined organic layers were washed (water then  $\text{NaHCO}_3$  and again with water), dried ( $\text{MgSO}_4$ ) and evaporated to dryness. The crude product was distilled under reduced pressure to yield a colourless oil, compounds 6(g-j), which solidified on cooling to give a white solid in each case.

##### Method 2.

Phosphoric acid (2 ml) was added dropwise to a well stirred mixture of thiophene (0.16 moles) and the acid anhydride (0.16 moles) at 70°C, then the whole mixture was stirred under reflux for 1 hour. A further portion of phosphoric acid (1 ml) was then added, dropwise, and stirring under reflux was continued for a further hour. Water (100 ml) and diethylether (200ml) were added successively to the cooled

mixture. The organic layer was separated, washed (2 x 100 ml, 10% Na<sub>2</sub>CO<sub>3</sub>), dried (MgSO<sub>4</sub>) and then evaporated to dryness. The crude product were purified by distillation at reduced pressure.

Table 5.1 gives a summary of the results for the 2-alkanoylthiophenes (compounds 6a-j), whose structural formulae is given in Fig. 5.1.

The spectral data for compound (6a), the first in the series are as follows:

$\nu_{\max}$  (film) (cm<sup>-1</sup>) 3100w (aromatic C-Hstr), 2950m (aliphatic C-Hstr), 2900m (aliphatic C-Hstr), 1660st (C=Ostr).  $\delta_{\text{H}}$ (CDCl<sub>3</sub>) (ppm) 1.35 (6 H, d, 2CH<sub>3</sub>), 3.5 (1 H, sept, CH), 7.1-8.0 (3 H, mult, thiophene 3, 4 and 5-H).  $\delta_{\text{C}}$ (CDCl<sub>3</sub>) (ppm) 19.35 (2CH<sub>3</sub>), 37.14 (CH), 128.04 (thiophene C<sub>4</sub>), 131.55 (thiophene C<sub>3</sub>), 133.37 (thiophene C<sub>5</sub>), 143.56 (thiophene C<sub>2</sub>), 197.25 (C=O).

The other compounds in the series gave essentially very similar spectra, differing only in the detail associated with the length of the side chain. The data for compound (6j) are typical:

$\nu_{\max}$  (film) (cm<sup>-1</sup>) 3080w (aromatic C-Hstr), 2960m, 2920m, 2870w, (aliphatic C-Hstr), 1670st (C=Ostr).  $\delta_{\text{H}}$ (CDCl<sub>3</sub>) (ppm) 0.9 (3 H, t, CH<sub>3</sub>), 1.3 (30 H, br, s, 15CH<sub>2</sub>), 2.9 (2 H, t, COCH<sub>2</sub>), 6.6-7.5 (3 H, mult, thiophene 3, 4 and 5-H).  $\delta_{\text{C}}$ (CDCl<sub>3</sub>) (ppm) 14.10 (CH<sub>3</sub>), 22.66 (CH<sub>2</sub>CH<sub>3</sub>), 24.81, \*29.67 (13CH<sub>2</sub>), 31.95 (CH<sub>2</sub>CH<sub>2</sub>CH<sub>3</sub>), 39.47 (COCH<sub>2</sub>), 127.91 (thiophene C<sub>4</sub>), 131.48 (thiophene C<sub>3</sub>) 133.11 (thiophene C<sub>5</sub>), 144.60 (thiophene C<sub>2</sub>), 193.36 (C=O).

\* This peak is the largest and is representative of a number of the central CH<sub>2</sub> groups.

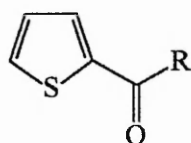


**Figure 5.1**

Compound 6

Table 5.1 summary of results for compounds 6 a-j

| R   | Yield (%) | Boiling/Melting point °C [mm Hg] | Literature Boiling/Melting point °C [mm Hg] | Micro Analysis Found [Calculated %] |
|-----|-----------|----------------------------------|---------------------------------------------|-------------------------------------|
| (a) | 80        | 78 @ [0.1]                       | 245 <sup>(160)</sup>                        | -                                   |
| (b) | 56*       | 190 @ [2]                        | 87-92 @ [3] <sup>(161)</sup>                | -                                   |
| (c) | 85        | 103-104 @ [0.1]                  | 275 <sup>(95)</sup>                         | -                                   |
| (d) | 84        | 114-116 @ [0.1]                  | 170-171 @ [22] <sup>(162)</sup>             | -                                   |
| (e) | 76        | 127-128 @ [0.1]                  | 140-143 @ [1] <sup>(96)</sup>               | -                                   |
| (f) | 79        | 159-165 @ [2]                    | 179-180 @ [8] <sup>(163)</sup>              | -                                   |
| (g) | 89        | 33.0-35.0                        | 36 <sup>(164)</sup>                         | -                                   |
| (h) | 79        | 40.0-41.5                        | 42.5 <sup>(165)</sup>                       | -                                   |
| (i) | 79        | 45.0-46.5                        | -                                           | C=74.8,H=10.93<br>[C=74.94,H=10.8]  |
| (j) | 93        | 48.5-49.5                        | 51 <sup>(166)</sup>                         | -                                   |

\* Method 2 was employed in this case and method 1 for all the rest.

### 5.3.2 Step 2: Huang-Minlon modification to the Wolff-Kishner reduction.

Hydrazine hydrate (5 ml, 99-100%) and the ketone (0.03 moles) were dissolved in diethylene glycol (65 ml); the solution was heated and stirred at 120-140°C for 1 hour, then cooled to approximately 80°C. A solution of potassium hydroxide (5.0 g, 0.09 moles) in hot diethylene glycol (16 ml) was added, and the mixture was gently heated under reflux for 1 hour. The solution was distilled until the internal temperature of the solution was 190-200°C, then heated under reflux for another hour. The solution was cooled and diluted with water (50 ml), then extracted with ether (3 x 50 ml). The combined ethereal solutions were washed successively with water, 2M hydrochloric acid, and water, dried ( $\text{Na}_2\text{SO}_4$ ) and then evaporated to dryness.

Table 5.2 gives a summary of the results for the for the 2-alkylthiophenes (compounds 5a,c-j), whose structural formulae is given in Fig. 5.2. The spectroscopic data presented below are for compound (5a):

$\nu_{\text{max}}$  (film) ( $\text{cm}^{-1}$ ) 3100w (aromatic C-Hstr), 2980st (aliphatic C-Hstr).  $\delta_{\text{H}}$ ( $\text{CDCl}_3$ ) (ppm) 0.95 (6 H, d,  $2\text{CH}_3$ ), 1.9 (1 H, sept,  $\text{CH}$ ), 2.7 (2 H, d,  $\text{CH}_2$ ), 6.7-7.5 (3 H, mult, thiophene 3, 4 and 5 H).  $\delta_{\text{C}}$ ( $\text{CDCl}_3$ ) (ppm) 22.21 ( $2\text{CH}_3$ ), 30.71 ( $\text{CH}$ ), 39.15 ( $\text{CH}_2$ ), 122.85 (thiophene  $\text{C}_5$ ), 124.73 (thiophene  $\text{C}_3$ ), 126.49 (thiophene  $\text{C}_4$ ), 144.15 (thiophene  $\text{C}_2$ ).

The following spectral data is for compound (5j), which is typical of the remainder of the series:

$\nu_{\text{max}}$  (film) ( $\text{cm}^{-1}$ ) 3080 (aromatic CHstr), 2920st, 2860m (aliphatic CHstr).  $\delta_{\text{H}}$ ( $\text{CDCl}_3$ ) (ppm) 0.9 (3 H, t,  $\text{CH}_3$ ) 1.3 (32 H, br, s,  $16\text{CH}_2$ ), 2.8 (2 H, t, Th- $\text{CH}_2$ ), 6.7-7.1 (3 H, mult, thiophene 3, 4 and 5 H).  $\delta_{\text{C}}$ ( $\text{CDCl}_3$ ) (ppm) 14.09 ( $\text{CH}_3$ ), 22.73 ( $\text{CH}_2\text{CH}_3$ ), 29.35, \*29.60, 29.93 (15  $\text{CH}_2$ ), 31.88 (Th- $\text{CH}_2$ ), 122.65 (thiophene  $\text{C}_5$ ), 123.82 (thiophene

C<sub>3</sub>), 126.54 (thiophene C<sub>4</sub>), 145.77 (thiophene C<sub>2</sub>).

\* This peak is the largest and is representative of a number of the central CH<sub>2</sub> groups.

### 5.3.3 Step 3: Friedel-Crafts acylation.

The appropriate carboxylic acid chloride (0.1 moles) was reacted as described in section 5.3.1 method 1.

Table 5.3 gives a summary of the results for the for the 2-n-alkyl-5(3'-carbmethoxypropanoyl)-thiophene (compounds 4a,c,d,g-j), whose structural formula is given in Fig. 5.3. The spectroscopic data presented below are for compound (4a):

$\nu_{\max}$  (KBr) (cm<sup>-1</sup>) 2980str, 2920m, 2870w, (aliphatic C-Hstr), 1740st (ester C=Ostr), 1660st (ketone C=Ostr), 1240st (C-Ostr).  $\delta_{\text{H}}$ (CDCl<sub>3</sub>) (ppm) 0.85 (6 H, d, 2CH<sub>3</sub>), 1.8 (1 H, sept, CH), 2.5 (2 H, t, Th-COCH<sub>2</sub>), 2.65 (2 H, d, Th-CH<sub>2</sub>), 3.15 (2 H, t, H<sub>2</sub>CCO<sub>2</sub>Me), 3.55 (3 H, s, OCH<sub>3</sub>), 6.40, 8.20 (2 H, A-B doublet, J = 3 Hz thiophene 3 and 4 H).  $\delta_{\text{C}}$ (CDCl<sub>3</sub>) (ppm) 22.14 (2CH<sub>3</sub>), 28.05 (COCH<sub>2</sub>), 30.64 (CH), 33.50 (H<sub>2</sub>CCO<sub>2</sub>Me), 39.80 (Th-CH<sub>2</sub>), 126.42 (thiophene C<sub>3</sub>), 132.26 (thiophene C<sub>4</sub>), 141.29 (thiophene C<sub>2</sub>), 154.15 (thiophene C<sub>5</sub>), 173.04 (CO<sub>2</sub>Me), 190.44 (Th-C=O). The following spectral data is for compound (4j), which is typical of the rest of the series:

$\nu_{\max}$  (KBr) (cm<sup>-1</sup>) 2960str, 2920m, 2850w, (aliphatic C-Hstr), 1740st (ester C=Ostr), 1660st (ketone C=Ostr), 1240st (C-Ostr).  $\delta_{\text{H}}$ (CDCl<sub>3</sub>) (ppm) 0.9 (3 H, t, CH<sub>3</sub>), 1.3 (32 H, br, s, 16CH<sub>2</sub>), 2.65 (2 H, t, Th-CH<sub>2</sub>), 2.7 (2 H, t, COCH<sub>2</sub>), 3.2 (2 H, t, H<sub>2</sub>CCO<sub>2</sub>Me), 3.7 (3 H, s, OCH<sub>3</sub>), 6.40, 8.00 (2 H, A-B doublet, J = 3 Hz, thiophene 3 and 4 H).  $\delta_{\text{C}}$ (CDCl<sub>3</sub>) (ppm) 14.09 (CH<sub>3</sub>), 22.73 (CH<sub>2</sub>CH<sub>3</sub>), 28.12 (ThCOCH<sub>2</sub>), \*29.67, 30.64 (14CH<sub>2</sub>), 31.36, (CH<sub>2</sub>CH<sub>2</sub>CH<sub>3</sub>), 31.95 (ThCH<sub>2</sub>), 33.50 (CH<sub>2</sub>CO<sub>2</sub>Me), 125.44 (thiophene C<sub>3</sub>), 132.26 (thiophene C<sub>4</sub>), 140.96 (thiophene C<sub>2</sub>), 155.76 (thiophene C<sub>5</sub>), 178.10 (CO<sub>2</sub>Me), 190.44 (Th-C=O).

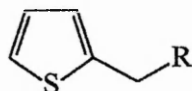


Figure 5.2

Compound 5

Table 5.2 summary of results for compounds 5 a, c-j.

| R   | Yield (%) | Boiling point °C [mm Hg] | Literature Boiling point °C [mmHg]    | Micro analysis Found % [Calculated %] |
|-----|-----------|--------------------------|---------------------------------------|---------------------------------------|
| (a) | 61        | 60-62 @ [2]              | 165-165.5 <sup>(167)</sup>            | -                                     |
| (c) | 61        | 75-78 @ [2]              | 79-82 @ [1] <sup>(168)</sup>          | -                                     |
| (d) | 62        | 120 @ [15]               | 117.5 @ [15] <sup>(100)</sup>         | -                                     |
| (e) | 96        | 140 @ [2]                | 130.5-131.5 @ [11.1] <sup>(100)</sup> | -                                     |
| (f) | 63        | 154-157 @ [1.5]          | 170 @ [16] <sup>(169)</sup>           | -                                     |
| (g) | 93        | 180 @ [1]                | 212-214 @ [15] <sup>(99)</sup>        | -                                     |
| (h) | 83        | 200 @ [1]                | 192 @ [5] <sup>(100)</sup>            | -                                     |
| (i) | 69        | 199 @ [1]                | -                                     | C=78.4, H=11.69<br>[C=78.20, H=11.88] |
| (j) | 79        | 209-211 @ [1]            | 182 @ [0.6] <sup>(101)</sup>          | -                                     |



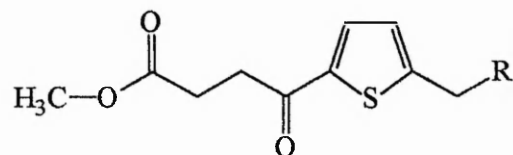


**Figure 5.3** Compound 4

**Table 5.3** Summary of results for compound 4 a, c, d, g-j.

| R   | Yield (%) | Boiling/Melting point °C | Micro analysis Found % [Calculated %] |
|-----|-----------|--------------------------|---------------------------------------|
| (a) | 84        | 164-166 @ 0.7mm Hg.      | C=61.51, H=7.07<br>[C=61.39, H=7.14]  |
| (c) | 55        | 165-169 @ 2 mm Hg        | C=63.99, H=7.77<br>[C=63.8, H=7.86]   |
| (d) | 73        | 162-167 @ 0.9 mm Hg      | C=65.01, H=8.09<br>[C=64.83, H=8.17]  |
| (g) | 74        | 49-51                    | C=70.2, H=9.62<br>[C=70.01, H=9.71]   |
| (h) | 71        | 53-54                    | C=71.1;H=9.95<br>[C=71.04;H=10.02]    |
| (i) | 90        | 74-76                    | C=71.7;H=10.1<br>[C=71.51;H=10.16]    |
| (j) | 95        | 55-57                    | C=72.01;H=10.22<br>[C=71.95;H=10.29]  |

#### 5.3.4 Step 4: Huang-Minlon reduction of 2-(3'-carbmethoxypropanoyl)-5-alkylthiophene.

These were reduced by the method described earlier. (section 5.3.2)

Table 5.4 gives a summary of the results for the for the 4'-(2-alkyl-5-thienyl)-butanoic acids (compounds 1a, c, g-j), whose structural formula is given in Fig. 5.4. The spectroscopic data presented below are for compound (1a):

$\nu_{\max}$  (KBr) ( $\text{cm}^{-1}$ ) 3600br (OHstr), 1720st (C=Ostr).  $\delta_{\text{H}}$ ( $\text{CDCl}_3$ ) (ppm) 0.95 (6 H, d, 2 $\text{CH}_3$ ), 2.0 (1 H, sept,  $\text{CH}$ ), 2.3-3.0 (8 H, mult, 4 $\text{CH}_2$ ), 6.05, 7.25 (2 H, AB doublet  $J = 3\text{Hz}$  thiophene 3 and 4 H), 9.7 (1 H, s, disappears on  $\text{D}_2\text{O}$  shake,  $\text{CO}_2\text{H}$ ).  $\delta_{\text{C}}$ ( $\text{CDCl}_3$ ) (ppm) 22.21 (2 $\text{CH}_3$ ), 26.36 ( $\text{CH}_2\text{CH}_2\text{CO}_2\text{H}$ ), 29.22 (Th $\text{CH}_2$ ), 30.58 ( $\text{CH}$ ), 33.05 ( $\text{CH}_2\text{CO}_2\text{H}$ ), 39.41 (Th- $\text{CH}_2\text{CH}$ ), 123.95 (thiophene  $\text{C}_4$ ), 124.41 (thiophene  $\text{C}_3$ ), 141.35 (thiophene  $\text{C}_2$ ), 142.26 (thiophene  $\text{C}_5$ ), 179.59 ( $\text{CO}_2\text{H}$ ). The following spectral data are for compound (1j), which is typical of the remainder of the series:

$\nu_{\max}$  (KBr) ( $\text{cm}^{-1}$ ) 3600br (OHstr), 2900st, 2850st (aliphatic C-Hstr), 1700st (C=Ostr).  $\delta_{\text{H}}$ ( $\text{CDCl}_3$ ) (ppm) 0.9 (3 H, t,  $\text{CH}_3$ ), 1.3 (32 H, br, s, 16 $\text{CH}_2$ ), 2.6-3.0 (8 H, mult, 4 $\text{CH}_2$ ), 6.1, 7.3 (2 H, AB doublet  $J = 3\text{ Hz}$ , thiophene 3 and 4 H), 11.4 (1 H, br, s, disappears on  $\text{D}_2\text{O}$  shake,  $\text{CO}_2\text{H}$ ).  $\delta_{\text{C}}$ ( $\text{CDCl}_3$ ) (ppm) 14.10 ( $\text{CH}_3$ ), 22.70 ( $\text{CH}_2\text{CH}_3$ ), 26.80, \*29.69 ( $\text{CH}_2$ ), 30.55 (Th $\text{CH}_2$ ), 33.05 ( $\text{CH}_2\text{CO}_2\text{H}$ ), 123.95 (thiophene  $\text{C}_4$ ), 124.41 (thiophene  $\text{C}_3$ ), 141.35 (thiophene  $\text{C}_2$ ), 142.26 (thiophene  $\text{C}_5$ ), 179.59 ( $\text{CO}_2\text{H}$ ).

\* This peak is the largest and it represents a number of the central  $\text{CH}_2$  groups.

#### 5.3.5 Step 5: Base hydrolysis of 2-n-alkyl-5(3'-carbmethoxypropanoyl)thiophene.

A solution of 2-n-alkyl-5(3'-carbmethoxypropanoyl)thiophene (0.02 moles) and potassium hydroxide (10 g, 0.2 moles) in ethanol (100 ml) and water (25 ml) was boiled under reflux for 2 hours. When the solution was cool it was diluted with water

and acidified with conc. hydrochloric acid. The precipitate was filtered off, washed with water and then dried.

Table 5.5 gives a summary of the results for the 3'-(2-alkyl-5-thienyl)-propanoic acids (compounds 2 a, c, d, g-j) whose formula is shown in Fig. 5.5. The spectroscopic data presented below are for compound (2a):

$\nu_{\max}$  (KBr) ( $\text{cm}^{-1}$ ) 3600-2500br (OHstr), 1700st (acid C=Ostr), 1655st (ketone C=Ostr).  $\delta_{\text{H}}$ ( $\text{CDCl}_3$ ) (ppm) 0.95 (6 H, d,  $2\text{CH}_3$ ), 2.0 (1 H, mult,  $\text{CH}$ ), 2.9 (4 H, t,  $\text{COCH}_2\text{-CH}_2$ ), 3.3 (2 H, d, Th- $\text{CH}_2$ ), 6.6, 8.3 (2 H, AB doublet  $J = 4.5\text{Hz}$ , thiophene 3 and 4 H), 11.9 (1 H, br, flat, disappears on  $\text{D}_2\text{O}$  shake,  $\text{CO}_2\text{H}$ ).  $\delta_{\text{C}}$ ( $\text{CDCl}_3$ ) (ppm) 22.14 ( $2\text{CH}_3$ ), 28.12 ( $\text{COCH}_2$ ), 30.64 ( $\text{CH}$ ), 33.24 ( $\text{CH}_2\text{CO}_2\text{H}$ ), 39.87 (Th- $\text{CH}_2$ ), 126.42 (thiophene  $\text{C}_3$ ), 132.33 (thiophene  $\text{C}_4$ ), 141.09 (thiophene  $\text{C}_2$ ), 154.47 (thiophene  $\text{C}_5$ ), 178.36 ( $\text{CO}_2\text{H}$ ), 190.30 ( $\text{C}=\text{O}$ ). The following spectral data are for compound (2j), which is typical of the remainder of the series:

$\nu_{\max}$  (KBr) ( $\text{cm}^{-1}$ ) 3600br (OHstr), 2900st, 2850m (aliphatic CHstr), 1700st (acid C=Ostr), 1650st (ketone C=Ostr).  $\delta_{\text{H}}$ ( $\text{CDCl}_3$ ) (ppm) 0.9 (3 H, s,  $\text{CH}_3$ ), 1.3 (32 H, br, s,  $16\text{CH}_2$ ), 2.6-2.75 (4 H, mult,  $\text{CO-CH}_2\text{-CH}_2$ ), 3.2 (2 H, t, Th- $\text{CH}_2$ ), 6.7, 8.2 (2 H, AB doublet  $J = 4.5\text{Hz}$  thiophene 3 and 4 H), 12.1 (1 H, br, flat disappears on  $\text{D}_2\text{O}$  shake  $\text{CO}_2\text{H}$ ).  $\delta_{\text{C}}$ ( $\text{CDCl}_3$ ) (ppm) 14.02 ( $\text{CH}_3$ ), 22.60 ( $\text{CH}_2\text{CH}_3$ ), 27.98 ( $\text{COCH}_2$ ), \*28.96, 30.65, 31.36 ( $15\text{CH}_2$ ), 31.69 (Th $\text{CH}_2$ ), 33.24 ( $\text{CH}_2\text{CO}_2\text{H}$ ), 125.51 (thiophene  $\text{C}_3$ ), 132.39 (thiophene  $\text{C}_4$ ), 140.76 (thiophene  $\text{C}_2$ ), 156.09 (thiophene  $\text{C}_5$ ), 177.45 ( $\text{CO}_2\text{H}$ ), 190.30 ( $\text{C}=\text{O}$ ).

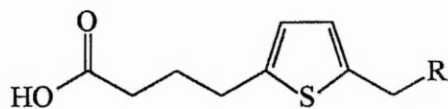


Figure 5.4 Compound 1

Table 5.4 Summary of results for compounds 1 a, c, g-j.

| R   | Yield (%) | Melting point °C | Micro analysis<br>Found %<br>[Calculated %] |
|-----|-----------|------------------|---------------------------------------------|
| (a) | 62        | 41.0 - 43.0      | C=63.7, H=7.98<br>[C=63.69;H=8.02]          |
| (c) | 15        | 41.0 - 42.5      | C=66.2, H=8.68<br>[C=66.11;H=8.72]          |
| (g) | 39        | 60.0 - 62.0      | C=72.21, H=10.36<br>[C=72.08;H=10.46]       |
| (h) | 58        | 60.0 - 62.0      | C=73.0;H=10.7<br>[C=73.04;H=10.74]          |
| (i) | 58        | 66.0 - 67.5      | C=73.3;H=10.6<br>[C=73.47;H=10.86]          |
| (j) | 79        | 60.5 - 62.5      | C=73.8;H=10.91<br>[C=73.88;H=10.98]         |

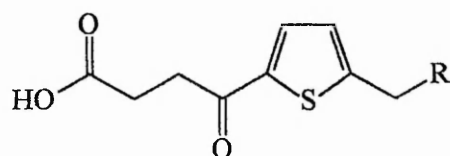


Figure 5.5 Compound 2

Table 5.5 Summary of results for compounds 2 a, c, d, g-j.

| R   | Yield (%) | Melting point °C | Micro analysis<br>Found %<br>[Calculated %] |
|-----|-----------|------------------|---------------------------------------------|
| (a) | 77        | 104.0 - 106.0    | C=59.83, H=6.66<br>[C=59.98;H=6.72]         |
| (c) | 55        | 102.5 - 103.5    | C=62.8, H=7.4<br>[C=62.66;H=7.52]           |
| (d) | 73        | 103.5 - 104.5    | 63.93, H=7.84<br>[C=63.80;H=7.86]           |
| (g) | 60        | 112.0 - 114.0    | C=69.5;H=9.3<br>[C=69.43;H=9.54]            |
| (h) | 97        | 113.5 - 115.5    | C=70.58;H=9.8<br>[C=70.54;H=9.87]           |
| (i) | 98        | 115.0 - 117.0    | C=70.7;H=9.9<br>[C=71.04;H=10.02]           |
| (j) | 90        | 116.0 - 117.2    | C=71.4;H=10.0<br>[C=71.51;H=10.16]          |

## 5.4 Preparation of compounds 3

### 5.4.1 Step 1: esterification of thiophene-2-ethanoic acid.

Thiophene-2-ethanoic acid (14.2 g, 0.1 moles), N,N-dicyclohexylcarbodiimide (22.7 g, 0.11 moles), methanol (3.52 g, 0.11 moles) and 4-N-pyrrolidinopyridine (1.48 g, 0.01 moles) were dissolved in ether (250 ml) and stirred at room temperature for 1 hour. The N,N-dicyclohexylurea which precipitated was filtered off; the filtrate was evaporated and the crude product was passed through a column of silica gel using light petroleum ether and chloroform as eluent (approx 15 g silica to 1 g of crude product) to give (15 g, 96%) methyl thiophene-2-ethanoate.  $\nu_{\max}$  (film) ( $\text{cm}^{-1}$ ) 3100<sub>w</sub> (aromatic C-H<sub>str</sub>), 2950<sub>m</sub> (aliphatic C-H<sub>str</sub>), 1740<sub>str</sub> (ester C=O<sub>str</sub>).  $\delta_{\text{H}}$ (CDCl<sub>3</sub>) (ppm) 3.4 (3 H, s, CH<sub>3</sub>), 3.7 (2 H, s, CH<sub>2</sub>), 6.5-7.1 (3 H, mult, thiophene 3, 4 and 5 H).

### 5.4.2 Step 2: Friedel-Crafts acylation.

The appropriate acid chloride (0.1 moles) was reacted as described in section 5.3.1 method 1.

Table 5.6 gives a summary of the results for the for the 2-(2'-carbmethoxyethyl)-5-alkanoylthiophene (compounds 10g-j), whose structural formula is given in Fig. 5.6.

The other compounds in the series gave essentially very similar spectra, differing only in the detail associated with the length of the side chain. The spectral data given here is for compound (10j) which are typical of the series:

$\nu_{\max}$  (KBr) ( $\text{cm}^{-1}$ ) 3100<sub>w</sub> (aromatic C-H<sub>str</sub>), 2920<sub>st</sub>, 2850<sub>m</sub> (aliphatic C-H<sub>str</sub>), 1740<sub>st</sub> (ester C=O<sub>str</sub>), 1680<sub>st</sub> (ketone C=O<sub>str</sub>).  $\delta_{\text{H}}$ (CDCl<sub>3</sub>) (ppm) 0.9 (3 H, t, CH<sub>2</sub>), 1.3 (30 H, br, s, 15CH<sub>2</sub>), 2.8 (2 H, t, COCH<sub>2</sub>), 3.6 (3 H, s, OCH<sub>3</sub>), 3.8 (2 H, s, Th-CH<sub>2</sub>), 6.55, 7.75 (2 H, AB doublet J = 3 Hz, thiophene 3 and 4-H).  $\delta_{\text{C}}$ (CDCl<sub>3</sub>) (ppm) 14.09 (CH<sub>3</sub>), 24.80, 27.60, 29.67\*, 31.88, 35.78 (18CH<sub>2</sub>), 39.18 (COCH<sub>2</sub>), 52.40, 127.91 (thiophene

C<sub>3</sub>), 131.55 (thiophene C<sub>4</sub>), 143.95, 143.56 (thiophene C<sub>2</sub> and C<sub>5</sub>), 169.79 (CO<sub>2</sub>Me), 193.16 (C=O).

\* Largest peak with the majority of the CH<sub>2</sub>'s

#### 5.4.3 Step 3: Huang-Minlon reduction of 2-(2'-carbmethoxvethyl)-5-alkanovl-thiophene.

These were reduced by the method described earlier. (section 5.3.2)

Table 5.7 gives a summary of the results for the for the 2-alkylthiophene-5-ethanoic acids (compounds 3g-j), whose structural formula is given in Fig. 5.7.

The other compounds in the series gave essentially very similar spectra, differing only in the detail associated with the length of the side chain. The spectral data given here is for compound (3j) which are typical for the series:

$\nu_{\max}$  (KBr) (cm<sup>-1</sup>) 3600br (OHstr), 1720st (C=Ostr).  $\delta_{\text{H}}$ (CDCl<sub>3</sub>) (ppm) 0.9 (3 H, t, CH<sub>3</sub>), 1.3 (32 H, s, 16CH<sub>2</sub>), 3.6 (2 H, t, Th-CH<sub>2</sub>), 3.8 (2 H, s, Th-CH<sub>2</sub>-CO<sub>2</sub>H), 6.55, 7.75(2 H, AB doublet J = 3Hz, thiophene 3 and 4 H) 11.3 (1 H, br, flat disappears on D<sub>2</sub>O shake, CO<sub>2</sub>H)  $\delta_{\text{C}}$ (CDCl<sub>3</sub>) (ppm) 14.02 (CH<sub>3</sub>), 22.60, 27.98, \*29.97, 31.36, 33.69 (19CH<sub>2</sub>), 123.95 (thiophene C<sub>4</sub>), 124.41 (thiophene C<sub>3</sub>), 141.35 (thiophene C<sub>2</sub>), 142.26 (thiophene C<sub>5</sub>), 177.92 (CO<sub>2</sub>H).

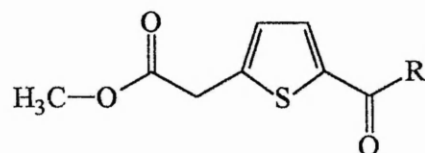


Figure 5.6 Compound 10

Table 5.6 Summary of results for compounds 10 g-j.

| R   | Yield (%) | Melting point °C | Micro analysis<br>Found %<br>[Calculated %] |
|-----|-----------|------------------|---------------------------------------------|
| (g) | 70        | 49.0-51.2        | C=68.7; H=9.44<br>[C=68.81;H=9.36]          |
| (h) | 68        | 52.0-54.0        | C=69.9; H=9.8<br>[C=70.01;H=9.71]           |
| (i) | 92        | 48.5-50.5        | C=70.6; H=9.9<br>[C=70.54;H=9.87]           |
| (j) | 85        | 55.5-57.5        | C=70.85; H=10.0<br>[C=71.04;H=10.02]        |

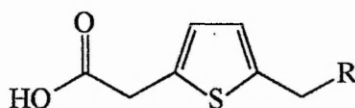


Figure 5.7 Compound 3

Table 5.7 Summary of results for compounds 3 g-j.

| R   | Yield (%) | Melting point °C | Micro analysis<br>Found %<br>[Calculated %] |
|-----|-----------|------------------|---------------------------------------------|
| (g) | 52        | 65.0 - 66.5      | C=70.8; H=10.2<br>[C=70.96;H=10.13]         |
| (h) | 63        | 67.0 - 68.0      | C=72.1; H=10.5<br>[C=72.08;H=10.46]         |
| (i) | 79        | 68.5 - 70.5      | C=72.2; H=10.7<br>[C=72.58;H=10.60]         |
| (j) | 72        | 71.0 - 73.0      | C=73.0; H=10.8<br>[C=73.04;H=10.74]         |



## **5.5 Synthesis of 2-nitrothiophene-5-ethanoic acid**

### **5.5.1 Nitration of thiophene-2-ethanoic acid**

From the two general methods of nitration described section 5.7.3.1 an intractable polymeric tar was produced.

### **5.5.2 Nitration of 2'-(2-carbmethoxyethyl)-thiophene.**

For general method see section 5.7.3.1

#### **5.5.2.1 Saponification of 2'-(2-carbmethoxyethyl)-5-nitrothiophene.**

##### **Method 1.**

A solution of 2-(2'-carbmethoxyethyl)-5-nitrothiophene (3.5 g, 0.017 moles) in 2M HCl was boiled under reflux for 5 hours ( $H_2S$  gas was detected). When cool the mixture was discarded because an intractable polymeric tar was produced.

##### **Method 2.**

A solution of 2-(2'-carbmethoxyethyl)-5-nitrothiophene (3.5 g, 0.017 moles) in 2 M NaOH was boiled under reflux for 0.5 hours. The mixture was then cooled and acidified. This produced an intractable polymeric tar which was discarded.

##### **Method 3.**

A solution of 2-(2'-carbmethoxyethyl)-5-nitrothiophene (0.02 moles) and potassium hydroxide (10 g, 0.2 moles) in ethanol (100 ml) and water (25 ml) was boiled under reflux for 2 hours. The cooled solution was diluted with water, acidified with conc. hydrochloric acid. This produced an intractable polymeric tar which was discarded.

##### **Method 4.**

A mixture of 2-(2'-carbmethoxyethyl)-5-nitrothiophene (1 g,  $5 \times 10^{-3}$  moles) in methanol (65 ml) and water (18 ml) and potassium hydrogen carbonate (1 g,  $1 \times 10^{-2}$

moles) was heated under reflux for 2 hours. The solution was then cooled and diluted with water, acidified with concentrated hydrochloric acid and then extracted with dichloromethane. The organic extract was washed with water and dried ( $\text{MgSO}_4$ ) and evaporated to dryness to yield the original starting material.

### **Method 5.**

A mixture of 2-(2'-carbmethoxyethyl)-5-nitrothiophene (1 g,  $5 \times 10^{-3}$  moles), methylsulphonic acid (0.5 g,  $5.21 \times 10^{-3}$  moles) and formic acid (250 ml) was boiled under reflux for 5 hours. The mixture was cooled, diluted with water and extracted with dichloromethane. The organic extract was dried ( $\text{MgSO}_4$ ) and evaporated to dryness. Starting material was recovered, so the reaction was repeated with an extended reflux (24 hours) but still no product was produced.

### **5.6 Chloromethylation of nitrothiophene**

A rapid stream of gaseous hydrogen chloride was passed into a cold ( $0-5^\circ\text{C}$ ) vigorously stirred mixture of 2-nitrothiophene (3.3 g, 0.0255 moles) and formalin (37%, 2 ml) with  $\text{ZnCl}_2$  (2.7g, 0.02 moles) catalyst for about 30 minutes. The mixture was poured into an equal volume of water. The product was extracted with diethyl ether, dried ( $\text{Na}_2\text{SO}_4$ ) and evaporated to leave a yellow liquid. This was then distilled to obtain the pure product, which was found to be bis-(5-nitrothienyl)-methane.

### **5.7 Preparation of 2-acetylamidothiophene**

#### **5.7.1 Method 1**

##### **5.7.1.1 Preparation of methyl 2-aminothiophene-3-carboxylate.**

*P*-dithiane-2,5-diol (76 g, 0.5 moles) and methyl cyanoacetate (99 g, 1 mole) were stirred in methanol (300 ml). Triethylamine (15 ml) was added over 15 minutes, the temperature being maintained at below  $50^\circ\text{C}$  by an ice water/bath. When the

additions were complete the reaction was stirred at room temperature for 90 minutes and then poured into water (2000 ml). The resulting precipitate was filtered off and washed with water, dissolved in dichloromethane, dried ( $\text{MgSO}_4$ ) and evaporated to dryness. The residue was recrystallized from petroleum ether b.p. 80-100°C to give the product. (63g, 40%), m.p. 76-77 °C, Lit m.p. 77-78 °C.<sup>(170)</sup>

#### 5.7.1.2 Preparation of methyl 2-acetylamidothiophene-3-carboxylate.

A solution of methyl 2-aminothiophene-3-carboxylate (10 g, 0.064 moles) and triethylamine (8 g, 0.079 moles) in dry ether was stirred at 0°C while a solution of acetic anhydride (8 g, 0.078 moles) in dry ether was added, dropwise. When the addition was complete the mixture was stirred at room temperature for 1 hour. This solution was then filtered, washed with water (50 ml),  $\text{NaHCO}_3$  (2 x 25 ml) and again with water (50 ml) then dried ( $\text{MgSO}_4$ ) and evaporated to dryness; the product was then recrystallized from ethanol. (12.9g, 95%), Mp = 159-161°C.  $\nu_{(\text{max})}$  (KBr) ( $\text{cm}^{-1}$ ) 3301 (N-Hstr), 3113 (aromatic C-Hstr), 2918, 2849 (aliphatic C-Hstr), 1701st (ester C=Ostr), 1678st (amide C=Ostr), 1235st (C-Ostr).  $\delta_{\text{H}}$ ( $\text{CDCl}_3$ ) (ppm) 2.1 (3 H, s, Th-NHCOCH<sub>3</sub>); 3.9 (3 H, s Th-CO<sub>2</sub>CH<sub>3</sub>), 6.2 (br, flat disappears on D<sub>2</sub>O shake NH), 6.5, 7.5 (2 H, AB doublet J=6 Hz, thiophene 4 and 5 H)

#### 5.7.1.3 Preparation of 2-acetylamidothiophene-3-carboxylic acid.

A solution of 2-acetylamidothiophene-3-carboxylic acid methyl ester (2 g, 9.39 x 10<sup>-3</sup> moles) and potassium hydroxide (5 g, 0.089 moles) in ethanol (50 ml) and water (10 ml) was heated under reflux for 2 hours. When the solution was cool it was diluted with water and acidified with conc. hydrochloric acid. The resulting precipitate was filtered off, washed with water and recrystallised from ethanol to give the title

amide (1.1 g, 58%), Mp = 165-167°C.  $\nu_{\max}$  (KBr) ( $\text{cm}^{-1}$ ) 3500-2000br (OHstr), 3336m (N-Hstr), 3100w (aromatic C-Hstr), 2916st (aliphatic C-Hstr), 1698st (acid C=Ostr), 1642st (amide C=Ostr).  $\delta_{\text{H}}$ ( $\text{CDCl}_3/\text{D.M.S.O.}$ ) (ppm) 2.2 (3 H, s,  $\text{COCH}_3$ ), 4.1 (br, s, disappears on  $\text{D}_2\text{O}$  shake NH), 6.55, 7.45 (2 H, AB doublet  $J = 6$  Hz, thiophene 4 and 5 H), 11.05 (br, s, disappears on  $\text{D}_2\text{O}$  shake  $\text{CO}_2\text{H}$ ).

#### 5.7.1.4 Decarboxylation of 2-acetylthiophene-3-carboxylic acid.

A mixture of 2-acetylthiophene-3-carboxylic acid (1 g,  $5.4 \times 10^{-3}$  moles), copper(I) oxide (4 g, 0.028 moles) in quinoline (70 ml) was heated and stirred at approximately 180°C until the liberation of carbon dioxide ceased. When the solution had cooled to room temperature it was extracted with dichloromethane, then filtered to remove any copper(I) oxide. The solution was then washed thoroughly with water, dilute hydrochloric acid (several times), and finally with water, dried ( $\text{MgSO}_4$ ) and evaporated to dryness. Any excess quinoline that remained was removed by distillation at reduced pressure. The resulting crude product was recrystallised from 1:1 petroleum ether b.p. 60-80 °C/ethyl acetate to yield 2-acetylthiophene (0.34 g, 45%), Mp. 157-159°C, Lit m.p. 154-157°C<sup>(171)</sup>.  $\nu_{\max}$  (KBr) ( $\text{cm}^{-1}$ ) 3241 (N-Hstr), 3107w (aromatic C-Hstr), 3045st (aliphatic C-Hstr), 1646st (amide C=Ostr).  $\delta_{\text{H}}$ ( $\text{CDCl}_3/\text{D.M.S.O.}$ ) (ppm) 2.1 (3 H, s,  $\text{COCH}_3$ ), 4.0 (br, flat disappears on  $\text{D}_2\text{O}$  shake N-H), 6.5-6.8 (3 H, mult, thiophene 3, 4 and 5 H).  $\delta_{\text{C}}$ ( $\text{CDCl}_3/\text{D.M.S.O.}$ ) (ppm) 22.73 ( $\text{CH}_3$ ), 111.03 (thiophene  $\text{C}_3$ ), 116.62 (thiophene  $\text{C}_5$ ), 125.76 (thiophene  $\text{C}_4$ ), 140.00 (thiophene  $\text{C}_2$ ), 167.00 ( $\text{C}=\text{O}$ ).

#### 5.7.2 Method 2: The Beckmann rearrangement.

##### 5.7.2.1 Preparation of 2-acetylthiophene oxime.

Sodium hydroxide (56 g, 1.4 moles) was added in portions with shaking to a

solution of 2-acetylthiophene (34.5 g, 0.274 moles) and hydroxylamine hydrochloride (30 g, 0.432 moles) in methylated spirits (500 ml) and water (50 ml) cooling as necessary. When the additions were complete the resulting solution was heated under reflux for 5 minutes, cooled and then poured into a solution of conc. hydrochloric acid (150 ml) in water (1000 ml). The resulting precipitate was filtered off and washed with cold water several times. The solid was then dried in a vacuum desiccator. (24.5 g, 63%).  $\nu_{\max}$  (KBr) ( $\text{cm}^{-1}$ ) 3250br (OHstr), 3100w (aromatic C-Hstr), 2900 (Aliphatic C-Hstr).  $\delta_{\text{H}}$ ( $\text{CDCl}_3/\text{D.M.S.O.}$ ) (ppm) 2.4 (3 H, s,  $\text{CH}_3$ ), 4.4 (br, s,  $\text{OH}$ ), 7.0-7.7 (3 H, mult, thiophene 3, 4 and 5 H).

#### 5.7.2.2 Beckmann rearrangement.<sup>(155)</sup>

A suspension of 2-acetylthiophene oxime (14.1 g, 0.1 moles) in dry ether (375 ml) was cooled to  $0^\circ\text{C}$ , phosphorus pentachloride (25 g, 0.12 moles) was added with efficient stirring and cooling over 2 hours, the mixture was stirred at  $0^\circ\text{C}$  for 2 hours then stirred at room temperature for 12 hours. The clear solution was poured onto ice (250 g) and carefully neutralised to pH 6-7 with aqueous 5M sodium hydroxide while maintaining the temperature at  $0^\circ\text{C}$  by the addition of ice. The aqueous phase was extracted with dichloromethane (3 x 50 ml), the combined organic phases were washed with water and dried ( $\text{MgSO}_4$ ), treated with charcoal and evaporated to dryness. The residue was triturated with petroleum ether b.p.  $60-80^\circ\text{C}$  and the resulting precipitate was recrystallized from petroleum ether b.p.  $60-80^\circ\text{C}$ /ethyl acetate. (1.75 g, 12.5%) m.p.  $157-159^\circ\text{C}$ .  $\nu_{\max}$  (KBr) ( $\text{cm}^{-1}$ ) 3241 (N-Hstr), 3108 (aromatic C-Hstr), 3046 (aliphatic C-Hstr), 1642 (C=Ostr).  $\delta_{\text{H}}$ ( $\text{CDCl}_3/\text{D.M.S.O.}$ ) (ppm) 2.1 (3 H, s,  $\text{CH}_3$ ), 3.6 (s, disappears on  $\text{D}_2\text{O}$  shake,  $\text{NH}$ ), 6.6-6.9 (3 H, mult, thiophene 3, 4 and 5 H).

#### 5.7.3 Method 3: The reductive acetylation of 2-nitrothiophene.

### 5.7.3.1 Nitration of thiophene.

#### Method 1.

Thiophene (84 g, 1 mole) was dissolved in acetic anhydride (340 ml). Fuming nitric acid (80 g, 1.2 moles) was dissolved in glacial acetic acid (600 ml). Each solution was then divided into two halves. One half of the nitric acid solution was cooled to between 5-10°C, then one half of the thiophene solution was added dropwise to the solution with efficient stirring. Care was taken to prevent the temperature rising to ambient temperatures and if it did the addition of the thiophene solution was halted until the temperature again fell below 10°C. When all of that fraction of thiophene solution had been added the temperature was reduced to 5-10°C and the second nitric acid solution was added to the flask quickly. The nitration was continued by adding the second portion of the thiophene solution dropwise. Once all additions had been made the mixture was allowed to stir at ambient temperatures for a further two hours. The solution was then poured into an equivalent volume of ice. The nitrothiophenes were then filtered off and the aqueous phase was extracted several times with dichloromethane. The nitrothiophenes were then dissolved in dichloromethane and the combined organic fractions were washed with water (2x), sodium hydrogen carbonate (3x) and water and then dried (MgSO<sub>4</sub>).

The mixture of 2-nitrothiophene and 3-nitrothiophene can be separated using a method that takes advantage of their differing reactivity towards chlorosulphonic acid<sup>(172)</sup>. The 2-nitrothiophene does not react with the chlorosulphonic acid whereas the 3-nitrothiophene reacts to give 3-nitrothiophene-2-sulphonic acid. The 3-nitrothiophene-2-sulphonic acid is water soluble and therefore can be removed by washing an organic extract of the nitrothiophene with water. The method was achieved

by cooling the solution to 0°C and adding chlorosulphonic acid (30 g, 0.258 moles) (approximately 25 mole percent) dropwise. When all the acid had been added the solution was stirred for a further 30 minutes at room temperature; it was then cautiously added to an equal volume of ice/water. The aqueous layer was further extracted with dichloromethane and the combined organic phases were washed with water, sodium hydrogen carbonate (3x) and then water. This was then dried ( $\text{MgSO}_4$ ) and evaporated to leave pure 2-nitrothiophene. (105 g, 81%)

### **Method 2.**

Copper(II) nitrate trihydrate (2.5 g, 0.0104 moles) was dissolved in acetic anhydride (20ml) and then cooled to -10°C. A solution of the thiophene (0.01 moles) in acetic acid (20ml) was then added dropwise at such a rate as to prevent the temperature of the solution from rising above -5°C. When all the addition had been made the solution was stirred at 0°C for 1 hour then allowed to warm to room temperature. This mixture was then poured onto ice/HCl and when all the ice had melted the solid was filtered off. The aqueous layer was washed with dichloromethane and combined with a solution of the solid, which was then washed with water (50 ml), sodium hydrogen carbonate (3 x 50 ml), water (50 ml) then dried ( $\text{MgSO}_4$ ). The organic phase was then treated as in method 1 to remove the 3-nitrothiophene to yield pure 2-nitrothiophene. (1.02 g, 79%) Mp. = 43-45°C.

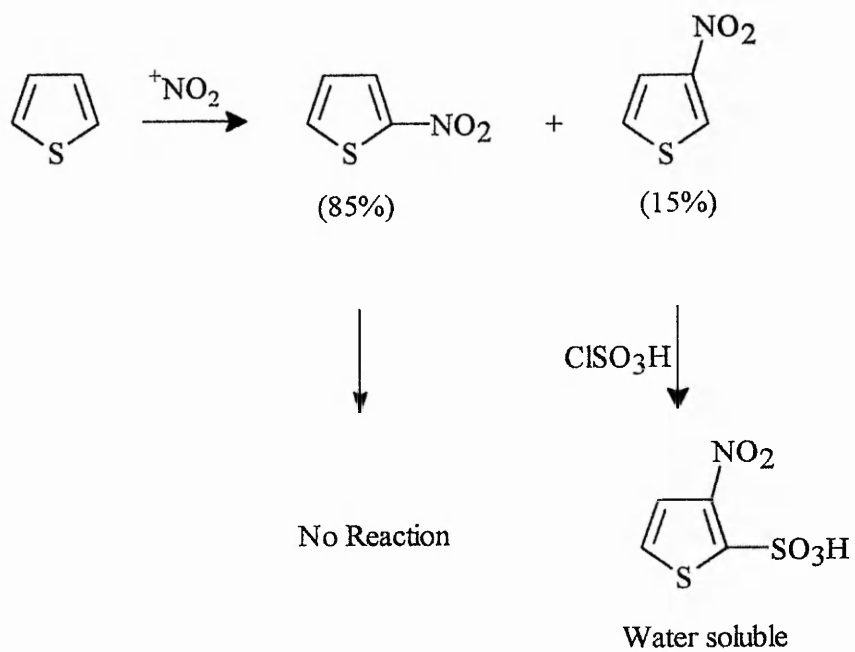


**Figure 5.8** The purification of 2-nitrothiophene.



### 5.7.3.2 Reductive acetylation of 2-nitrothiophene.

A solution of 2-nitrothiophene (51.6 g, 0.4 moles) in acetic anhydride (90 g, 0.88 moles) and acetic acid (144 g, 2.4 moles) was stirred with an overhead stirrer and heated to 55-60°C. Once the reaction mixture had attained that temperature the source of heat was removed and reduced iron (67.2 g, 1.2 moles) was added in small portions. The temperature of the mixture rose after each addition of iron and it was allowed to cool back to 55-60°C before adding more. When all the iron had been added the reaction mixture was heated to 60-70°C and stirred for a further 45 minutes. When the mixture was cool it was poured into 2M hydrochloric acid (approximately an equal volume to the reaction mixture) and left to stand overnight. The solution was filtered and the solid product extracted into ethyl acetate. The aqueous layer was further extracted with ethyl acetate and the combined organic layers were washed with water, sodium hydrogen carbonate (several times) and then water, dried (MgSO<sub>4</sub>) and evaporated to dryness. The solid was recrystallized from 1:1 petroleum ether bp 60-80°C/ethyl acetate to yield 2-acetamidothiophene, (52.2 g, 93%) Mp. 157-159°C.  $\nu_{\max}$  (KBr) (cm<sup>-1</sup>) 3241m (N-Hstr), 3107w (aromatic C-Hstr), 3045m (aliphatic C-Hstr), 1646str (amide C=Ostr).  $\delta_{\text{H}}$ (CDCl<sub>3</sub>/D.M.S.O.) (ppm) 2.1 (3 H, s, CH<sub>3</sub>), 4.0 (br, flat disappears on D<sub>2</sub>O shake) NH), 6.5-6.8 (3 H, mult, thiophene 3, 4 and 5 H).  $\delta_{\text{C}}$ (CDCl<sub>3</sub>/D.M.S.O.) (ppm) 22.73 (CH<sub>3</sub>), 111.03 (thiophene C<sub>3</sub>), 116.62 (thiophene C<sub>5</sub>), 125.76 (thiophene C<sub>4</sub>), 140.00 (thiophene C<sub>2</sub>), 167.00 (C=O).

### 5.8 Preparation of N-alkylated 2-acetamidothiophene.<sup>(173)</sup>

A solution of 2-acetamidothiophene (7.1 g, 0.05 moles), finely powdered sodium hydroxide (7.0 g, 0.175 moles), potassium carbonate (14.0 g, 0.1014 moles) and myristyltrimethylammonium bromide (1.7 g, 0.075 moles) in benzene (50 ml) was

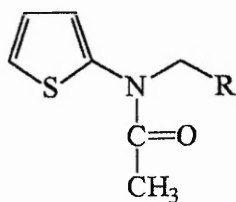
heated under reflux with efficient overhead stirring. A solution of the appropriate n-alkylbromide (0.075 moles) in benzene (10 ml) was added dropwise to the mixture. This was heated under reflux for a further 5 hours. The solution was cooled, diluted with benzene and washed with water several times, dried ( $\text{MgSO}_4$ ) and evaporated to dryness. The resulting solid was purified by column chromatography on silica gel using dichloromethane as the solvent.

Table 5.8 gives a summary of the results for the for the N-alkyl-2-acetamidothiophenes (compounds 30 g,h,j,k), whose structural formula is given in Fig. 5.8.

The spectra are essentially the same and the data for compound (30j) which is representative of the series is given below:

$\nu_{\text{max}}$  (KBr) ( $\text{cm}^{-1}$ ) 3072w (aromatic C-Hstr), 2924m, 2854st (aliphatic C-Hstr), 1672st (amide C=Ostr), 1543m (thiophene C=Cstr).  $\delta_{\text{H}}$ ( $\text{CDCl}_3$ ) (ppm) 0.88 (3 H, t,  $\text{CH}_3$ ), 1.26 (32 H, br, s,  $16\text{CH}_2$ ), 1.96 (3 H, s,  $\text{COCH}_3$ ), 3.64 (2 H, d,  $\text{N-CH}_2$ ), 7.1 (3 H, mult, thiophene 3, 4 and 5 H).  $\delta_{\text{C}}$ ( $\text{CDCl}_3$ ) (ppm) 14.12 ( $\text{CH}_3$ ), 22.48 ( $\text{CH}_2\text{CH}_3$ ) 22.71 ( $\text{COCH}_3$ ), 26.70 ( $\text{NCH}_2\text{CH}_2\text{CH}_2$ ), 27.78 ( $\text{NCH}_2\text{CH}_2$ ), 29.38, 29.49, 29.60, \*29.72, (13 $\text{CH}_2$ ), 31.95 ( $\text{CH}_2\text{CH}_2\text{CH}_3$ ), 50.04 ( $\text{N-CH}_2$ ), 124.56, 125.25, 125.78 (thiophene  $\text{C}_3$ ,  $\text{C}_4$ , and  $\text{C}_5$ ), 145.87 (thiophene  $\text{C}_2$ ), 171.26 ( $\text{C=O}$ ).

\* This peak is the largest and is representative of a number of the central  $\text{CH}_2$  groups.



**Figure 5.8**

compound 30

Table 5.8 Summary of results for compounds 30 g, h, j, k.

| R   | Yield (%) | Melting point °C | Micro analysis                                         |
|-----|-----------|------------------|--------------------------------------------------------|
|     |           |                  | Found %<br>[Calculated %]                              |
| (g) | 43        | 29.0-30.0        | C=71.28, H=10.38, N=4.11<br>[C=71.17, H=10.46, N=4.15] |
| (h) | 58        | 34.0-36.0        | C=72.31, H=10.80, N=3.77<br>[C=72.27, H=10.76, N=3.83] |
| (j) | 51        | 43.5-45.5        | C=73.01, H=11.10, N=3.67<br>[C=73.23, H=11.02, N=3.56] |
| (k) | 73        | 54.5-55.9        | C=74.80, H=11.43, N=3.08<br>[C=74.77, H=11.44, N=3.12] |

## 5.9 Formylation of N-alkyl-2-acetamidothiophene.

A mixture of N-alkyl-2-acetamidothiophene ( $5.089 \times 10^{-3}$  moles), N,N-dimethylformamide (0.47 g,  $6.412 \times 10^{-3}$  moles) and phosphoryl chloride (0.98 g,  $6.371 \times 10^{-3}$  moles) in dry 1,2-dichloroethane (10 ml) was stirred at room temperature for 14 hours. The mixture was then poured onto crushed ice and neutralised to pH 6.0-7.0 with anhydrous sodium acetate. The crude product was purified by column chromatography on silica gel using chloroform as the elutant.

Table 5.9 gives a summary of the results for the for the N-alkyl-2-acetamidothiophene-5-carboxaldehydes (compounds 29 g,h,j,k), whose structural formula is given in Fig. 5.9.

The spectra are essentially the same and the data for compound (29j) which is representative of the series is given below:

$\nu_{\max}$  (KBr) ( $\text{cm}^{-1}$ ) 3107w (aromatic C-Hstr), 2922st, 2892st (aliphatic C-Hstr), 1662st (amide C=Ostr), 1548m (thiophene C=Cstr).  $\delta_{\text{H}}$ ( $\text{CDCl}_3$ ) (ppm) 0.85 (3 H, t,  $\text{CH}_3$ ), 1.25 (32 H, br, s,  $16\text{CH}_2$ ), 2.25 (3 H, s,  $\text{COCH}_3$ ), 3.8 (2 H, t,  $\text{N-CH}_2$ ), 6.4, 8.0 (2 H, AB doublet  $J = 5.4$  Hz, thiophene 3 and 4 H), 9.8 (1 H, s,  $\text{CHO}$ ).  $\delta_{\text{C}}$ ( $\text{CDCl}_3$ ) (ppm) 14.09 ( $\text{CH}_3$ ), 22.60 ( $\text{COCH}_3$ ), 26.75 ( $\text{NCH}_2\text{CH}_2\text{CH}_2$ ), 27.79 ( $\text{NCH}_2\text{CH}_2$ ), \*29.61 ( $14\text{CH}_2$ ), 31.88 ( $\text{CH}_2\text{CH}_2\text{CH}_3$ ), 50.13 ( $\text{N-CH}_2$ ), 122.1 (thiophene  $\text{C}_5$ ), 134.45 (thiophene  $\text{C}_3$  and  $\text{C}_4$ ), 152.78 (thiophene  $\text{C}_2$ ), 169.33 ( $\text{C=O}$ ), 183.11 ( $\text{CHO}$ ).

\* This peak is the largest and is representative of a number of the central  $\text{CH}_2$  groups.

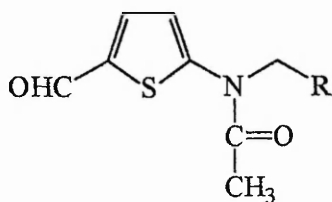


Figure 5.9 compound 29

Table 5.9 Summary of results for compounds 29 g, h, j, k.

| R   | Yield (%) | Melting point °C | Micro analysis<br>Found %<br>[Calculated %]            |
|-----|-----------|------------------|--------------------------------------------------------|
| (g) | 43        | 42.5-43.5        | C=68.70, H=9.87, N=3.79<br>[C=69.00, H=9.66, N=3.83,]  |
| (h) | 70        | 51.0-52.5        | 70.00, H=10.03, N=3.58<br>[C=70.18, H=9.99, N=3.56]    |
| (j) | 91        | 58.0-59.5        | C=71.54, H=10.11, N=3.29<br>[C=71.21, H=10.29, N=3.32] |
| (k) | 67        | 55.0-57.0        | C=72.55, H=10.70, N=3.01<br>[C=72.90, H=10.77, N=2.93] |

### 5.10 Synthesis of the triphenylphosphine salt of 4-nitrobenzylbromide

A solution of triphenylphosphine (10 g, 0.0382 moles) and 4-nitrobenzylbromide (5 g, 0.0231 moles) in 1,2-dichlorobenzene (20 ml) was boiled gently under reflux for 5 minutes. The mixture was cooled to room temperature and diluted with diethyl ether and the solid product was filtered off, washed with dry diethyl ether and dried in a vacuum desiccator. (10.7 g, 97%).

### 5.11 Wittig Reaction

Butyllithium (2.4 ml, 1.6 M in hexane) was added to a stirred solution of dry tetrahydrofuran (20 ml) and 4-nitrobenzyltriphenylphosphine bromide (1.7 g,  $3.56 \times 10^{-3}$  moles) at 0°C under a dry nitrogen atmosphere. After all the butyllithium had been added the solution was stirred at room temperature for 2 hours. A solution of the N-alkyl-2-acetamidothiophene-5-carboxaldehyde (2.375 moles) in dry tetrahydrofuran was then added quickly and the whole was stirred at room temperature for a further 1 hour or until all the N-alkyl-2-acetamidothiophene-5-carboxaldehyde had reacted (T.L.C.). The solution was poured into water and extracted with chloroform. The organic layer was separated and washed several times with water, dried ( $\text{MgSO}_4$ ), and evaporated to dryness. The resulting crude product was passed down a silica chromatography column using 1:1 chloroform/light petroleum ether b.p. 60-80°C. The J values for the AB doublet of the alkene suggests the configuration is *trans* giving E-1-(5'-(N-alkyl)-2'-acetamidothienyl)-2-(4''-nitrophenyl)-ethene.

Table 5.10 gives a summary of the results for the for the E-1-(5'-(N-alkyl)-2'-acetamido-thienyl)-2-(4''-nitrophenyl)-ethenes (compounds 54 g,h,j,k), whose structural formula is given in Fig. 5.10.

The spectra are essentially the same and the data for compound (54j) which is

representative of the series is given below:

$\nu_{\max}$  (KBr) ( $\text{cm}^{-1}$ ) 3012w (aromatic C-Hstr), 2923st, 2852str (aliphatic C-Hstr), 1654st (amide C=Ostr), 1594m (CH=CHstr), 1515st, 1342str ( $\text{NO}_2$ str).  $\delta_{\text{H}}$ ( $\text{CDCl}_3$ ) (ppm) 0.88 (3 H, t,  $\text{CH}_3$ ), 1.25 (32 H, br, s,  $16\text{CH}_2$ ), 2.04 (3 H, s,  $\text{COCH}_3$ ), 3.67 (2 H, t,  $\text{N-CH}_2$ ), 5.7, 8.0 (2 H, AB doublet,  $J = 3.3$  Hz, thiophene 3 and 4 H), 5.3, 8.9 (2 H AB doublet  $J = 15.84$  Hz,  $\text{CH}=\text{CH}$  trans isomer), 5.0, 10.75 (4 H AB doublet  $J = 8.58$  Hz, benzene 2 and 3-H).  $\delta_{\text{C}}$ ( $\text{CDCl}_3$ ) (ppm) 14.12 ( $\text{CH}_3$ ), 22.53 ( $\text{COCH}_3$ ), 22.70 ( $\text{CH}_2\text{CH}_3$ ), 26.68 ( $\text{NCH}_2\text{CH}_2\text{CH}_2$ ), 27.82 ( $\text{NCH}_2\text{CH}_2$ ), 29.36, 29.54, 29.65\* ( $10\text{CH}_2$ ), 31.91 ( $\text{CH}_2\text{CH}_2\text{CH}_3$ ), 50.01 ( $\text{N-CH}_2$ ), 124.22 (benzene  $\text{C}_3$  and thiophene  $\text{C}_3^{\S}$ ), 126.04 (thiophene  $\text{C}_4^{\S}$ ), 126.20; 126.26 (alkene  $\text{HC}=\text{CH}^{\S}$ ), 126.70 (benzene  $\text{C}_2$ ), 140.53 (thiophene  $\text{C}_2$ ), 143.07 (benzene  $\text{C}_1$ ), 145.80 (benzene  $\text{C}_2$ ), 146.83 (thiophene  $\text{C}_5$ ) 170.89 ( $\text{C}=\text{O}$ ).

\* largest peak comprising of most of the carbon atoms of the alkyl side chain.

§ These assignments have not been made with 100% certainty; absolute identification could possibly be achieved by radioisotope labelling with  $^{13}\text{C}$  giving doublets or triplets for neighbouring carbon atoms.

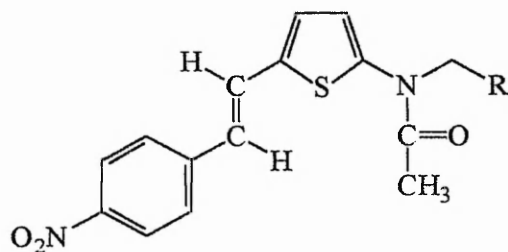


**Figure 5.10** Compound 54

Table 5.10 Summary of results for compounds 54 g, h, j, k.

| <b>R</b> | <b>Yield (%)</b> | <b>Melting point °C</b> | <b>Micro analysis<br/>Found %<br/>[Calculated %]</b>  |
|----------|------------------|-------------------------|-------------------------------------------------------|
| (g)      | 67               | 113.5-114.8             | C=69.62; H=8.53; N=5.83<br>[C=69.38; H=8.32; N=5.78]  |
| (h)      | 65               | 105.5-106.9             | C=69.64; H=8.71; N=5.21<br>[C=70.27; H=8.66; N=5.47]  |
| (j)      | 61               | 98.0-99.5               | C=71.35; H=9.15; N=5.08<br>[C=71.07; H=8.95; N=5.18]  |
| (k)      | 60               | 87.4-88.8               | C= 72.47; H=9.66; N=4.60<br>[C=72.43; H=9.46; N=4.70] |



## 5.12 LANGMUIR-BLODGETT FILM EXPERIMENTAL

### 5.12.1 Monolayer spreading.

Most monolayer-forming materials are applied to the subphase by first dissolving them in a solvent. The necessary properties of the solvent are discussed by Gaines<sup>(31)</sup>: it must be able to dissolve an adequate quantity of the monolayer material (concentrations of 0.1-1 mgml<sup>-1</sup> are typical); it must not react chemically with the material or dissolve in the subphase; finally, the solvent must evaporate within a reasonable time frame so that none remains in the condensed monolayer. A solvent which evaporates too quickly may be a problem, as this could prevent an accurate determination of the concentration of the solution. A report by Mingins *et al* has shown that different solvents can influence the pressure area isotherms for particular monolayer materials.

Solvents which are commonly used for monolayer spreading include n-hexane (bp = 69°C), benzene (bp = 80°C), chloroform (bp = 61°C), and diethyl ether (bp = 35°C). For the spreading of materials which are not soluble in such non-polar solvents, special techniques have to be devised. One approach is to use mixed solvents, which give sufficient solubility to the monolayer material but do not induce serious water-solubility problems; examples include hexane-ethanol, benzene-ethanol, and chloroform-methanol. Chloroform-alcohol-water mixtures have been used to spread biological materials.

The application of the spreading solution to the subphase was accomplished by dropping the solution from a microsyringe held only a millimetre or so from the subphase surface. The drops were applied to the centre of the subphase surface and allowed to spread out and evaporate before the next drop was applied. In this way if

any impurities do happen to remain on the surface they are pushed to the extremities away from the surface pressure measurement and 'dipping' area. There is available an automated spreading apparatus which is controlled by the microcomputer; this would be particularly useful if trying to deposit a very large number of layers, since the floating monolayer would need to be replenished frequently.

The most fundamental requirement for a material to be of use in Langmuir-Blodgett film formation is that it should be practically insoluble in the water subphase. However, the conventional concept of bulk solubility is not really meaningful in this context, and figures for such a quantity could only give at best a rough estimate of whether or not a monolayer of the material is likely to be stable at the air-water interface. The two most valuable properties of the water-surface monolayer which can be studied are its pressure-area relationship at constant temperature and the change in surface area with time at constant pressure.

#### **5.12.2 Pressure-area isotherms.**

If a material forms an insoluble monolayer at the air-water interface, then as the surface area of the trough is reduced the surface pressure will increase. By plotting the calibrated output from the pressure sensor against that from the barrier potentiometer, a pressure-area ( $\pi$ -A) curve, or isotherm can be obtained. The pressure-area isotherm of an 'ideal' LB film material, stearic acid, is shown in Fig. 5.11. This isotherm represents the 'ideal' situation in which there are three distinct regions, corresponding to two-dimensional 'gas', 'liquid', and 'solid' phases. The presence or absence of any or all of such phases in the isotherm of the novel materials should give clues as to how their monolayers are behaving as compared to the ideal materials. Materials that register a finite surface pressure at very large molecular areas and

whose isotherms have very gentle slopes with increasing pressure are likely to have their molecules or part of the molecules lying flat on the water surface when uncompressed, the act of compression only gradually altering their orientation such that the hydrocarbon chains point vertically. Usually the best materials are ones that display low surface pressure prior to the quite steep "solid" phase. The isotherms are plotted as area per molecule ( $a_m$ ) against surface pressure ( $\pi$ ).  $a_m$  is calculated by the trough controlling software using Eqn. 5.1.

$$a_m = A \cdot \frac{M}{cVN_A} \quad (5.1)$$

A = Trough area (calculated by software from barrier position)

M = R.M.M. of the compound.

c = Concentration of the compound in the solution.

V = Volume of the solution placed onto the subphase.

$N_A$  = Avogadro's number.

The errors in c and V are quite small; in the case of c the errors arise from the weighing of the solid and the volume of the solvent the solid is dissolved in. Typically there is  $\pm 0.01 \text{ cm}^3$  accuracy in  $10 \text{ cm}^3$  of solvent which equates to  $\pm 0.1\%$  error, and the weighing of the solid is  $\pm 0.005\text{g}$  in  $1.0\text{g}$  which is  $\pm 0.5\%$  error. V depends on the method used to dispense the solution but usually  $\pm 0.5\mu\text{l}$  in  $100\mu\text{l}$  giving  $\pm 0.5\%$  error. Each barrier position on the trough can typically be measured to an accuracy of  $\pm 0.3^\circ$  in  $180^\circ$  which leads to an error of  $\pm 0.3\%$  for A. Therefore the total error for  $a_m$  is approximately  $\pm 1.5\%$ .

The accuracy of  $a_m$  is not always as high as might be expected when the precision with which A, c, and V are known, since the presence of water soluble

impurities in the bulk material or any dissolution of the monolayer itself before the isotherm is finished will give rise to an  $a_m$  value that is too small. As  $a_m$  is the area per molecule the film must only be one molecule thick on the subphase. A good indication of bilayers or multilayers on the subphase is very low values for  $a_m$  (ie. below the expected limiting value for an alkyl chain found by calculations using a computer chemical modelling package). Extrapolation of the steep, linear high pressure region of the isotherm to zero pressure gives the limiting  $a_m$  of the "solid" phase. Such comparisons can help to indicate the orientation of molecules in the film, which in turn may elucidate some of the possible intermolecular interactions. Langmuir found that films of long chain fatty acids gave the same cross-sectional  $a_m$ , irrespective of chain length. He concluded that the films were one molecule thick and that the molecules were oriented nearly vertically on the water surface, the film thickness being the chain length. Few materials exhibit the three distinct "phases" shown by stearic acid, but the shapes of their isotherms help to elucidate the behaviour of the molecule as the film is compressed. Many compounds exhibit "solid" regions, but often after a series of other phase changes.

Compression of the monolayer to a surface pressure that is just below the point of collapse, followed firstly by relaxation through expansion and then by recompression, can yield some interesting information. If the isotherm tends towards lower and lower area then this is probably due to significant film dissolution. If the isotherm tends to be steeper in nature whilst the pressure at which the film collapses ( $\pi_c$ ) remains unchanged, then this could indicate some molecular reorganisation or interaction taking place. The point at which a film begins to collapse can be seen in two ways. The first is a marked reduction in the slope of the isotherm; secondly, it is

sometimes possible to see lines appearing on the film adjacent to the barriers. This is especially noticeable with highly coloured active molecules. In some materials this collapse can take place at very low  $\pi$ , and sometimes immediately upon spreading the film. These molecules are no good for Langmuir-Blodgett work; however, it is sometimes possible to improve the film forming capabilities of such materials by mixing them with a fatty acid such as stearic or arachidic acid<sup>(174)</sup>. This mixing has also been used to increase the mobility of rigid films (see section 5.12.4).

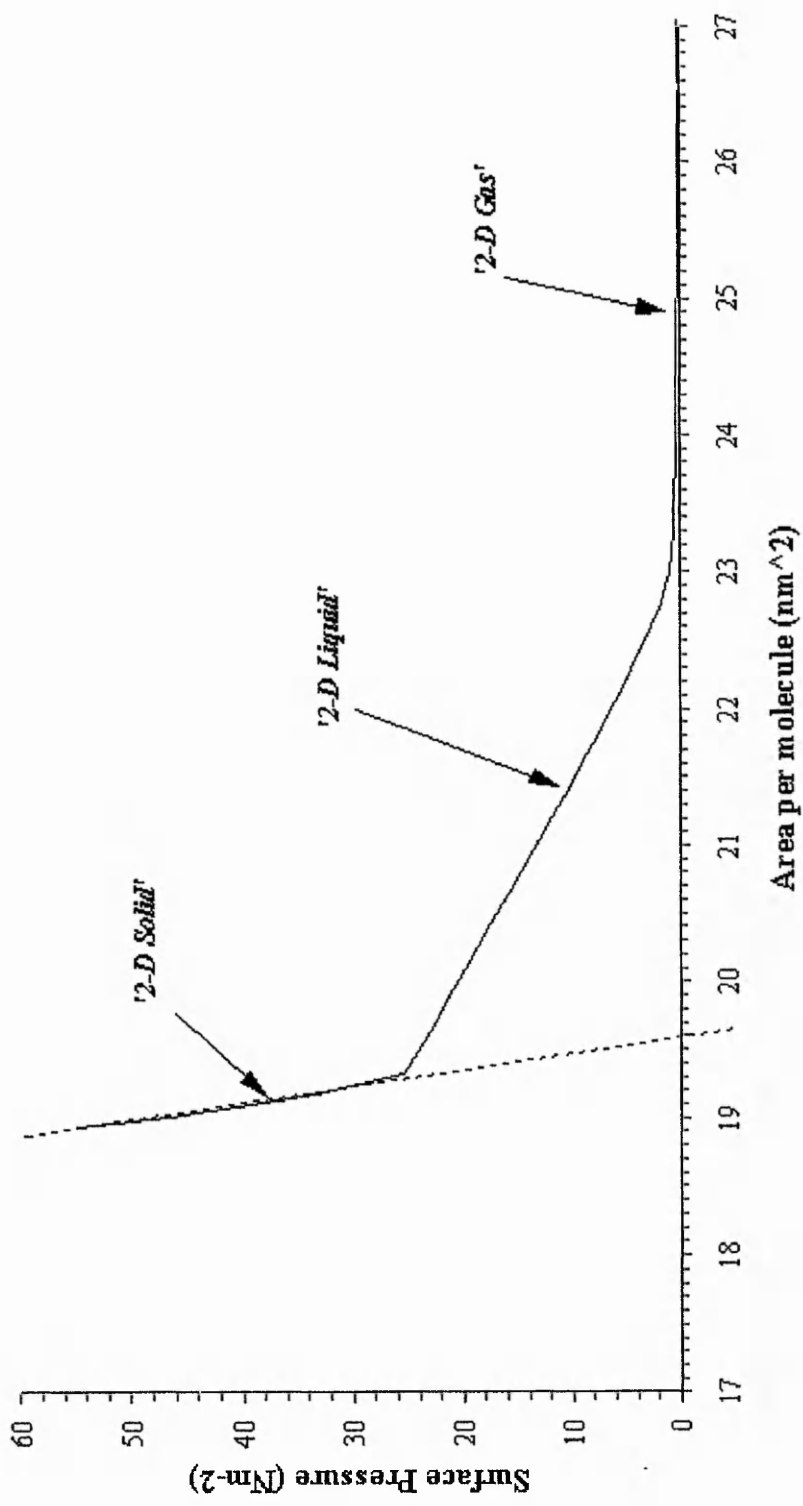


Figure 5.11 Area Pressure Isotherm of Stearic acid at pH = 5.5.  $a_m = 19.6 \text{ nm}^2$

### 5.12.3 Monolayer Stability Studies.

The rate of dissolution and or collapse of the monolayer on the water surface should not be too large; indeed, in order for the compound to be of practical use for LB film formation an ideal Langmuir film would display no decrease in surface area with time when held at a constant surface pressure in its psuedo-solid phase. However, in practice all monolayer films show some decay in area with time due to some or all of the following effects:-

- (a) Collapse (buckling) of the film;
- (b) rearrangement;
- (c) dissolution of material into the subphase;
- (d) evaporation.

Normally a monolayer can be prevented from collapsing by keeping the surface pressure below that at which the film becomes unstable; however, in some cases this pressure is too low for efficient transfer to a substrate. The rate of dissolution may depend on several factors, including temperature, pH, and the concentration of various ions in the subphase. With most of the classical fatty acid materials this process can be rendered insignificant by partial salt formation, but dissolution can be quite rapid, and thus a major problem, with many of the more novel materials. The optimum conditions for slowing the collapse of the film must therefore be ascertained by experimentation. Gaines<sup>(31)</sup> has studied Langmuir films which dissolve at a considerable rate and has found that they show an initial rapid desorption, followed by a process obeying the equation:

$$\ln(N) = -kt + C \quad (5.2)$$

where  $N$  is the number of molecules remaining on the surface at time  $t$ , and  $k$ ,  $C$  are constants. The optimum conditions for reduced solubility can be found by measuring the area of a collapsing film as a function of time for a range of different subphase parameters and noting which gives the smallest value of  $k$ .

An appropriate surface pressure for each material was determined by inspecting the isotherms generated during the  $a_m$  studies and selecting a pressure which was approximately half way up the steepest part of the graph. By compressing a freshly deposited film until it reached that pressure, and holding it at that pressure via a negative feedback loop between the barriers and the pressure sensors for a long period of time, the rate of loss of monolayer area due to either dissolution into the subphase or collapse of the film could be determined. This was evaluated by drawing a best fit straight line through the slope and then calculating the gradient of the line.

#### **5.12.4 Monolayer mobility.**

Although it is desirable that a monolayer should be well-ordered and close packed, it is also necessary that it remains mobile on the water surface in order that film transfer to a suitable substrate can be facilitated. If a film is too rigid, then as the substrate traverses the air/subphase interface the film will fracture and deposition will take the form of the transfer of film fragments, with large cracks and holes between them.

The 'suction test' provides a simple check on monolayer mobility; the film is held at constant pressure, and a small amount of material is removed using the vacuum nozzle. An adequately mobile film should realign immediately to maintain the preset surface pressure. Very rigid monolayers can often be made more mobile by mixing the material with a fatty acid or by using a slow evaporating solvent. In some cases



rigidity sets in slowly with time and so the problem can be circumvented by always depositing from a freshly spread monolayer, although this can be rather tedious.

#### **5.12.5 Langmuir-Blodgett Film Deposition.**

Three possible modes of Langmuir-Blodgett film deposition have been recognized<sup>(175)</sup> and are illustrated in Fig. 3.1. With most materials deposition is Y-type, with pick up occurring on both insertion and withdrawal of the substrate from the subphase. With this mode the first monolayer is deposited on the first upstroke of a hydrophilic material (giving an odd number of layers) or on the first downstroke of a hydrophobic material (giving an even number of layers). Y-type deposition produces a highly symmetrical packing arrangement unless different materials are used for successive layers (as with the alternate layer trough design). At high subphase pH, fatty acids will sometimes only deposit on the downstroke, thus forming X-type films. This type of deposition is energetically unfavourable compared to Y-type deposition, and there is x-ray evidence for molecular rearrangement during transferral to give films that are essentially Y-type in nature. Z-type deposition, in which pick up occurs only on the upstroke, has been observed in a lightly substituted anthracene derivative<sup>(176)</sup> and in asymmetrically substituted copper phthalocyanine<sup>(177)</sup>. An important parameter used to characterize Langmuir-Blodgett film deposition is the deposition (or transfer) ratio (see section 3.1.4).

The success of deposition and the quality of the multilayer films depend critically on the structure of the first monolayer, since any faults in it might be propagated into subsequent layers. In addition, the first layer is unique in that it is the only one directly bonded to the substrate. Thus, there will be a fundamental difference between the forces involved in this process and those involved in bonding succeeding

layers to each other. Particular care was therefore taken when depositing the first layer, dipping being commenced immediately after the final surface treatment of the substrate, at low speeds ( $\sim 2 \text{ mm min}^{-1}$ ), and a drainage time of at least 30 minutes was allowed before depositing further layers.

New monolayers were spread and the optimum conditions ascertained from the  $a_m$  and time stability experiments were applied. After the film had stabilised on the subphase a substrate was dipped down and up through the air-surface interface. This was performed at different dipping speeds to find the best conditions. The actual transfer ratio was calculated by finding the area of film that disappeared during the length of the dip process and subtracting the figure found from the time stability experiment; the resulting figure was then divided by the area of the substrate and converted to a percentage.

#### **5.12.6 Second Harmonic Generation.**

The standard experimental arrangement for the SHG measurements has been described in detail<sup>(178)</sup>. Light from a Q-switched NdYAG laser, linearly polarized parallel (p) to the plane of incidence, was directed at  $45^\circ$  onto the vertically mounted samples. The p-polarised component of the second harmonic radiation was detected in the transmission geometry.

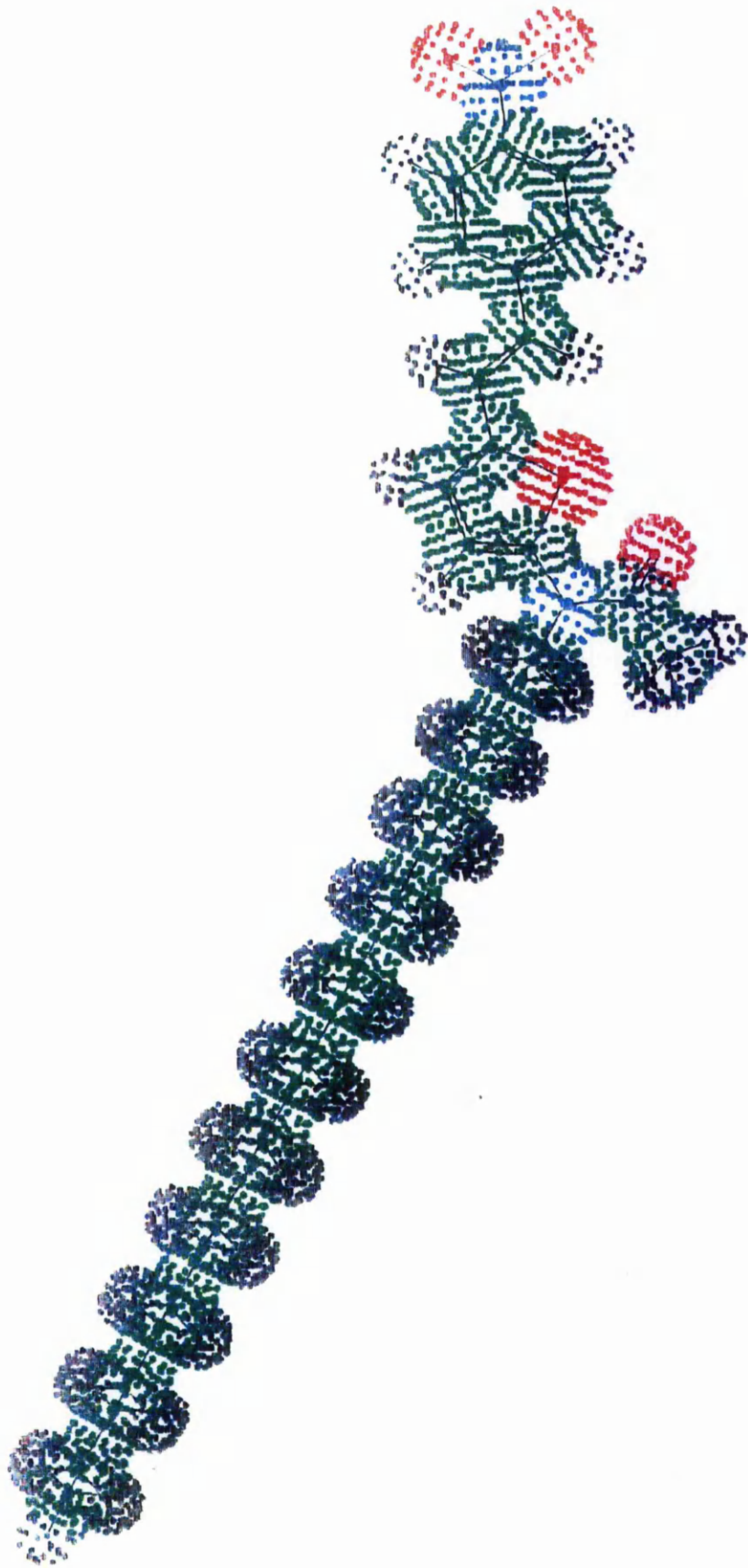


**Figure 18.** A chem-X Energy minimised molecular model of the E-configuration of compound 54K

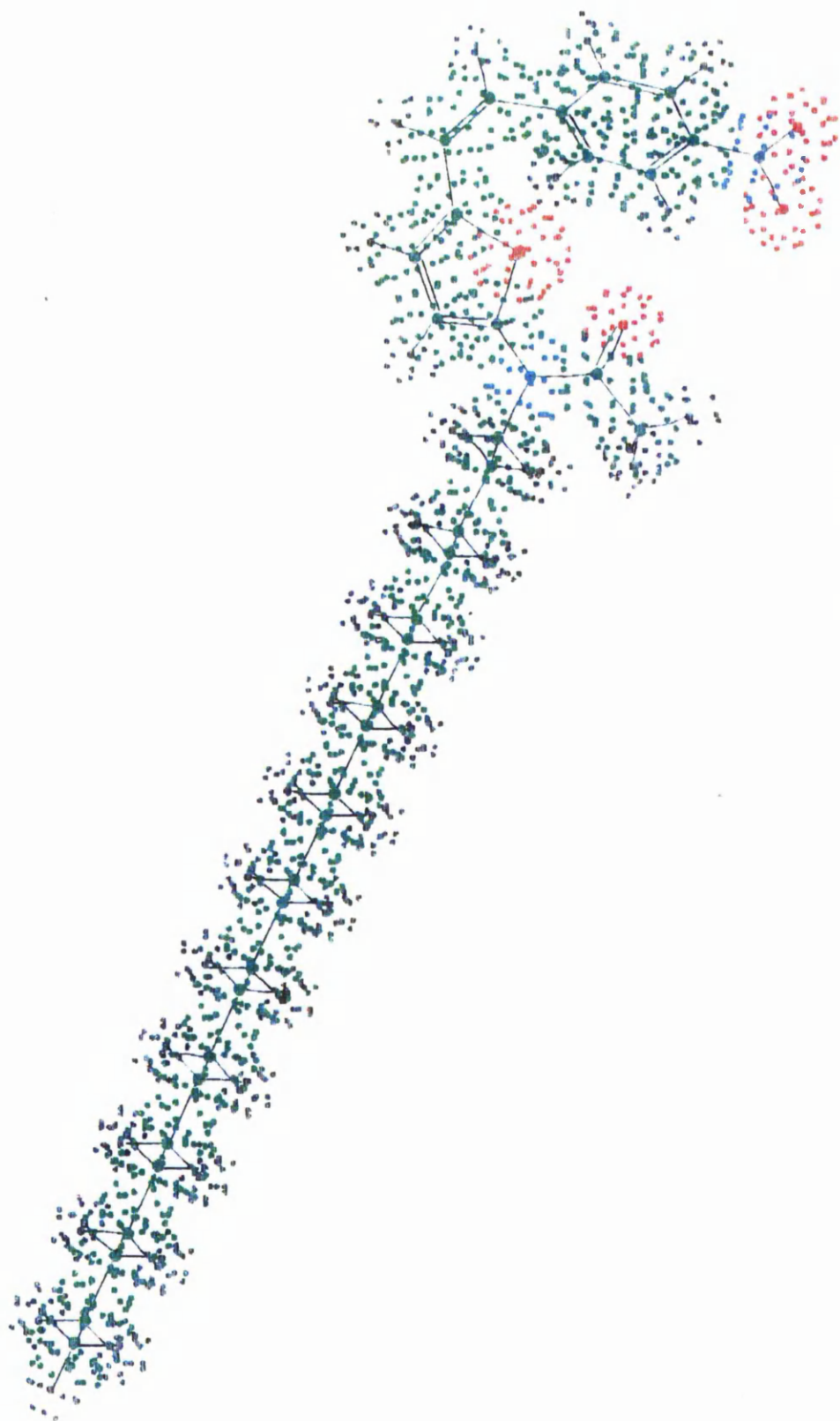


**Figure 19.** A chem-X Energy minimised molecular model of the Z-configuration of compound 54K

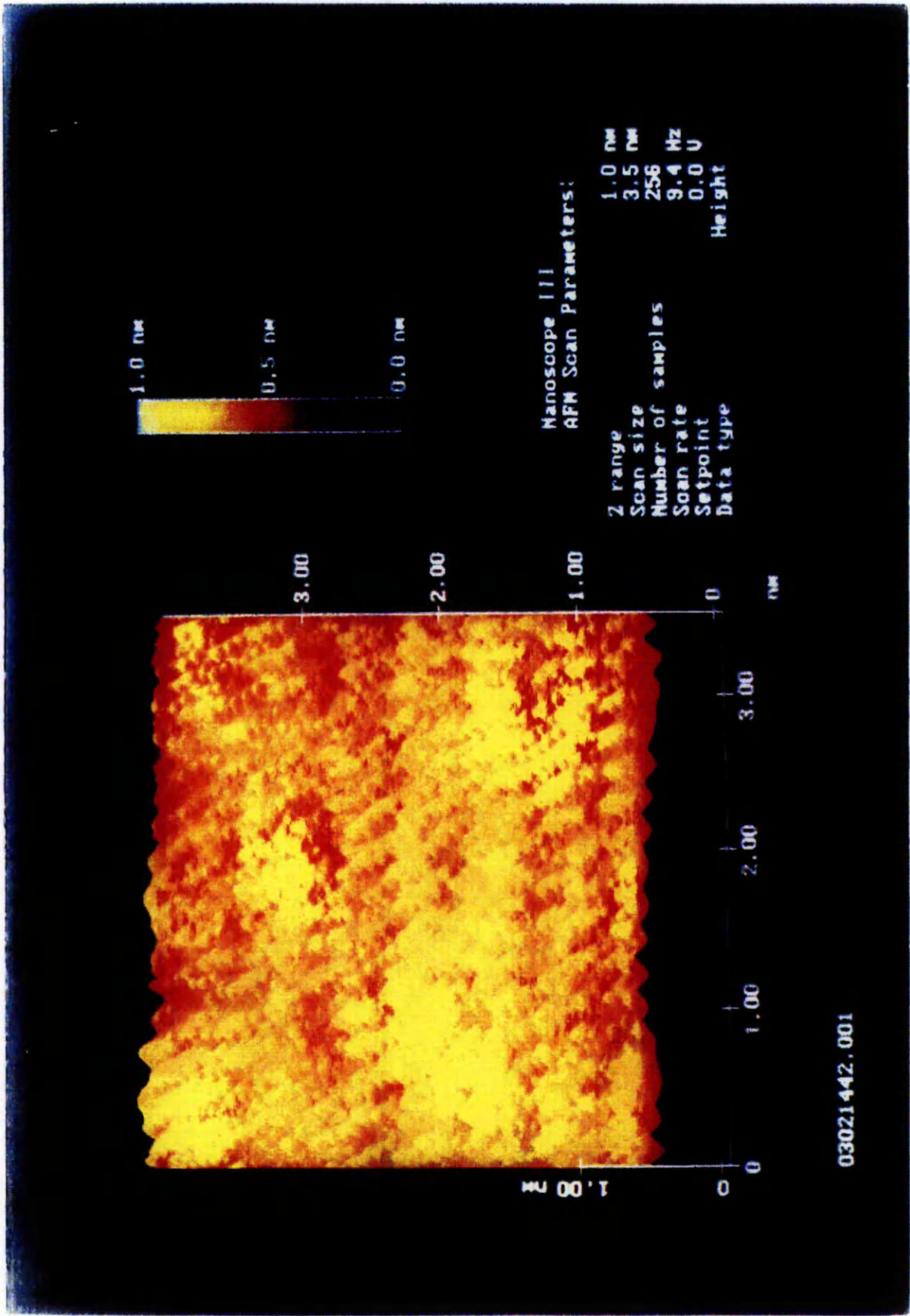


Figure 20. Atomic force micrograph of compound 54K on a (100) n-type silicon wafer

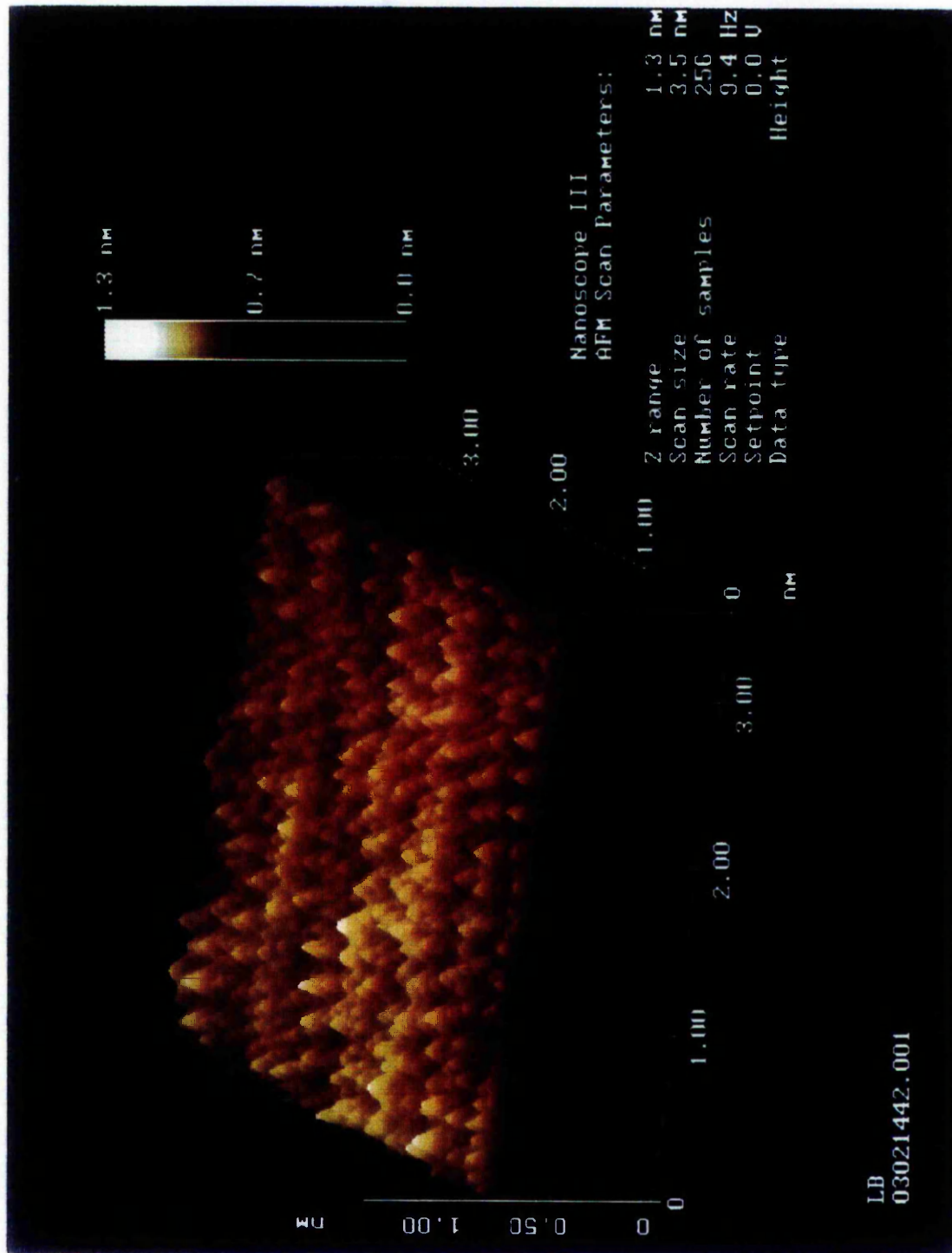


Figure 21. Atomic force micrograph of compound 54K on a (100) n-type silicon wafer

# Conclusions

## CONCLUSIONS

For each individual molecule in the simple amphiphilic thiophene series the pH of the subphase has very little effect on the area per molecule. If anything the area per molecule at pH = 9.0 is slightly larger than that observed at pH = 4.0, which could be accounted for by the association of the acid groups into dimers with a large cadmium ion in the middle. The area per molecule for the molecules in group two are larger than those in groups one and three. This is probably a consequence of the carbonyl group next to the thiophene moiety in the group two molecules preventing the molecules from packing as close together as those in groups one and three, which do not have this carbonyl group. The longer the hydrophobic 'tail' on the molecules, the more stable the subsequent films are to dissolution and/or collapse; furthermore, the molecules in group two are less stable than those of corresponding length in group three. This is again probably due to the lower packing density caused by the carbonyl group, and hence leading to reduced intermolecular interactions, relative to the group three molecules. When comparing molecules of the same overall length but with the thiophene moiety in a different position along the carbon chain (cf. 1h with 3j), it can be seen that there is very little difference in monolayer stability.

Compound 54 k, the D- $\pi$ -A molecule, shows a steady increase in area per molecule as the pH of the subphase increases, which is probably due to the higher pH resulting in a greater tendency for the molecules to associate with the large cadmium ions in the subphase, causing them to have greater stability and slightly larger area per molecule. The isotherms of the mixtures of compound 54 k and arachidic acids show a phase change that exhibits a progressively greater similarity to that of 'the ideal' produced by stearic acid as the percentage of arachidic acid in the mixture is



increased, which is as to be expected. The further phase change seen in the isotherms of compound 54 k at pH = 5.0 giving a local maximum at an area per molecule of approximately  $47 \text{ nm}^2$ , could be due to the monolayer being initially compressed to a state where the region of conjugation, being fairly rigid due to the aromatic rings, is lying flat on the surface of the subphase; further compression may lead this region of conjugation to reorientate, resulting in a fall in the surface pressure, until the monolayer eventually adopts a more ordered packing arrangement.

The more stable monolayer of pure compound 54 k at the higher pH and the subsequent improved transfer ratio from the subphase to the substrate, is again probably due to the association of a large cadmium ion with each pair of molecules of compound 54 k. This association is possible because the cadmium chloride in the subphase should be totally dissociated in the aqueous medium and therefore free to stabilise the compound on the subphase. This results in a dimer structure consisting of one cadmium ion and two molecules of compound 54 k associating through the  $\text{NO}_2^-$  'head' group in a similar way to the carboxylate group in stearic acid.

The SHG studies performed on structures consisting of  $n$  pairs of alternating layers of 67% 54 k : 33% cadmium arachidate gave results which were inconsistent, the greatest SHG being obtained from the  $n = 7$  structure, however, most of the data did reflect an increase in SHG with increasing  $n$  ( $n = 3 < n = 5 < n = 9$ ), a single monolayer of the mixture deposited directly onto the substrate gave greater SHG than did the  $n = 9$  structure. This apparently anomalous result for the monolayer was probably due to a more favourable orientation of the chromophore in the monolayer bonded directly to the substrate compared with that adopted in subsequent layers. In addition, the slightly lower pH used in the formation of alternate layer structures may

have been unfavourable to the deposition of the active component; the resulting poor quality may account for the scatter of the data, including the erroneous position in the sequence for  $n = 7$ .

It can be seen from the SHG results of the monolayer mixtures of compound 54 k and cadmium arachidate that the higher the concentration of compound 54 k the greater the amount of SHG, up to a certain point (around the 70% active molecules). More experiments will have to be carried out to ascertain the best possible ratio.

The superior transfer ratio of the mixtures when forming the alternate layer structures rather than monolayer films may be due to the arachidic acid component being more stable at a slightly lower pH employed in this set of studies; however, more experiments will have to be performed to confirm this.

It is likely that the optimum conditions will result from a trade off between having the maximum possible amount of compound 54 k and improving:-

- (a) the quality of deposition,
- (b) the molecular orientation within the film,
- (c) the dielectric environment of the active species, and
- (d) the possible stabilisation of the layers by the interdigitation of the spacer molecules with the active molecules.

The possible future of this work could be to synthesise a compound with the benzene and thiophene moieties transposed, as in compound (55) in Fig 4.18. This would probably be better because the free amine would be on the benzene ring and therefore more stable.

It might also be an idea, in addition to the first suggestion, to increase the electron density in the  $\pi$ -system by replacing the thiophene ring by a 2,2'-bithiophene

system and/or to increase the length of the  $\pi$ -system by adding  $(\text{CH}=\text{CH}\text{-thiophene})_n$  moieties into the molecule. These would have the further beneficial effect that the alkyl chain would not have to be as long to provide insolubility, thus the dilution of the non-linear optical effect due to the relatively large spacing of the  $\pi$ -systems in the molecular lattices of the Langmuir-Blodgett multilayers would be reduced.

# References

## REFERENCES

1. Williams, D.J., *Angew. Chem. Int. Ed. Engl.*, **23**, 690-703 (1984).
2. Roberts, G.G., *Contemp. Phys.*, **23**, 109-128 (1984).
3. Girling, I.R., Kolinsky, P.V., Cade, N.A., Earls, J.D. and Peterson, I.R., *Opt. Commun.*, **55**, 289-292 (1985).
4. Girling, I.R., Cade, N.A., Kolinsky, P.V., Earls, J.D., Cross, G.H. and Peterson, I.R., *Thin Solid Films*, **134**(1-4), 101-112, (1985).
5. Neal, D. B.; Petty, M. C.; Roberts, G. G.; Ahmad, M. M.; Feast, W. J.; Girling, I. R.; Cade, N.A.; Kolinsky, P. V.; Peterson, I. R., *Electronic Letters*, **22**(9), 460-462 (1986).
6. Neal, D. B.; Petty, M. C.; Roberts, G. G.; Ahmad, M. M.; Feast, W. J.; Girling, I. R.; Cade, N.A.; Kolinsky, P. V.; Peterson, I. R., *I.E.E.E. Transactions on Ultrasonics Ferroelectrics and Frequency Control* **33**(6), 800-801 (1986).
7. Butcher, P. N., *N.L.O. Phenomena* Ohio State University (1965).
8. Harper, P.G., Wherrett, B.S. (Eds.), *Non-Linear Optics*, Proceedings of the 16<sup>th</sup> Scottish Universities Summer School in Physics (1975), Academic Press.
9. Hecht, E., Zajac, A. *Optics*, Addison-Wesley (1974).
10. Yariv, A., *Introduction to Optical Electronics*, 2<sup>nd</sup> Edition, Holt, Rinehart and Winston (1976).
11. Garito, A.F., Singer, K.D., Teng, C.C., in *Non-Linear Optical properties of organic and polymeric materials*. Ed. Williams, D.J., *ACS Symposium Series 233*, Washington (1983).
12. Twieg, R.J., Jain, K., in *Non-Linear Optical properties of organic and polymeric materials*. Ed. Williams, D.J., *ACS Symposium Series 233*, Washington (1983).
13. Oudar, J.L., Chemla D.S., *Opt. Commun.*, **13**, 164 (1975).
14. Oudar, J.L., Le Person, H., *Opt. Commun.*, **15**, 258 (1975).
15. Badan, J., Hierle, R., Périgaud, A., Zyss, J., in *Non-Linear Optical properties of organic and polymeric materials*. Ed. Williams, D.J., *ACS Symposium Series 233*, Washington (1983).
16. Fabian, J., Hartmann, H., *Light absorption of organic colorants*, Springer-Verlag, New York (1980).

17. Griffiths, J., *Colour and Constitution of organic molecules*, Academic press (1976).
18. Kitaigorodsky, A.I., *Molecular crystals and molecules*, Academic press, New York (1973).
19. Nayar, B.K., in *Non-Linear Optical properties of organic and polymeric materials*. Ed. Williams, D.J., *ACS Symposium Series 233*, Washington (1983).
20. Meredith G.R., in *Non-Linear Optical properties of organic and polymeric materials*. Ed. Williams, D.J., *ACS Symposium Series 233*, Washington (1983).
21. Pushkara Rao, V.; Jen, Alex K-Y.; Wong, K. Y.; Drost, K. J., *Tetrahedron Letters*, **34**, 11, 1747-1750, (1993).
22. Zyss, J., *J. Non-Crystalline Solids*, **47**, (2), 211 (1982).
23. Oudar, J.L., Hierle, R., *J. App. Phys.*, **48**, (7), 2699 (1977).
24. Zyss, J., Chemla, D.S., Nicoud, J.F., *J. Chem. Phys.*, **74** (9), 4800 (1981).
25. Sigelle, M., Zyss, J., Hierle, R., *J. Non-Crystalline Solids*, **47**, (2), 287 (1982).
26. Bass, M., Bua, D., Mozzi, R., Monchamp, R.R., *Appl. Phys. Lett.*, **15**, 393, (1969).
27. Rao, V. P.; Jen, A. K-Y., Wong, K. Y.; Drost, K. J., *Tetrahedron Letters*, **34**(11), 1747-1750, (1993).
28. Cheng, L. T.; Tam, W.; Meredith, G. R.; Rikken, G.; Meijer, E. W., *SPIE Proc.*, **61**, 1147, (1989).
29. Smith, P.W., Tomlinson, W.J., *I.E.E.E. Spectrum*, June, **26**, (1981).
30. Roberts, G. G., *Contemp. Phys.*, **2**, 109, (1984).
31. Gaines, G.L., *'Insoluble Monolayers at Liquid-Gas Interfaces'* Wiley Interscience publishers (1966).
32. Barraud, A.; Rosilio, C.; Raudel-Textier, A., *J. Coll. Int. Sci.*, **62**, 509 (1977).
33. Barraud, A., *Thin Solid Films*, **99**, 317 (1983).
34. Veale, G.; Peterson, I.R., A., *J. Coll. Int. Sci.*, **103**, 178, (1985).
35. Tieke, B.; Wegner, G.; Naegele, D.; Rinsdorff, H., *Angew. Chem. Int. Ed Engl.*, **15**, 764, (1976).
36. Simpson, W.H.; Reucroft, P.J., *Thin Solid Films*, **6**, 167, (1970)

37. Procarione, W.L.; Kaufman, J.W., *Chem. Phys. Lipids*, **12**, 251, (1974).
38. Wei, L.Y.; Woo, B.Y., *Biophys. J.*, **13**, 215, (1973).
39. Vincett, P.S.; Barlow, W.A.; Boyle, F.T.; Finney, J.A.; Roberts, G.G., *Thin Solid Films* **99**, 265, (1979).
40. Baker, S.; Petty, M.C.; Roberts, G.G.; Twigg, M.V., *Thin Solid Films*, **99**, 53, (1983).
41. Baker, S.; Roberts, G.G.; Petty, M.C., *IEE Proc.*, **130-I**, 260, (1983).
42. Hua, Y.L.; Roberts, G.G.; Ahmad, M.M.; Petty, M.C.; Hanack, M.; Rein, M., *Phil. Mag. B*, **53**, 105, (1986).
43. Sugi, M.; Saito, M.; Fukui, T.; Iizima, S., *Thin Solid Films*, **88**, L15, (1982).
44. Girling, I. R.; Cade, N. A.; Kolinski, P. V.; Earls, J. D.; Cross, G. H.; Peterson, I. R., *Thin Solid Films*, **132**, 101, (1985).
45. Holcroft, B.; Petty, M. C.; Roberts, G. G.; Russell, G. J., *Proc. 2<sup>nd</sup> International Conference on Langmuir-Blodgett Films*, *Thin Solid Films*, **134**, 83, (1985).
46. Fukuda, K.; Nakahara, H.; Kato, T., *J. Coll. Int. Sci.*, **54**, 430, (1976).
47. Girling, I. R.; Cade, N. A.; Kolinsky, P. V.; Jones, R. J.; Peterson, I. R.; Ahmad, M. M.; Neal, D. B.; Petty, M. C.; Roberts, G. G.; Feast, W. J., *Journal of the Optical Society of America B-Optical Physics*, **4**(6), 950-955, (1987).
48. Heesemann, J., *J. Am. Chem. Soc.*, **102**, 2167, (1980).
49. Vandevyver, M.; Barraud, A., *J. Mol. Elec.*, **4**, 207-221, (1988).
50. Roberts, G. G.; Vincett, P. S.; Barlow, W. A., *J. Phys. C.*, **11**, 2077, (1978).
51. Allara, D.; Swalen, J. D., *J. Phys. Chem.*, **86**, 2700, (1982).
52. Novotny, N.; Swalen, J. D.; Rabe, J. P., *Langmuir*, **5**, 485-489, (1989).
53. Zanoni, R.; Naselli, C.; Bell, J.; Stegeman, G. I.; Seaton, C. T., *Phys. Rev. Lett.*, **57**, 2838-2340, (1986).
54. Gleed, D. G.; Hillebrands, B.; Lee, S.; Stegeman, G. I.; Sambles, J. R.; Geddes, N. J., *J. Phys. Condens. Mater.*, **1**, 3663-3669, (1989).
55. Lee, S.; Hillebrands, B.; Stegeman, G. I.; Laxhuber, L. A.; Swalen, J. D., *J. Chem. Phys.*, **91**, 1882-1884, (1989).
56. Brundle, C. R.; Hopster, H.; Swalen, J. D., *J. Chem. Phys.*, **70**, 5190, (1979).

57. Mori, C.; Noguchi, H.; Mizuno, M.; Watanabe, T., *Jap. J. Appl. Phys.*, **19**, 725, (1980).
58. Peterson, I. R.; Russell, G. J.; Roberts, G. G., *Thin Solid Films*, **109**, 371, (1983).
59. Peterson, I. R.; Russell, G. J.; Neal, D. B.; Petty, M. C.; Roberts, G. G.; Ginnai, T., *Phil. Mag. B*, **54**, 71, (1986).
60. Vincett, P. S.; Barlow, W. A., *Thin Solid Films*, **71**, 305, (1980).
61. Matsuda, A.; Sugi, M.; Fukui, T.; Iizima, S., *J. App. Phys.*, **48**, 771, (1977).
62. Tredgold, R. H.; Allen, R. A.; Hodge, P., *Thin Solid Films*, **155**, 343-352, (1987).
63. Tredgold, R. H.; Vickers, A. J.; Hoorfar, A.; Hodge, P.; Khoshdel, E., *J. Phys. D Appl. Phys.*, **18**, 1139-1145, (1985).
64. von Frieling, M.; Bradaczek, H.; Durfee, W. S., *Thin Solid Films*, **159**, 451-459, (1988).
65. Kamata, T.; Umemura, J.; Takenaka, T., *Chem. Lett.*, 1231-1234, (1988).
66. Fromherz, P.; Oelschlagel, U.; Wilke, W., *Thin Solid Films*, **159**, 421-427, (1988).
67. Buhaenko, M. R.; Grundy, M. J.; Richardson, R. M.; Roser, S. J., *Thin Solid Films*, **159**, 253-265, (1988).
68. Russell, G. J.; Petty, M. C.; Peterson, I. R.; Roberts, G. G.; Lloyd, J. P.; Kan, K. K., *J. Mat. Sci. Lett.*, **3**, 25, (1984).
69. Nicklow, R. M.; Pomerantz, M.; Segmuller, A., *Phys. Rev.*, **B23**, 1081, (1981).
70. Russell, T. P.; Karim, A.; Mansour, A.; Fletcher, G. P., *Macromolecules*, **21**, 1890-1893, (1988).
71. Anastasiadis, S. H.; Russell, T. P.; Satija, S. K.; Majkrazak, C. F., *Phys. Rev. Lett.*, **62**, 1852-1855, (1989).
72. Karim, A.; Mansour, A.; Fletcher, G. P.; Russell, T. P., *Physica*, **156/157**, 430-433, (1989).
73. Chidsey, C. E. D.; Lui, G.; Rowntree, P.; Scoles, G., *J. Chem. Phys.*, **91**, 4421-4423, (1989).
74. Swalen, J. D., *Annu. Rev. Mater. Sci.*, **21**, 373-408, (1991).



75. Rabe, J., *Angew. Chem. Int. Ed. Engl.*, **28**, 117-122, (1989).
76. Wang, P.; Singleton, J. L.; Wu, X. L.; Shansuzzoha, M.; Netzger, R. M.; Panetta, C. A.; Kim, J. W.; Hiemer, N. E., *Synthetic Metals*, **56**(2-3), 3824-3829, (1993).
77. Wang, P.; Wu, X. L.; Shansuzzoha, M.; Lee, W. J.; Netzger, R. M., *Synthetic Metals*, **56**(2-3), 3104-3109, (1993).
78. Garnaes, J.; Schwartz, D. K.; Viswanathan, R.; Zasadzinski, J. A. N., *Synthetic Metals*, **57**(1), 3795-3800, (1993).
79. Schwartz, D. K.; Garnaes, J.; Viswanathan, R.; Chiruvolu, S.; Zasadzinski, J. A. N., *Physical Review E*, **47**(1), 452-460, (1993).
80. Roberts, G. G., *Adv. in Chem. Ser.*, **218**, 225-270, (1988).
81. Baker, S.; Roberts, G. G.; Petty, M. C., *Proc. Inst. Electr. Eng.*, Part 1, **130**, 260-263 (1983).
82. Wohltjen, H.; Barger, W.; Snow, A. and Jarvis, N. J., *IEEE Trans Electron Devices*, **32**, 1170, (1985).
83. Fu, C. W.; Batzel, D. A.; Rikert, S. E.; Ko, W. H.; Fung, C. D.; Kenney, M. E., *Transducer 87 Tech Dig.*, 4<sup>th</sup> Int. Conf. on Solid State Sensors and Actuators, 1987, Institute of Electrical Engineers of Japan, Tokyo, 677, (1987).
84. Brown, A. D., *Sensors and Actuators*, **6**, 151-168, (1984).
85. Moriizumi, T.; Sriyudthsak, M., *Proc. 2<sup>nd</sup> Int. Meet. on Chemical Sensors, Bordeaux*, 431, (1986).
86. Moriizumi, T., *Thin Solid Films*, **160**, 413-429, (1988).
87. Morizumii, T., *Proc. Int. Symp. on Future Electron devices, 1985*, Research and Development Association for Future Electron Devices, Tokyo, 73, (1985).
88. Miyahara, Y.; Moriizumi, T.; Shiokawa, S.; Matsuoka, H.; Karube, I.; Suzuki, S., *J. Chem. Soc. Jpn.*, **6**, 823 (1983).
89. Miyahara, Y.; Moriizumi, T., *Sens. Actuators*, **7**, 1, (1985).
90. Takatu, I.; Moriizumi, T., *Sens. Actuators*, **11**, 309, (1987).
91. Katsube, T.; Hara, M., *Trans. '87 Tech Dig.*, 4<sup>th</sup> Int. Conf. on Solid State Sensors and Actuators, Institute of Electrical Engineers of Japan, Tokyo, 816, (1987).
92. Muramatsu, H.; Tamitani, E.; Karube, I., *Proc. Ann. Meet. Jap. Soc. of App. Phys.*, **Oct.**, no. 29-ZB-4, (1986).

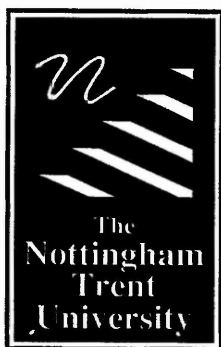
93. Ulman, Abraham, *An introduction to ultrathin organic films: From Langmuir-Blodgett to self-assembly*. 111, Academic Press Limited (1991).
94. Schomaker, V., Pauling, L., *J. Am. Chem. Soc.*, **61**, 1769, (1939).
95. Wheland, G.W., Pauling, L., *J. Am. Chem. Soc.*, **57**, 2086, (1935).
96. Barker, J.M., Huddleston, P.R., Shutler, S.W., *J. Chem. Soc., Perkin Trans. 1*, 2489, (1975).
97. Bell, R.P. and Skinner, B.G., *J. Chem. Soc.*, 2955, (1952).
98. Tarbell, D.S. and Herz, A.H., *J. Amer. Chem. Soc.*, **75**, 1668, (1953).
99. Tarbell, D.S. and Petropoulos, J.C., *J. Amer. Chem. Soc.*, **74**, 244, (1952).
100. Galenkamp, H. and Faber, A.C., *Rec. Trav. Chim.*, **77**, 850, (1958).
101. Nightingale, D.V. and Hocker, H.B., *J. Org. Chem.*, **18**, 1529, (1953).
102. Nightingale, D.V., Hocker, H.B. and Wright, O.L., *J. Org. Chem.*, **18**, 244, (1953).
103. Ferrero, C. and Helg, R., *Helv. Chim. Acta*, **42**, 2111, (1959).
104. Gol'dfarb, Y.L., Goroshkina, G.I. and Fedorou, B.P., *Izv. Akad. Nauk. SSSR., Otd. Khim, Nauk.*, 340, (1956).
105. Gol'dfarb, Y.L. and Kovsakova, I.S., *Izv. Akad. Nauk. SSSR., Otd. Khim, Nauk.*, 546, (1954).
106. Hoehn, W.M., *U.S. Patent 2,880,229* (Mar 31 1959). C.A. 53; P15034, (1959).
107. Kulka, M., *J. Amer. Chem. Soc.*, **76**, 5469, (1954).
108. Pines, H. and Shaw, A.W., *J. Org. Chem.*, **20**, 373, (1955).
109. Royer, R., Demerseman, P., Cheutin, A., Allegrine, E. and Michelet, R., *Bull. Soc. Chim. Fr.*, Mém 1379, (1957).
110. Schlatter, M.J., *J. Amer. Chem. Soc.*, **76**, 4952, (1956).
111. Webber, S.H., Stofberg, J., Spoelstra, D.B. and Kleipol, R.J.C., *Rev. Trav. Chim.*, **75**, 1433, (1956).
112. Graebe, C. and Ullmann, F., *Ber.*, **29**, 824, (1896).

113. Staedinger, H., Goldstein, H. and Schlenker, E., *Helv. Chim. Acta.*, **4**, 334, (1921).
114. Auwers, K. and Rietz, E., *Ber.*, **40**, 3514, (1907).
115. Bargellini, G. and Martegiani, E., *Atti. Acad. Nazl. Lincei. Rend., Classe Sci. Fis., Mat. Nat.*, (**5**) 20 II, 183, (1911).
116. Stadnikoff, G. and Weizmann, A., *Brennstoff-Chem.*, **8**, 344, (1927).
117. Dermer, O.C. and Billmeier, R.A., *J. Amer. Chem. Soc.*, **64**, 464, (1942).
118. Dermer, O.C., Mori, P.T. and Suguiton, S., *Oklahoma Acad. Sci.*, **29**, 74, (1948).
119. Rebstock, M.C. and Stratton, C.D., *J. Amer. Chem. Soc.*, **77**, 3082, (1955).
120. Wynberg, H. and Bantjes, A., *J. Amer. Chem. Soc.*, **82**, 1447, (1960).
121. Farrar, M.W. and Levins, R., *J. Amer. Chem. Soc.*, **72**, 4433, (1950).
122. Walker Jr., H.G., Sanderson, J.J. and Hauser, C.R., *J. Amer. Chem. Soc.*, **53**, 514, (1931).
123. Dalal, S.R. and Shah, R.C., *Chem. and Ind.*, **140**, (1957).
124. Rivikin, S.H., *Zh. Obshch. Khim.*, **5**, 277, (1935).
125. Bassilos, H.F., Makar, S.M. and Salem, A.Y., *Bull. Soc. Chim. Fr.*, Mém, [5], **21**, 72, (1954).
126. Bassilos, H.F., Makar, S.M. and Salem, A.Y., *Bull. Soc. Chim. Fr.*, Mém, **25**, 1430, (1958).
127. Bassilos, H.F. and Salem, A.Y., *Bull. Soc. Chim. Fr.*, Mém, **19**, 586, (1952).
128. Brown, H.C. and Marino, G., *J. Amer. Chem. Soc.*, **81**, 3308, (1959).
129. Brown, H.C., Botto, B.A. and Jensen, F.R., *J. Org. Chem.*, **23**, 417, (1958).
130. Brown, H.C. and Jensen, F.R., *J. Amer. Chem. Soc.*, **80**, 2296, (1958).
131. Brown, H.C. and Young, H.L., *J. Org. Chem.*, **22**, 719, (1957).
132. Hartough, H.D. and Kosak, A.I., *J. Amer. Chem. Soc.*, **68**, 2639, (1946); **69**, 1012, (1947).
133. Hartough, H.D. and Kosak, A.I., *J. Amer. Chem. Soc.*, **70**, 867, (1948).

134. Hartough, H.D. and Kosak, A.I., *J. Amer. Chem. Soc.*, **69**, 3093, (1947).
135. Hartough, H.D. and Kosak, A.I., *J. Amer. Chem. Soc.*, **69**, 3098, (1947).
136. Schoegal, K. and Pelousek, H., *Annalen*, **651**, 1, (1962).
137. Otsuji, Y., Kimura, T., Sugimoto, Y., Imoto, E., Omori, Y. and Okawa, T., *Nippon Kagaku Zasshi*, **80**, 1021, (1959); C.A. 55; 5467, (1967).
138. Noyce, D.S., Alipinski, C. and Nichols, R.W., *J. Org. Chem.*, **37**, 2615, (1972).
139. Pirsonn, P., Schonne, A. and Christiaens, L., *Bull. Soc. Chim. Belg.*, **79**, 575, (1970).
140. MacDowell, D.W.H., Jourdenais, R.A., Naylor, R.W. and Wisowaty, J.C., *J. Org. Chem.*, **37**, 4406, (1972).
141. Pennanen, S., *Acta. Chem. Scand.*, **26**, 2907, (1972).
142. Buu-Hoi, N.P., Hoon, N. and Khoi, N.G., *Rec. Trav. Chim.*, **69**, 1083, (1950).
143. Macdonald, D.W.H. and Ballas, F.L., *J. Org. Chem.*, **39**(15), 2239, (1974).
144. For a review, see Reusch, in Augustine, Ref. 486, 171-211
145. For a review, see Vedejs *Org. React.*, **22**, 401-422, (1975); For a discussion of the experimental conditions see Fieser; *Fieser*, Ref. 46 Vol 1, 1287-1289.
146. For a review, see Todd *Org. React.*, **4**, 378-422, (1948).
147. Huang-Minlon, *J. Am. Chem. Soc.*, **68**, 2487, (1946); **71**, 3301, (1949).
148. Cram, Sahyun, Knox, *J. Am. Chem. Soc.*, **84**, 1734, (1967).
149. Yamaura, Ueda, Hirata, *Chem. Commun.*, 1049, (1967); Todd, Hayashi, Hirata, Yamamura, *Bull. Chem. Soc. Jpn.*, **45**, 264, (1972).
150. March, J. *Advanced Organic Chemistry Reactions, Mechanisms and Structure Fourth Edition.*, Wiley-Interscience (1992).
151. Pommer, *Angew. Chem. Int. (Engl.)* **16**, 423-429, (1977).
152. Cadogan, J. I. G. *Organophosphorus Reagents in Organic Synthesis*, Academic Press: New York, (1979).
153. Johnson, A. W., *Ylide Chemistry*, Academic Press, New York, (1966).
154. Ramirez, Pilot, Desai, Smith, Hansen, McKelvie, *J. Am. Chem. Soc.*, **89**, 6273, (1967).

155. Koziara, A., Zawadzki, S., Zweirzak, A., *Synthesis Communications*, **July**, 527-529, (1979).
156. Adaptation of Meth-Cohn, O.; Narine, B., *Synthesis Communications*, **February**, 133-135, (1980).
157. Ställberg-Stenhagen, S.; Stenhagen, E., *Nature*, **156**, August, (1945).
158. Neal, D. B.; Petty, M. C.; Roberts, G. G.; Ahmad, M. M.; Feast, W. J.; Girling, I. R.; Cade, N. A.; Kolinsky, P. V., Peterson I. R., *Proceedings of the Sixth I.E.E.E. International Symposium on Applications of Ferroelectrics.*, **June**, (1986).
159. Ashwell, G. J.; Jackson, P. D.; Lochun, D.; Thompson, P. A.; Crossland, W. A.; Bahra, G. S.; Brown, C. R.; Jasper, C., *Proceedings of the Royal Society of London Series-A Mathematical and Physical Sciences.*, **445**, (1924 385-398 (1994).
160. Spurlock, J.J., *J. Am. Chem. Soc.*, **75**, 1115-1117, (1953).
161. Hartough, H.D.; Kosak, A.I., *J. Am. Chem. Soc.*, **69**, 3093-3096, (1947).
162. Badger, G.M.; Rodda, H.J.; Sasse, W.H.F., *J. Chem. Soc.*, 4162-4168, (1954).
163. Hartough, H.D.; Kosak, A.I., *J. Am. Chem. Soc.*, **69**, 3098-3099, (1947).
164. Buu, H.N.P.; Lavit, D.; Xuong, N.D.; Royer, R., *J. Chem. Soc.*, 547-549, (1953).
165. Cagniant, P., *Bull. Soc. Chim. France.*, 359-366, (1955).
166. Zyl, G.V.; Langenberg, R.J.; Tah, H.H., *J. Am. Chem. Soc.*, **78**, 1955-1958, (1956).
167. Ceasar, P.D., *J. Am. Chem. Soc.*, **70**, 3623-3625, (1948).
168. Campaigne, E.; Diedrich, J.L., *J. Am. Chem. Soc.*, **70**, 391-392, (1948).
169. Buu, H.N.P.; Lavit, D.; Xuong, N.D., *J. Chem. Soc.*, 1581-1583, (1955).
170. Gewald, K., *Chem. Ber.*, **98**(11), 3571-3577, (1965). from chem. abs. **64:3451g**.
171. Dann, O. and Möller, E. F., *Chem. Ber.*, **80**, 23-36, (1947) from chem. abs. **41:3091d**.
172. Ostman Borje, *Acta Chem. Scand.* **22**(5), 1687-1689, (1968).
173. Koziara, A., Zawadzki, S., Zweirzak, A., *Synthesis Communication*. 527-529 **July**, (1979).

174. Kuhn, H., Möbius, D., Bücher, H., *Physical Methods of Chemistry*. Weissberger, A., Rossiter, B., (Eds.), 1, Part 3b, Wiley (1972).
175. Roberts, G.G., Vincett, P.S., Barlow, W.A., *Phys. Technol.*, **12**, 69, (1981).
176. Vincett, P.S., Barlow, W.A., Boyle, F.T., Finney, J.A., Roberts, G.G., *Thin Solid Films*, **60**, 265, (1979).
177. Baker, S., Roberts, G.G., Petty, M.C., *IEEE Proc.*, **130-I**, 260, (1983).
178. Girling, I. R.; Cade, N. A.; Kolinsky, P. V.; Earls, J. D.; Cross, G. H.; Peterson, I. R., *Thin Solid Films*, **132**, 101-112, (1985).



## **Libraries & Learning Resources**

**The Boots Library: 0115 848 6343  
Clifton Campus Library: 0115 848 6612  
Brackenhurst Library: 01636 817049**